AN ABSTRACT OF THE DISSERTATION OF

Naoyuki Ochiai for the degree of Doctor of Philosophy in Soil Science presented on September 10, 2010.

Title: Movement of Zoospores of *Phytophthora citricola* in Saturated Porous Media

Abstract approved:

Maria I. Dragila Jennifer L. Parke

The genus *Phytophthora* comprises numerous plant pathogens in both natural and managed ecosystems. For *Phytophthora spp*. that infect roots, dispersal occurs in soil water through a combination of advection and swimming of specialized motile propagules (zoospores). Specific biological and physico-chemical processes, however, remain poorly understood, due to difficulties in studying phenomena in opaque media and lack of a theoretical framework for analyzing transport of motile microorganisms. The goal of this research was to elucidate the impacts of advection and swimming on zoospore movement in a saturated, ideal soil. The work was accomplished in two stages, (i) conceptualization of 3-dimensional topography and flow field heterogeneity at the subpore-scale, and (ii) observation of behavior of zoospore suspensions infiltrated into saturated media. Chapter 2 introduces a 3-dimensional particle tracking method and presents two studies investigating particle transport in simplified 'ideal pores'. The first study describes 'avoidance' by latex microspheres of a volume surrounding orthogonal grain contacts and the second describes 'capture', translation, and retention of microspheres under conditions unfavorable to deposition. Chapter 3 expands on the first study and demonstrates,

with the aid of computational fluid dynamics, that low flow zones associated with orthogonal grain contacts are minimally connected to the main flow. Thus, probability of entry into these regions for large, non-Brownian particles by advection alone is low. In zoospore infiltration experiments, zoospore plumes 'converged' rather than dispersing as expected. To assess the possibility of zoospore auto-aggregation driving this 'convergence', Chapter 4 delves into the 'pattern swimming' observed in free-swimming zoospore suspensions, concluding that the concentrating is an example of bioconvection. Chapter 5 introduces a conceptual model to explain the anomalous zoospore plume behavior. Random walk simulations replicated plume convergence but were less successful at modeling anisotropic dispersion. At low infiltration rates (<100 $\mu m\ s^{-1}$), simulations predict that zoospores will remain at or near the soil surface, resulting in greater opportunity to find host tissues or to be transported with surface water. Further investigation is necessary to develop a robust theoretical framework with appropriate conceptualization of the subpore hydrodynamic environment for predicting transport of zoospores and other motile microorganisms in porous media.

Movement of Zoospores of *Phytophthora citricola* in Saturated Porous Media

by

Naoyuki Ochiai

A DISSERTATION

submitted to

Oregon State University

in partial fulfillment of

the requirements for the

degree of

Doctor of Philosophy

Presented September 10, 2010

Commencement June 2011

Doctor of Philosophy dissertation of Naoyuki Ochiai presented on September 10, 2010

APPROVED:

Co-Major Professor, representing Soil Science

Co-Major Professor, representing Soil Science

Chair of the Department of Crop and Soil Science

Dean of the Graduate School

I understand that my dissertation will become part of the permanent collection of Oregon State University libraries. My signature below authorizes release of my dissertation to any reader upon request.

Naoyuki Ochiai, Author

ACKNOWLEDGEMENTS

The author expresses his sincere appreciation to members of the Parke and Dragila labs who assisted both materially and emotionally to the successful conclusion of this research, to Celeste Jones who contributed to many aspects of the data collection and processing, to Marshall Richmond, John Serkowski, and Cindi Rakowski of Pacific Northwest National Laboratory for their assistance with the computational fluid dynamics and finally, to Yoshie, my partner in life and Reon, my inspiration.

CONTRIBUTION OF AUTHORS

Dr. Marshall Richmond provided the computational fluid dynamics (CFD) modeling and writing and editing of text related to CFD modeling in Chapter 3.

TABLE OF CONTENTS

TABLE OF CONTENTS (Continued)

LIST OF FIGURES

LIST OF FIGURES (Continued)

LIST OF FIGURES (Continued)

LIST OF FIGURES (Continued)

LIST OF TABLES

Chapter 1: General Introduction

GOALS AND SCOPE OF RESEARCH

The genus *Phytophthora* comprises over 50 plant pathogens of economic and ecological significance in both forest and agricultural systems worldwide (Erwin and Ribiero, 1996). Due to their morphological and ecological similarity to fungi, *Phytophthora* and other water molds (Oomycetes) were previously classified within the Kingdom Fungi, but now are placed in the Kingdom Stramenopiles, alongside brown algae and diatoms, with which they share the common characteristic of having a unicellular motile (zoosporic) life stage. In *Phytophthora*, the zoosporic stage is not only a vestige of their aquatic ancestry, but continues to play a prominent role in their lifecycle, serving as the primary means of local dispersal. For the majority of *Phytophthora spp*., which are root-infecting, this dispersal takes place in the soil and is the combined result of passive transport with infiltrating water and active movement due to swimming. Despite the ecological importance of soil dispersal, relatively little is known about the transport and movement of zoospores in soils and porous media. This is perhaps understandable, given the inherent difficulties in studying the internal processes of an opaque medium such as soil (Ochiai et al, 2006).

In addition, the classical colloid filtration theory (CFT) (Yao et al)., 1971) commonly employed to study microbial transport, described in greater detail below, may be inadequate for investigating the transport of motile organisms. First, the underlying conceptualization of the pore space, typically the Happel Sphere-in-Cell single collector model, does not capture features, i.e. the topography and resulting heterogeneity of hydrodynamic conditions, relevant to motile microorganisms. Furthermore, other common conceptualization of pores as capillary bundles or body-and-throat networks also do not included these features. While there are some promising novel conceptualizations of the pore space, particularly those

involving packed spheres, their validity remain uncertain. Second, CFT relies on the advective dispersive equation (ADE) to describe dispersion of the microbial population as it is transported through the column. This approach assumes that transport processes 'average out' over large length-scales and that the non-Fickian behaviors of individuals at small scales result in Fickian behavior of populations at larger scales. However, as is demonstrated in Chapter 5 of this dissertation, this is not a valid assumption for the transport of *Phytophthora* zoospores.

The four manuscripts presented in this dissertation, then, represent two distinct phases of research: (i) understanding the 3-dimensional topography and hydrodynamic environment of individual pores and (ii) understanding the combined influence of passive transport and active swimming in the dispersal of zoospores in a saturated ideal 'soil'. The first manuscript (Chapter 2) describes a direct visualization method I developed using epifluorescence microscopy to track the movement of fluorescent particles in 3-dimensions. This method is applied to observation of fluorescent microspheres passed through an isolated glass bead-pair micromodel representing an idealized 3-dimensional pore. The results of two preliminary studies are presented. The first investigates the behavior of latex microspheres with respect to orthogonally-oriented grain-to-grain contacts and the second explores the nature of particle retention under chemical conditions unfavorable to particle deposition. The second manuscript (Chapter 3) expands on the observations of the first study in Chapter 2, utilizing computational fluid dynamics to investigate the nature of the low flow zone associated with orthogonal grain-to-grain contacts and to evaluate the potential of these zones to serve as colloid retention sites. The goal of the second phase of research was to investigate the saturated transport of zoospores through an ideal soil. The interpretation of results is informed by insights gained in the first stage of research. Zoospore plumes passed through sand columns exhibited anomalous breakthrough. Contrary to expectations, plumes converged, i.e.

narrowed in width and increased in concentration and exhibited non-Gaussian distribution. The third manuscript (Chapter 4) probes the possibility of auto-attraction of zoospores as an explanation for this plume convergence by delving into the nature of spontaneously-forming concentrated swimming masses often observed in free suspensions of zoospores. The fourth manuscript (Chapter 5) presents the results of the zoospore column experiments and introduces a novel conceptual model of zoospore swimming behavior to explain the observed plume convergence. Monte Carlo (conditionally-biased random walk) simulations are then used to evaluate the potential of the conceptual model to explain the anomalous plume behavior.

LITERATURE REVIEW

Zoospore morphology. Under specific environmental conditions (in general, low nutrient availability & near saturation), kidney-shaped, unicellular, membrane-bound zoospores are produced within specialized structures called sporangia (or sporangiophores) on infected host tissue. Zoospores vary slightly in size and shape by species and possess two different flagella (hence their *heterokont* designation) that are attached near the soma midpoint, deep within a groove running along the ventral side of the zoospores (Carlile, 1983). The tinsel-type anterior flagellum is thought to enable forward propulsion, while the smooth, somewhat longer posterior flagellum is responsible for changes in direction (Holwill, 1982).

Zoospore motility & taxis. Much of what is known about zoospore motility is based on observations of free-swimming zoospores. Unconfined zoospores swim at velocities ranging from 80 to 240 $\mu m \cdot s^{-1}$, or approximately 10 to 20 times body length per second, depending on species and temperature (Ho and Hickamn, 1967, Allen and Newhook, 1973, Katsura and Miyata, 1967). They tend to swim in a helical path along their long axis, gradually changing direction while unhindered, but

drastically reorienting when coming upon an obstacle (Allen and Newhook, 1973). Zoospores have been observed to swim smoothly in shallow suspensions that may constrain their ability to rotate (Ho and Hickman, 1967).

Zoospores exhibit a number of directional-swimming behaviors, including both positive and negative chemotaxis, electrotaxis, autotaxis, negative geotaxis, and positive rheotaxis. In chemotaxis, zoospores are attracted to root exudates (e.g. Chang-Ho and Hickman, 1970, Morris and Ward, 1992) or pure substances (e.g. Allen and Newhook, 1973, Khew and Zentmeyer, 1973), but are repelled by high concentrations of cations H^+, K^+, NH_4^+, and Na^+, Mg^{2+}, Ca^{2+}, and La^{3+} (Allen and Harvey, 1974, Cameron and Carlile, 1980). In electrotaxis, Morris and Gow (1993) demonstrated that zoospores were attracted to electrical fields by modulation of zoospore turning frequency. For autotaxis, there is some evidence that encysting zoospores may release compounds that recruit other zoospores (Thomas and Peterson, 1990, Reid et al. 1995, Galiana et al. 2008, Kong and Hong, 2010). Cameron and Carlile (1977) demonstrated that the tendency of zoospores to accumulate at the water surface was not due to aerotaxis but, rather, due to negative geotaxis. The mechanism for this upward-swimming tendency is not known, but it may be because the zoospores have an 'upward tilt' due to their center of gravity being offset from their center of buoyancy, as in the case of the alga *Chlamydomonas nivalis* (Kessler, 1985, Roberts, 2006). In regards to rheotaxis, Katsura and Miyata (1967) observed that in the presence of moving fluid, zoospores can and do swim upstream as long as the ambient fluid velocity is less than the free-swimming speed of the zoospores.

Movement of zoospores in porous media. Despite the importance of dispersal in soils, relatively little is known about behavior and fate of zoospores in soil water, perhaps due to the inherent difficulties in studying the internal processes of an opaque medium (Ochiai et al, 2006). It has been reported that zoospores tend to encyst more rapidly when confined than when free-swimming (Ho and Hickman,

1967, Bimpong and Clerk, 1970). Based on these observations, it is suggested that zoospore encystment can be triggered, even in the absence of chemical signals, by repeated collisions with pore walls. This phenomenon is commonly referred to as 'contact stimulus.' However, it appears that the degree to which contact stimulus causes early encystment is species-specific and may not be particularly relevant for some species (Young et al., 1979, Benjamin and Newhook, 1982).

Autonomous dispersal of zoospores in soil. The autonomous dispersal speed and range of zoospores dispersal within soils or ideal media such as glass beads is significantly lower than would be suggested by the swimming speeds of unconfined zoospores. Duniway (1976) found that zoospores only moved 2.5 to 3.5 cm through coarse-textured soils, a distance that would be covered in approximately 3 to 4 minutes if a zoospore were able to swim at 150 $\mu m\ s^{-1}$, unobstructed and in a single direction. Furthermore, estimates of motility based on maximum distance traveled by some members of a zoospore population may be misleading. For example, although Newhook et al (1981) observed some zoospores swimming up to 6 cm in 10 hr through coarse sand, these represented only 0.1 to 0.2% of the original population. The movement or spread of a population of zoospores can be modeled as a diffusive process and the estimated rate of zoospore dispersion can be expressed by a motility coefficient, analogous to a diffusion coefficient. Newhook et al. (1981) estimated the motility coefficient of *P. cinnamomi* zoospores in coarse sand to be on the order of 0.004 $m \cdot s^{-2}$, which is only slightly higher than the diffusion coefficient of an ionic species such as HCl but several orders of magnitude higher than the estimated diffusivity of similar-sized inert particles ($\sim 10^{-13}\ m \cdot s^{-2}$). The inability of zoospores to quickly disperse through pore networks is not surprising since, given their random changes in direction, there is relatively little chance that zoospores will happen upon pathways that would enable them to escape from one pore to the next. Thus, while autonomous movement of zoospores is recognized to occur over short distances (a few mm or cm) in slow moving or stationary water,

passive transport of zoospores in infiltrating water is seen as an important means of zoospore dispersal over greater spatial scales (Newhook et al, 1981).

Passive transport of zoospores in soil. Less is known about the facilitated transport of zoospores through soil by moving water. It has been demonstrated, at least in a single case for *P. capsici*, that free-swimming zoospores exhibit positive rheotaxis, provided that the velocity of the liquid is equal to or less than the zoospore swimming speed (Katsura and Miyata, 1967). This observation suggests that zoospores can either 'sense' the direction of the current and swim against it or may become oriented upstream due to a combination of the zoospore morphology and hydrodynamics. In either case, this upstream swimming is likely to have significant implications for zoospore transport in infiltrating water such as would be experienced during rain or irrigation events. However, the lack of other studies focused on this phenomenon make it impossible to draw any conclusions about its validity and generalizability. In the context of 'contact stimulus' discussed above, it has been suggested that transport by flowing water might lead to increased encystment due to an increasing collision frequency (Carlile, 1983). This, however, has not been borne out by the data. Young et al. (1979) demonstrated that zoospores could be passed through a column of glass beads at relatively high velocities and remain motile, provided the pore necks are of sufficient size to let the zoospores pass. Newhook et al. (1981) observed that only 25% of zoospores allowed to infiltrate into saturated natural soil cores by gravity broke through when expected. An additional 50% of zoospores, most of which were still motile, were recovered after successive flushings, bringing the total of exiting zoospores to approximately 75%. The unrecovered zoospores presumably lysed, encysted, or entered immobile regions of the pore space, i.e. dead-end pores.

Knowledge gap: combined effects of passive transport and autonomous movement. As discussed earlier, it is recognized that zoospore dispersal in soil is achieved by a combination of passive transport and active swimming. However,

perhaps due to the logistic and theoretical challenges posed by such studies, few attempts have been made to investigate both aspects simultaneously. It is not at all certain that zoospores behave the same in moving water as they do in still water or that they behave the same in confined space as they do in free suspension. Thus, it is important to experimentally investigate zoospore swimming behavior in the context of moving water and in porous media to understand the processes involved in soil dispersal.

Colloid filtration theory. In contrast to the case of *Phytophthora* zoospores, there is a growing body of knowledge regarding the transport of bacteria, viruses, and other micro-organisms through porous media. This is motivated by the relevance of such processes to a wide range of disciplines including bioremediation (Loffler and Edwards, 2006), water filtration (e.g. Hijnen et al., 2007), contaminant and pathogen transport (e.g. Semenov et al., 2009). The majority of these studies rely on colloid filtration theory (CFT) (Harvey and Garabedian, 1991) as a theoretical framework (Tufenkji, 2007). Briefly, CFT couples a model of particle-grain interaction to the well-known advection dispersion equation (ADE). The ADE is used to model the dispersion of the particle population as it moves through a porous medium. The particle-grain interaction model describes the process of particle attachment to media grains and comprises a transport step, whereby a particle is transported to the vicinity of the media grain, and an attachment step, whereby the particle becomes associated (or doesn't) with the media grain. The former step is quantified by the collector efficiency (η), and the latter by the attachment efficiency (α). CFT models particle transport and retention reasonably well under chemical conditions which are favorable to particle attachment, i.e. when particles and grain surfaces are oppositely charged so there is no energy barrier to attachment. CFT, however, tends to underestimate particle retention (e.g. Redman et al., 2004) and incorrectly predict the distribution of retained particles under chemical conditions that are unfavorable to particle attachment (Tufenkji, and Elimelech, 2004, Johnson et al., 2007).

The physical model underlying CFT. In CFT, the porous media is conceptualized as a bed of uniform cells. This allows calculations of the transport and attachment steps to be performed for a single unit cell and the results can be extrapolated to the entire media. The most commonly invoked physical model of a unit cell is the Happel Sphere-in-Cell (Rajagopalan and Tien, 1976, Nelson and Ginn, 2005). Briefly, the Happel Sphere-in-cell consists of a spherical 'collector' surrounded by fluid shell whose thickness represents the porosity. The frequency at which particles contact the collector are calculated by performing a trajectory analysis whereby particles are 'released' upstream from the collector. Typically, three transport mechanisms are considered in this trajectory analysis: (i) interception (passive transport on fluid streamlines), (ii) sedimentation due to gravity (relevant if particles are denser than water), and (iii) Brownian motion (relevant for smaller particles). A number of formulas for collector efficiency (η) have been proposed including the original trajectory analysis presented by Rajagopalan and Tien 1976 and a semi-empirical correlation equation based on regression of media and particle parameters against rigorously-determined theoretical single collector efficiencies over a wide range of conditions (Tufenkji and Elimelech, 2004). Nelson and Ginn (2004) compared results of direct numerical simulations based on primary transport mechanisms to predictions based on the Rajagopalan and Tien (1976) trajectory analysis.

Colloid retention under chemically unfavorable conditions. As mentioned above, CFT predicts colloid retention in porous media with reasonable accuracy under favorable chemical conditions (in the absence of an energy barrier to deposition), but fails to predict retention in the presence of an energy barrier to deposition. A number of mechanisms have been proposed, then, to explain particle retention under unfavorable conditions. These include: (i) existence of attractive subdomains on media surfaces (Song and Elimelech, 1994), (ii) entrapment due to surface roughness (Morales et al. 2009), (iii) physical straining at narrow pore regions (Bradford et al., 2006), (iv) capture in the secondary energy minimum (e.g.

McDowell-Boyer, 1992, Hahn et al., 2004, Tufenkji and Elimelech, 2005), (v) association with grain surfaces via attractive nanodomains (Duffadar and Davis, 2007, 2008), (vi) wedging at grain-to-grain contacts (Johnson et al., 2007), and (vii) retention in pore regions of low drag (Tong et al., 2008, Torkzaban et al., 2008).

Ionic strength-dependence of colloid retention under chemically unfavorable conditions. Colloid retention under chemically unfavorable conditions is also observed to be dependent on the ionic-strength of the carrying solution, with increasing deposition associated with increasing ionic strength. This additional observation rules out mechanisms (i – iii), which are not ionic strength-dependent, but is consistent with the remaining mechanisms. Two models of colloid-surface interaction are proposed to explain this ionic-strength dependent retention. First, capture in the secondary minimum (iv) relies on a prediction by the DLVO theory (Derjaguin and Landau, 1941, Verwey and Overbeek, 1948) that the total interaction energy between two electrostatically repulsive surfaces reaches a maximum at very close separation distances but can also achieve a local minimum at some greater separation distance. This is due to the differential separation distance-dependence of the two primary components of the surface-surface interaction energy, repulsive electrostatic interactions and attractive London-van der Waals forces. The resulting energy minimum is referred to as the 'secondary minimum' to contrast it with the 'primary minimum' which occurs when the two surfaces are in direct contact with each other. DLVO theory further predicts that the depth and separation distance of the energy minimum depends on the ionic strength of the mediating fluid. Ions in the mediating fluid 'screen' the electrostatic interaction between the surfaces, effectively lowering the energy barrier between electrostatically repulsive surfaces. Colloids, then, can become associated with like-charged grain surfaces if they are 'captured' in a secondary energy minimum (Hahn et al., 2004). A second model of ionic-strength dependent association of like-charged colloids and grain surfaces involves the presence of attractive nano-domains on grain surfaces (Duffadar and

Davis, 2007 & 2008). This is similar to the proposed existence of attractive subdomains of media surfaces (i), but differs in the scale of the attractive domains. In the nano-domain model, individual attractive domains are very small compared to the interactive surface area of the colloids and the attractive force of a single attractive nano-domain would be much too weak to 'capture' colloids. However, the total attractive force between colloids and surfaces with attractive nano-domains is the specific attractive energy multiplied by the proportion of the interactive area occupied by attractive nanodomains. Net colloid-surface interactions may be attractive, if the total attractive force exceeds the total repulsive force. The net interaction energy in this model is expected to exhibit similar ionic-strength dependence to that predicted for the secondary minimum capture model. Again, ions in the mediating fluid function to 'screen' electrostatic interaction between colloids and surfaces, lowering the repulsive energy of the non-attractive domains.

Coupling of 'capture' mechanisms with pore-scale hydrodynamics. Both the secondary minimum capture and attractive nano-domain hypotheses propose reasonable mechanisms for colloids to become associated with media grains under chemically unfavorable conditions. Secondary minimum capture by itself, however, does not explain the observed retention of colloids in porous media. As demonstrated in numerous radial impinging jet studies, secondary minimum-captured colloids are simply translated along surfaces in the presence of fluid shear (Johnson and Tong, 2006, Nazemifard et al., 2006, de Kerchove et al, 2007, Kline et al., 2008, Liu et al, 2009). Although some researchers have proposed that there may be a resistive component to secondary energy minimum attraction analogous to the rolling resistance experienced by colloids attached in the primary minimum (Torkzaban et al., 2007), there is, as yet, no hypothesized mechanism to account for this force. In the absence of such a resistive force, secondary minimum-captured colloids should continue to move through the porous media, i.e. not be retained, albeit slowly. For captured colloids to become retained in porous media they must

somehow deposit on grain surfaces (in the primary minimum) or enter stagnant (or extremely low flow) regions of the pore. As to the former case, Johnson et al., 2007 proposed that colloids can deposit or become 'wedged' (iv) near grain-to-grain contacts when the 'repulsive' force of one of the impinging grain walls is able to push the colloid over the energy barrier of the other impinging wall. In support of the latter case, it is proposed that secondary minimum captured colloids are translated along grain surfaces to low flow zones associated with grain-to-grain contacts, where they would be prevented from further downstream transport (Kuznar and Elimelech, 2007, Tong et al., 2008, Torbzaban et al., 2008). The predicted retention of colloids at grain-to-grain contacts has been confirmed in a variety of experimental studies (Li et al., 2006, Yoon et al., 2006, Kuznar and Elimelech, 2007, Tong et al., 2008, Johnson et al., 2010). The attractive nano-domain model also predicts that colloids will translate across grain surfaces in the presence of fluid drag. However, direct contact of colloids with the collector surface introduces frictional and adhesive forces that could oppose lateral movement in the presence of shear. Colloids could, thus, be 'retained' in locations where the local fluid drag is unable to overcome the resistive colloid-surface torque.

Alternative physical models of pore space. In both the secondary minimum and attractive nano-domain models above, it is apparent that colloids will be retained only in regions of low fluid drag. To be able to correctly predict colloid retention under chemically unfavorable conditions, then, requires that we are able to accurately model the flow field, and particularly the low shear zones, of pores. In this sense, it is clear that the commonly-invoked Happel Sphere-in-Cell model is inadequate. Notably absent are grain-to-grain contacts, which have significant impact on the flow field, are essential features of granular porous media, and have been demonstrated to be locations of colloid retention. Traditional conceptualizations of soil pores as capillary bundles or body-and-throat networks are equally inadequate in representing the sub-pore heterogeneity of the flow field.

In the context of unsaturated flow, Tuller and Or (2002) proposed representation of pores as a combination of main pores with triangular cross section and slits representing matrices. The impinging walls at the corners create low flow zones analogous to the low flow zones that are analogous to those found in the vicinity of grain-to-grain contacts. However, this model does not capture the change in the flow field along the pore axis. Paraskeva et al., 1991, proposed representation of pores as constricted tubes. While this model captures the axial change in pore cross-sectional area, it does not account for the low flows zones associated with grain-to-grain contacts. Cushing and Lawler (1998) first proposed using face-centered cubic packed spheres as a unit pore. Such conceptualization of the pore space explicitly includes grain-to-grain contacts as well as represents the axial change in pore cross section. This general approach was extended by Johnson et al. (2007EST) to models using dense cubing packing. Finally, Ma et al. (2009) and Ma and Johnson (2010) have proposed a Hemispheres-in-Cell model, analogous to the Happel Sphere-in-Cell model which, again, explicitly includes grain to grain contacts and represents axial changes in the pore cross section. The last two conceptualizations of the pore space appear to have some traction, although it remains to be seen if they can be used to accurately predict colloid deposition under unfavorable conditions.

Knowledge gap: are all grain-to-grain contacts the same? There is a tacit assumption in the current literature that all grain-to-grain contacts are the same. However, it may be that the retention potential and functions of grain-to-grain contacts may vary with orientation relative to the main flow. If, for example, we consider the deposition of colloids into low flow zones associated with grain-to-grain contacts after capture in the secondary minimum (or attractive nano-domains) and translation along the grain surface, it would seem that grain-to-grain contacts occurring at the rear of the bead would be the preferred location for colloid retention (Torkzaban et al. 2004). This is because the majority of near-surface streamlines lead to the rear of the bead. In contrast, the low flow zones associated

with grain-to-grain contacts that are orthogonal to the direction of flow would receive few colloids, since very few streamlines lead to this region. Orientation-dependent deposition of colloids at grain-to-grain contacts under unfavorable conditions is apparent in some studies (Fig. 4 of Kuznar and Elimelech, 2006), but not all (Tong, et al., 2008, Johnson et al., 2010). In the latter studies, the orientation-dependence is perhaps not easily identified because local flow orientation, and thus grain-to-grain contact orientation, can be difficult to determine, even in simple, single-layer models. Despite the potential qualitative difference in function with orientation, only rear grain-to-grain contacts have be rigorously investigated (Torkzaban et al. 2008).

Microbial transport studies. CFT has been successfully applied to the study of microbial transport (Tufenkji, 2007). However, the morphology and metabolism of microbes introduce a number of complicating factors, including difficult-to-characterize microbe-grain surface interactions due to surface properties and appendages, time-dependent growth and decay of populations, alteration of grain surfaces and pore topography by biofilm development, enhanced diffusion and chemotaxis due to microbial motility (Ginn et al., 2002). Some of these complications, such as variability of microbe-grain interaction energies, may be dealt with within the ADE-CFT framework as long as they do not lead to violation of the assumption Fickian dispersion that underlies the ADE-CFT approach, however, other behaviors such as chemotaxis may result in non-Fickian plume dispersion and require alternative modeling techniques (Tufenkji, 2007).

Alternative approaches to modeling transport (random walk). Random walk models have been frequently employed to model the dispersal of a variety of biological agents, including microorganisms. A comprehensive review of the theory and application of random walk models in biological systems is provided by Codling et al. (2008). In the case of microorganisms, the random walk approach has been most commonly been employed to model bacterial chemotaxis in unrestricted space,

either in the absence (e.g. D'Orsogna et al., 2003, Nicolau et al., 2009) or presence of flow (e.g. Bearon, 2003, Locsei and Pedley, 2009). Random walks have also been limitedly employed to simulate transport of bacteria through porous media (Duffy et al., 1995) or in restricted pore-space (Kusy and Ford 2007). The Kusy and Ford (2007) investigation aptly illustrates a strength of the random walk approach, it inherent 'up-scaling', which enables researchers to simulate the behavior of populations, which is generally the scale of interest in transport studies, by specifying behaviors of individuals and characteristics of the micro-scale environment, which is typically the scale at which quantitative data is available.

Three-Dimensional Tracking of Colloids at the Pore Scale Using Epifluorescence Microscopy

Naoyuki Ochiai, Maria Ines Dragila, and Jennifer L. Parke

Vadose Zone Journal
Soil Science Society of America
5585 Guilford Road
Madison, WI 53711-5801
Published in Vol. 9 (2010)

ABSTRACT

The transport of micrometer- and submicrometer-sized particles of biotic and abiotic origin through both natural and engineered porous media is relevant to a wide variety of disciplines. While the influence on colloid transport of chemical factors such as colloid and media surface chemistry and the ionic strength of the carrying fluid are fairly well understood, the role of physical factors still needs clarification from a mechanistic standpoint. Along with recent recognition that pore-scale processes may depend on the coupling of chemistry and local hydrodynamics, which in turn depends on pore topography, there is a growing need for experimental systems that enable visualization of individual colloids in pores and pore networks that contain relevant three-dimensional features. We introduce a single camera–epifluorescence microscope system to track fluorescent colloids in three dimensions using the apparent diameter of out-of-focus colloids to estimate their *z*-axis location. The current system, using a plan achromat 5× objective, enables *z* estimation of 4.7-µm-diameter fluorescent microspheres across a range of 1200 µm with accuracy of approximately 34 µm. In addition to discussion of system limitations and potential improvements, we present results from two mini-studies illustrating the use of three-dimensional particle tracking to investigate (i) the behavior of colloids approaching orthogonally oriented grain-to-grain contacts, and (ii) the potential retention mechanisms in porous media under chemical conditions unfavorable to deposition. The ability to track individual colloids in three dimensions brings experimental capabilities closer in line with computer-modeling capabilities, setting the stage for synergistic pairing of experimental and theoretical investigations.

Abbreviations: AD, apparent image diameter, G2G, grain-to-grain contact, obG2G, oblique grain-to-grain contact, oG2G, orthogonal grain-to-grain contact, pG2G, parallel grain-to-grain contact.

INTRODUCTION

The generation, retention, and transport of suspended nanometer- to micrometer-sized particles, commonly referred to as *colloids*, through porous media is of interest to researchers and practitioners in a wide variety of disciplines such as microbial remediation, contaminant transport, and water filtration. Since the specific behavior of suspended particles in a given system depends on complex chemical, physical, and in some cases biological interactions of the particles, suspending fluid, and porous medium, it is not surprising that our ability to predict behavior based on known system parameters is still limited.

The traditional method of studying particle or colloid transport has been to pass a known particle suspension through a column of disturbed or undisturbed natural or engineered porous media and to infer internal processes based on the pattern of breakthrough. This methodology has been particularly useful in elucidating the nature of the chemical interaction between colloids and grain surfaces (e.g., Elimelech et al., 2000) and the mediating role of the carrying fluid cation valence and ionic strength (e.g., Huber et al., 2000) based on the theoretical framework for interactions of surfaces proposed by Derjaguin and Landau (1941) and Verwey and Overbeek (1948), commonly referred to as DLVO theory.

What has been less forthcoming from column breakthrough studies is an understanding of the physical processes controlling transport. This is largely due to a combination of not knowing what the relevant mechanisms are and the difficulty in discriminating the effects of individual mechanisms by studying breakthrough curves, which by their nature represent the integration of multiple mechanisms.

Given that pore-scale mechanisms may contribute significantly to macro-scale transport behavior, significant effort has been made to study such mechanisms by direct visualization, typically through microscopic observation of colloids in glass or silicon micromodels replicating regular or irregular pores and pore networks. These investigations have led to the identification of important features such as the air–

water interface, the verification of mechanisms such as straining and size exclusion, and the evaluation of predictive models based on fluid dynamics and transport theory (reviewed by Ochiai et al., 2006, Keller and Auset, 2007). The utility of such micromodels for investigating pore-scale mechanisms, however, is limited by the fact that they are essentially two dimensional.

Recent theoretical and experimental research recognizes the importance of three-dimensional pore structure on colloid transport and deposition, focusing particularly on grain-to-grain contacts (e.g., Johnson et al., 2007a, Torkzaban et al., 2008). Grain-to-grain contacts are one feature of the flow field among others that are likely to influence pore-scale colloid transport behavior. Commonly invoked conceptualizations of pores as capillaries, pore body and throat networks, or constricted tubes (Paraskeva et al., 1991) imply that pore cross-sections are circular, in reality, pore cross-sections of granular media are irregularly shaped and change rapidly with position along the pore axis. The resulting flow field simultaneously exhibits “flow-constricted” regions where adjacent grains approach and “free flow” sections away from grains that change rapidly with position along the pore axis. Given the increasing recognition that certain pore-scale mechanisms, such as retention in the secondary energy minimum, may be governed by coupled chemical and local hydrodynamic factors (Elimelech and O’Melia, 1990, Bradford et al., 2007, Johnson et al., 2007b), there is a growing need for experimental systems that allow direct investigation of colloids in real porous media or pore models that contain the above-mentioned characteristics of the flow field.

While fluid and particle transport in idealized three-dimensional pores (bead pairs or regular bead packings) has previously been investigated (Snyder and Stewart, 1966, Davis et al., 1976, Cushing and Lawler, 1998), increased computing power now enables theorists to simulate particle transport with a growing portfolio of rule sets governing particle behavior and particle–surface interactions (Johnson et al., 2007a, Torkzaban et al., 2008). On the other hand, experimenters continue to

face the challenge of developing methods to track the movement of individual colloids in realistic, three-dimensional pore networks. Novel three-dimensional imaging techniques such as magnetic resonance imaging and x-ray tomography enable visualization of the interior of a porous medium, as opposed to just the surface. Magnetic resonance imaging systems typically have maximum resolutions on the order of 30 μm (Manz et al., 2003), which is too coarse to resolve individual colloids. While highly specialized transmission x-ray microscopes are capable of resolutions on the order of 25 nm (Schneider, 2003), more commonly used synchrotron-based x-ray tomography offers resolutions on the order of 7.5 μm (Auzerais et al., 1996). Currently, light-based methods offer sufficient spatial resolution (on the order of 0.20 μm) and temporal resolution (generally limited by the frame rate of the image capture device) to track individual colloids, but are limited to visualizing the surface layer of porous media, where colloids may be subject to significant boundary effects. Recently, researchers have used epifluorescence and confocal microscopy to investigate colloid behavior in simplified three-dimensional pore network models consisting of a single layer of glass beads or sand grains (Kuznar and Elimelech, 2007, Smith et al., 2008, Tong et al., 2008). The visualization techniques used in these studies, however, were essentially two-dimensional. With recent technological advances in scanning speed, confocal microscopy offers high-speed three-dimensional imaging capability with the potential to track the movement of individual colloids in three dimensions (Moschakis et al., 2006). An alternative to the “slice and stack” approach to generate three-dimensional images represented by confocal microscopy is to view a single “slice” of the sample at a single depth and to estimate the height or depth of out-of-focus objects based on the characteristics of the out-of-focus images, such as image intensity, diffraction pattern (Speidel et al., 2003, Luo et al., 2006), or diffraction ring size (Wu et al., 2006).

Our group is developing an epifluorescence-based three-dimensional particle tracking method that exploits the apparent image diameter of out-of-focus colloids to estimate their axial position. We briefly review the theory underlying this visualization method, present data illustrating the capabilities and limitations of our current system, and discuss potential improvements. In addition, we present results from two mini-studies illustrating the use of three-dimensional particle tracking to investigate colloid behavior in simplified three-dimensional pores consisting of pairs of touching glass beads arranged within a flow cell. The first study investigated the behavior of colloids as they approach orthogonally oriented grain-to-grain contacts. In preliminary observations in single-bead-layer flow cells, we observed that the flow tended to locally reorient itself to be orthogonal to grain-to-grain contacts, even if these were off-angle with respect to the overall flow. We suspected that colloid behavior with respect to these orthogonally oriented grain-to-grain contacts would differ from the funneling and retention in low flow or hydrodynamically isolated zones hypothesized for grain-to-grain contacts (Tong et al., 2008, Torkzaban et al., 2007). The second study, presented here, explored the nature of colloid retention in porous media in the presence of an energy barrier to deposition. Previous work has consistently demonstrated higher colloid retention rates in porous media vs. impinging jet or parallel plate models under similar conditions, suggesting that retention in porous media is a function not only of the chemical conditions but also the hydrodynamic environment, which is governed by the pore topography.

MATERIALS AND METHODS

Fluorescent colloids and carrying solution. Colloids consisted of 4.7-µm-diameter fluoresbrite carboxylate-coated latex microspheres, with excitation and emission maxima at 441 and 486 nm, respectively, and a diameter coefficient of variation of 7% (Polysciences Inc., Warrington, PA). Colloid suspensions were created by adding stock suspension to 10 mmol L^{-1} KCl electrolyte solution (pH ~10). Both

the electrolyte solution and colloid suspensions were de-aired by vacuum before use.

Micromodels. The micromodels consisted of chambers molded from polydimethylsiloxane that were open at the top and had two spherical silver-dyed glass beads (Corpuscular Inc., Cold Spring, NY), approximately 1 mm in diameter (sphericity ³95%), embedded into the side walls of the chamber in various configurations (Fig. 2.1). In the experiments presented here, the bead orientations were orthogonal (the line connecting bead centers was perpendicular to the long axis of the chamber) and offset. In a given glass bead pair, the beads were not exactly the same size and the bead centers were not always at the same height. We determined the actual bead diameters and center heights for each micromodel by direct measurement and the relative locations of colloid reflections, respectively. A standard glass microscope slide (1 mm thick) placed on top of each micromodel and held in place by clips to seal the chamber served as our viewing window and allowed the chamber to be saturated during flow experiments.

Flow and imaging system. Micromodels were placed horizontally on the stage of an Axiostar epifluorescence microscope (Carl Zeiss, Jena, Germany) fitted with a cGFP filter set (Chroma Technology Corp., Rockingham, VT) (Fig. 2.1). Micromodels were connected to an upstream syringe pump (74900 series, Cole Parmer, Vernon Hills, IL) via 0.5-mm-i.d. Teflon tubing. For the orthogonal bead pair study, flow rates ranged between 138 and 1110 µL h^{-1}, corresponding to linear velocities in the open micromodel chambers of approximately 2.1 to 16.7 m d^{-1}. For the colloid retention study, the flow rate was 882 µL h^{-1}, corresponding to a linear velocity in the open micromodel chamber of 8.3 m d^{-1}. Based on our bead and chamber dimensions, we chose to use a 5× Plan Achromat objective, intended for air, and a standard 0.17-mm-thick glass cover slip. A combination of ultraviolet and bright-field illumination enabled simultaneous visualization of colloids and the microchamber beads. The ultraviolet light source was a 100-W mercury lamp (Osram, Danvers, MA) housed in

an HB 103W/2 lamp housing and powered by an ebq100 isolated power supply (Carl Zeiss, Jena, Germany). A red filter was placed over the bright-field light source to increase the color contrast between colloids and the background. High-definition (1960 by 1080 pixels) digital movies were captured at 29 frames s^{-1} with a consumer video camera (HDR-SR7 or HDR-SR11, Sony Corp., Tokyo) attached to the microscope with a C-mount adaptor.

Experimental procedure. Micromodels were prepared by first introducing a 95% ethanol solution to prevent retention of air bubbles in the chamber. To ensure complete displacement of the ethanol solution, at least 100 pore volumes of de-aired electrolyte solution (10 mmol L^{-1} KCl) were passed through the chamber before introduction of the colloid suspension. On occasion, if air bubbles formed within the chamber, the 95% ethanol was again introduced into the system at high flow rates to remove the bubbles and displaced by at least 100 pore volumes of de-aired electrolyte solution before reintroducing a colloid suspension.

Videos were transferred at full resolution to a personal computer before being analyzed. Video frames were time stamped and rendered to individual images, and individual colloid trajectories were generated using custom, semiautomated programs developed in Matlab version 14 (The Mathworks, Natick, MA). When building trajectories, frames were dropped to reduce the number of images to be processed to between 30 and 60.

THREE-DIMENSIONAL TRACKING: THEORY AND PERFORMANCE

Theory. A fluorescent colloid located on the objective's focal plane acts as a point light source and appears to the viewer as a slightly fuzzy point of light known commonly as an Airy disk. The fuzziness is due to the presence of tiny diffraction rings surrounding the main image. These diffraction rings are more visible for colloids not on the focal plane, i.e., out-of-focus colloids, giving the object the appearance of having a larger diameter. In addition to the apparent diameter of

diffraction rings (Olsen and Adrian, 2000, Wu et al., 2005), the diffraction pattern and image intensity (Speidel et al., 2003, Luo et al., 2006) change predictably with the distance of the object from the focal plane.

Our three-dimensional tracking method, similar to that proposed by Wu et al. (2005), exploits the relationship between the apparent image diameter (AD), and the distance (z) of the colloid relative to the focal plane. The theoretical AD–z relationship is summarized by the following equation by Olsen and Adrian (2000):

$$\mathrm{AD} = \left[M^2 d_\mathrm{p}^2 + 5.95(M+1)^2 \lambda^2 f^{\#2} + \frac{M^2 z^2 D_\mathrm{a}^2}{(s_\mathrm{o}+z)^2} \right]^{1/2} \quad (1)$$

where M is the magnification, d_p is the particle diameter, λ is the wavelength of light emitted by the colloid, *f*# is the focal number of the lens (the *f* number is the ratio of the focal length to the diameter of the aperture), s_o is the distance from the focal plane to the objective lens, D_a is the lens aperture, and z is the distance of the colloid from the focal plane. In most microscopic systems $s_\mathrm{o} >> z$, and the $(s_\mathrm{o} + z)^2$ term can be approximated by s_o^2. The resulting relationship between AD and z takes the form of a hyperbolic equation (Fig. 2A):

$$\mathrm{AD} \propto \left(y + xz^2 \right)^{1/2} \text{ or } z = \left(\frac{\mathrm{AD}^2 - y}{x} \right)^{1/2} \quad (2)$$

Note that both Eq. (1) and (2) are symmetric about the focal plane and thus make no distinction between colloids below or above the focal plane.

Generating apparent image diameter–distance calibrations. Since d_p, λ, *f*#, D_a, and s_o are constant and measurable, the dependence of AD on z, or conversely, the estimation of z as a function of AD, should be calculable a priori. In practice, however, estimates of z based on Eq. (1) and our system parameters did not always yield the best fit to the data, probably due to difficulties in calculating M, which included the unindexed zoom of the camera. Yet our data did exhibit the expected hyperbolic relationship, suggesting that the basic form of the correlation equation

(Eq. (2)) was correct. Using *x* and *y* from Eq. (2) as fitting parameters, we were able to generate a reasonably good fit to the data (R^2 > 0.95), however, parameters optimized for a given experiment did not always yield the same goodness-of-fit for different experiments run under slightly different conditions. Consequently, each experiment required its own parameter fitting, i.e., calibration.

Calibrating AD with *z* involved generating independent measurements of AD and *z* for a subset of colloids (the training set) and then fitting a calibration equation to the correlated data. The training set comprised at least 100 colloid-reflection pairs that were selected to provide an even distribution of colloid heights. Apparent image diameters were semiautomatically measured using custom image analysis programs developed in Matlab. The procedure involved isolating the images of individual colloids, thresholding to define the colloid edge, and manually delineating the location of the colloid center in the *x* axis and the edges of the colloid image in the *y* axis to calculate AD. As illustrated in Fig. 2.3, an individual colloid was followed across a series of images, enabling individual images to be seen in the context of its trajectory, which significantly improved the consistency of AD measurements. Errors in AD measurements were avoided when colloid images overlapped or when colloid edges appeared excessively "jagged," and it was difficult to accurately delineate the colloid edges.

Due to difficulties in obtaining direct measurements of *z*, the *z* values for the training set were estimated by geometric analysis of the *x*–*y* location of colloids and their reflections on the glass beads. The procedure for generating reflection-based *z* estimates is described in detail in supplemental information (Supplemental Document 1, Description of Reflection Method). While some error in the *z* estimates can be expected due to the imperfect sphericity of the beads and difficulties in pinpointing the true centers of the reflections, this method yielded the best available *z* estimates.

Although theory, as described by Eq. (1), predicts symmetry of the AD–*z* relationship about the focal plane, we frequently observed asymmetry in this relationship whereby the general shape of the AD–*z* relationship was similar above and below the focal plane but the slopes were clearly different. In such cases, we simultaneously fit two separate calibration equations of the form given by Eq. (2) to the training set data above and below the focal plane using the same value for *y* and different values for *x* (Fig. 2.2A). Similar asymmetry has been reported elsewhere and was attributed to the dominant influence of spherical aberrations in the lens system below the focal plane (Wu et al., 2005).

Performance of apparent image diameter based distance estimates. To assess the performance of the AD-based *z* estimates, we analyzed differences in the trajectories of colloids generated based on AD with those based on bead reflection, which we considered to be the best available proxy for direct measurements. The data for these comparisons consisted of a test set of 200 colloids drawn from the same experiment used to generate the training set to correlate AD with *z*.

The trajectories presented in Fig. 2.2B, typical of our current system, give a qualitative indication of the degree of similarity between bead-reflection-based and AD-based *z* estimates. Although fits were, in general, consistent, there were notable discrepancies at the beginnings and ends of the trajectories, especially obvious in trajectories for Particles 3 and 94 (Fig 3B). In most cases, this was the result of underestimations of AD for colloids near the edge of the field of view, where images were distorted by camera lens curvature. In the case of trajectory no. 3, discrepancies were greatest near the center of the field of view due to overestimation of AD where the colloid and reflection images overlapped as the colloid passed near the bead surface, making accurate delineation of the colloid edges difficult.

The residual histogram (Fig 3C), along with basic descriptive statistics, provides a more quantitative comparison of the AD and bead-reflection methods. The standard

deviation of the difference in AD- and bead-reflection-based *z* estimates was 50 μm (R^2 = 0.979) if data for all the colloids was used, and 34 μm (R^2 = 0.986) if only data for the colloids in the center 2000 μm of the field of view were used, indicating the significant impact of lens curvature near the edge of the field of view.

Relative to the range across which *z* values were estimated (−350 to 850 μm), the ~34-μm error, equivalent to approximately seven colloid diameters, was small. It is important to recognize, however, that many of the phenomena of interest to colloid researchers, such as capture in the secondary energy minimum, occur at separation distances <100 nm, significantly below the measurement error of the system presented here. The requisite axial resolution to study these phenomena may be achieved by increasing the magnification, but at the cost of the range and field of view. For example, Speidel et al. (2003) reported <5-nm precision tracking 261-nm particles at 100× magnification but only across a range of 3.5 μm and a 40- by 60-μm field of view. Thus, the optimal magnification for a given experiment will be depend on the scale of the phenomenon being studied and result from balancing requirements for axial precision, range, and field of view.

Improvements. In addition to increasing system magnification, there are several ways in which the resolution of the current system can be improved. First, the accuracy of AD measurements could be improved by optimizing the equipment along the optical chain. The glass slide viewing window could be replaced with a cover slip for which the objective was designed. The use of a higher quality objective and research-grade camera would also improve the quality of the captured images. Second, the experimental conditions could be optimized to ensure better AD measurements. Lowering colloid concentrations would decrease the incidence of overlapping images. Correct centering of the region of interest within the field of view would limit the need to use data from the edges of the field of view, which are subject to lens distortion. Third, the accuracy of AD–*z* calibrations could be improved by having more precise measurements of *z*. This could be accomplished by placing a

calibration scale with particles at known heights within the micromodels. Alternatively, to improve *z* estimates, it may be possible to use other image properties such as the diffraction pattern or intensity, as proposed by Speidel et al. (2003) and Luo et al. (2006), which also vary predictably with the distance of the object to the focal plane.

COLLOID TRANSPORT STUDIES

"Zone of Avoidance" Surrounding Grain Contacts

Grain-to-grain contacts have received much attention recently as ubiquitous features of granular porous media with potential relevance to both solute (Cardenas, 2008) and colloid transport (Johnson et al., 2007b, Torkzaban et al., 2007). In the context of colloid transport, this interest is largely motivated by observations of colloid accumulation at grain-to-grain contacts (G2Gs) in the presence of an energy barrier to deposition (Li et al., 2006, Yoon et al., 2006, Kuznar and Elimelech, 2007, Tong et al., 2008). This accumulation is hypothesized to be the result of either wedging or retention in low-flow zones (Johnson et al., 2007a) or deposition in hydrodynamically isolated regions surrounding the grain-to-grain contact point (Torkzaban et al., 2007). Hydrodynamically isolated regions have been theoretically demonstrated in models of flow around a pair of touching beads oriented such that the line connecting the bead centers is aligned with the flow (referred to subsequently as a *parallel orientation*) (Torkzaban et al., 2007, Cardenas, 2008) but not for other orientations of bead pairs or in more complex pore systems consisting of multiple beads. As illustrated by the dense cubic packing model used by Johnson et al. (2007a), in more complex granular packings, not all G2Gs are parallel (pG2G), but may be orthogonal (oG2G) or oblique (obG2G) with respect to the overall direction of flow. Based on our observations in single-layer bead packing models that flow tends to reorient itself to be orthogonal with respect to G2Gs and the current deficiencies in theory regarding colloid behavior in relation

to non-parallel G2Gs, as a first step, we set out to directly observe the behavior of colloids as they passed through a simplified pore system consisting of a pair of orthogonally oriented glass beads. Specifically, we were interested in if and in what manner colloids would accumulate in the vicinity of the oG2G and if we would observe a hydrodynamically isolated region surrounding oG2Gs analogous to that predicted for pG2Gs.

We observed the passage of approximately 10,000 4.7-µm colloids through pore constrictions created by orthogonal bead pairs at superficial velocities ranging between 2.1 and 16.7 m d^{-1} (Supplemental Video 1 (wmv): Passage of 4.7-µm fluorescent colloids at ~6.1 m d^{-1} between a 1-mm glass bead pair with the grain-to-grain contact oriented orthogonal to the direction of flow (oG2G)). Experimental conditions (ionic strength of 10 mmol L^{-1}, pH ~10) were considered to be unfavorable for colloid deposition in the primary minimum in this system. We did observe retention (~1%) of some colloids on the bead surfaces away from the G2Gs during the experiments, although we did not determine the nature of this attachment. After examining ~10,000 colloids, we noted that a certain volume of space surrounding the oG2Gs seemed to be "avoided" by the colloids. This observation was substantiated by the generation of three-dimensional trajectories of colloids passing between the glass bead pairs. As illustrated by the trajectory ensemble from a typical experiment, the path of almost all colloids arced either upward or downward as they encountered the bead pair, including those that appeared to be headed toward the G2G (Fig. 2.4B and 2.4C). The outline of the avoided zone created when the trajectories are collapsed into two dimensions (*x* and *z*) is approximately elliptical, with the major axis aligned to the direction of flow, and with major and minor diameters of approximately 750 and 450 µm (Fig. 2.4A).

Given that it is impossible to unambiguously determine whether or not colloids ever enter the "avoided" region near oG2Gs, we recognize that the use of the term *avoided zone* is presumptuous. We use this term, however, rather than *stagnation*

zone or *low-velocity zone*, which define the region in terms of its hydrodynamic properties, to focus on the zone's potential impact on colloid transport. It is probable that this region is a natural feature of the flow field that is visited, but only infrequently. Looking at the trajectories of colloids passing nearest the oG2G in Fig. 2.4A, we note that the streamlines of colloids passing above and below the oG2G originate from similar locations upstream. Streamlines which lead to the avoided zone, then, must originate in the space between these streamlines.

We did observe a colloid within the avoided region in one instance. This colloid may have settled into the avoided region after flow had been stopped for a period of approximately 1 h. When flow was resumed, the colloid remained in this region and did not appear to move (Fig. 2.5, Supplemental Video 1), even when the flow rate was increased by 500×. The stationary colloid was approximately 275 μm from the G2G and ~80 and 60 μm from the nearest bead surfaces, ruling out the possibility of the colloid being held in place by short-range chemical interaction with the bead surfaces. The existence of a stationary colloid suggests two possibilities regarding the hydrodynamic environment in the avoided region: (i) the entire region may be hydrodynamically isolated and experience zero flux, or (ii) the region may be hydrodynamically connected and thus experience some flux, but the colloid happened to be located at a stagnation point. If the region does experience flux, it seems reasonable that flux would be very low, meaning that the region is fed by only a very small portion of the upstream stream tube. Thus, only colloids traveling on that portion of the stream tube would be carried into the region. If the region is hydrodynamically isolated and does not experience any flux, colloids may enter only via mechanisms such as diffusion and settling.

The case for oG2Gs appears to differ markedly from that of pG2Gs, for which it is proposed that colloids captured in the secondary energy minimum, regardless of their initial capture location, are translated along the bead surface (Spielman and Cukor, 1973) to the vicinity of the pG2G because all near-surface streamlines lead

toward the rear of the bead. Once the colloids are brought near the G2G, they can become wedged or retained in low-flow zones (Johnson et al., 2007a) or deposited in hydrodynamically isolated regions (Torkzaban et al., 2007). In contrast, since only a very small portion of near-surface streamlines passes near oG2Gs, only those colloids captured in a very limited initial area have the potential of being translated to an oG2G.

There is naturally some concern whether the colloid behavior observed here is not simply an artifact of the isolated bead pair micromodel. Certainly, with the presence of other grains, the pores in continuous media would be smaller than in these models, which could impact the size and shape of the low-flow and avoided zones. In addition, in more complex media, the distinction between parallel, orthogonal, and oblique G2G orientations would be less clear because there are likely to be multiple stream tubes feeding and exiting G2Gs at different angles. Thus, a G2G might be simultaneously parallel with respect to one stream tube and orthogonal with respect to another, and colloids may be funneled to the G2G from one direction but not another. Furthermore, the convergence of stream tubes near G2Gs in complex packings may also reduce the size of low-flow zones, and hence the avoided zones.

Given these and other potential differences with “real” media, the scope of inference of the results presented here for the isolated bead pair model is limited. The result do suggest that G2Gs with primarily orthogonal orientation may represent zones of avoidance and, as such, may be poor candidates for retention, particularly of large (low diffusion coefficient) colloids, while those with more parallel characteristics may serve as retention regions. Further theoretical and experimental investigation is necessary to elucidate the mechanisms of avoidance and the relative importance (or insignificance) of such zones to transport of colloids in porous media.

Deposition of Colloids under Unfavorable Chemical Conditions

The (partially) reversible, ionic-strength-dependent retention of colloids in porous media under chemical conditions unfavorable to deposition in the primary energy minimum is often attributed to the attachment of colloids in the secondary minimum (e.g., McDowell-Boyer, 1992, Hahn et al., 2004, Tufenkji and Elimelech, 2005). Because analogous reversible retention is not observed in impinging jet or parallel plate studies under similar chemical and flow conditions (e.g., Redman et al., 2004, Johnson and Tong, 2006), however, researchers have concluded that retention in porous media results from a coupling of secondary energy minimum attachment with local hydrodynamic conditions that are a function of the local pore geometry (Johnson et al., 2007a, Torkzaban et al., 2008). Given the current interest in the contribution of pore topography and local hydrodynamic factors to colloid retention under unfavorable chemical conditions, we present a trajectory analysis of eight colloids that "attached" to glass beads in an oblique bead pair micromodel at low ionic strength and moderate flow rates to explore the nature of such retention. The isolated bead pair model used here lacked rear G2Gs, which have previously been implicated as potential locations for the retention of secondary-minimum-captured colloids (Tong et al., 2008, Torkzaban et al., 2008), but rather presented exposed rear stagnation points.

We observed approximately 350 colloids (4.7-μm diameter, carboxylate coated) passing through an oblique bead pair micromodel during a 14-min time period (Supplemental Video 2: Passage and retention of 4.7-mm fluorescent colloids at ~4.4 m d^{-1} between 1-mm glass bead pair with the G2G oriented obtusely to the direction of flow). The experimental conditions (10 mmol L^{-1} ionic strength, pH ~10, open chamber velocity ~8.3 m d^{-1}) were considered to be unfavorable to colloid deposition in the primary energy minimum. Although we did not directly measure colloid–bead interactions under these conditions, we assumed, based on published estimates for similar colloid, collector, and solution chemical parameters (Kuznar

and Elimelech, 2007), that a secondary energy minimum with an approximate depth of −5 kT was manifested at approximately 30 nm from the bead surface. During the experiment, we observed eight colloids (~2%) attach to the upper surfaces of the two beads. These attachment rates are notably higher than expected, considering that the single-collector transport efficiency based solely on interception is on the order of 3.7×10^{-5} (Yao et al., 1971).

The three-dimensional colloid trajectories suggested that the colloids traveled close to the bead surface for some distance before attaching (Fig. 2.6), however, given the large error in *z* estimates, we were not able to accurately evaluate the colloid–bead separation distance. The velocity profiles also indicated a relatively close approach of colloids to the bead surface as they passed over the beads, with velocity magnitudes generally falling to below 30 μm s^{-1}, less than 25% of the mean velocity (~118 μm s^{-1}) of all colloids as they crossed the bead-to-bead axis line (Fig. 2.7A and 2.7B). Colloid velocities either remained steady or declined slightly between the forward stagnation point and the bead meridian (see $0 < L/L_{max} < 0.5$ on abscissa of Fig. 2.7A and 2.7B, where L/Lmax is the normalized distance from the forward stagnation point). A sharper decline in velocities with respect to L/L_{max} was observed starting, in most cases, near the bead meridian, followed by a low-velocity (<3 μm s^{-1}) plateau before the colloids came to rest. Two exceptions were Particle 78, whose velocity began declining significantly before the bead meridian (~0.3 L/L_{max}) and reached a plateau (~2 μm s^{-1}) at ~0.41 L/L_{max} before falling to zero at ~0.59 L/L_{max}, and Particle 189, whose velocity appeared to decline steadily after the first observation point (0.15 L/L_{max}) before coming to rest at ~0.76 L/L_{max}. The decline in velocities past the bead meridian indicates that the colloids continuously shifted to slower streamlines as they were transported rearward. Had the colloids continued to follow their original streamlines, the velocities should have changed approximately in mirror image to the change before the bead midpoint. All of the retained colloids eventually came to rest somewhere between 0.50 and 0.85 L/L_{max}

of the respective beads. Three of the seven “attached” (Particles 188, 189, and 190) colloids were re-entrained following a 10-fold increase in the flow rate, while a fourth colloid (Particle 78) was re-entrained after a subsequent fivefold increase of the flow rate (Fig. 2.6A).

In exploring potential retention mechanisms, we considered two aspects of our observations: (i) apparent streamline crossing, i.e., “retention” of colloids at or near the bead surface after the bead meridian, and (ii) reversible or irreversible deposition before the rear stagnation point. These aspects correspond to the transport and attachments steps presented in classic filtration theory.

Streamline crossing. Classic filtration theory provides for three ways in which colloids are transported to a collector surface: diffusion, interception, and sedimentation. Interception is not a likely candidate here because it would have resulted in colloid contact with (and attachment to) a spherical collector either before or at the bead meridian. Diffusion also seems an unlikely candidate, given the predicted low diffusivity (~1×10^{-13} m^2 s^{-1}) of the colloids. It is highly improbable that random thermal movements would cause the colloids to continuously stray across streamlines in a given direction, i.e., toward the bead surface. Such directional shifting suggests the involvement of an attractive interaction between the colloid and the surface.

In the presence of fluid shear, colloids associated with a collector surface via the secondary energy minimum are observed, consistent with theoretical predictions, to translate across flat surfaces while maintaining a set distance from those surfaces (Johnson and Tong, 2006, Nazemifard and Bhattacharjee, 2006, de Kerchove et al., 2007, Kline et al., 2008, Liu et al., 2009). In expanding pore sections (as would be the case for the rear half of the glass beads in our micromodel), colloids “captured” in the secondary minimum would be expected to follow the surface topography rather than follow their original streamlines as these bend away from the surface, provided that the colloid–surface attraction is stronger than advective forces that would

otherwise keep the colloids on their original streamlines. Such colloids would appear to continuously cross to slower streamlines to maintain their distance from the collector surface.

Our observations may also be explained by mechanisms other than secondary minimum capture. Duffadar and Davis (2007, 2008) proposed that the presence of attractive nano-domains on an otherwise repulsive surface can result in ionic-strength-dependent reversible attachment and lateral rolling or skipping (analogous to "translation") in the presence of fluid shear similar to that predicted for secondary minimum retention. An important difference between this model and secondary energy minimum capture lies in the fact that colloids are predicted to be in direct contact with the collector surface, bringing into play frictional and adhesive forces that could oppose lateral movement. Again, the error of our *z* estimates was too large to be able to distinguish between colloids held in a secondary energy minimum at a distance from the surface (~30 nm) or in direct contact with the surface.

It is also possible that the observed streamline crossing of colloids was simply due to the colloids settling as they moved rearward, given the estimated Stoke's settling velocity of the colloids (~35 μm min^{-1}) and the time (~2 –10 min) between passing the bead meridian and coming to rest. The downsloping bead surface under the colloids as they move rearward presents a continuously falling "target" surface onto which the colloids can settle. The rates of bead surface change (drop) as a function of colloid location and velocity were in the 20 to 50 μm s^{-1} range for seven of the eight colloids, similar to the estimated Stoke's settling velocity, the exception being Particle 191, for which the bead surface drop was >125 μm s^{-1} for the majority of its trajectory. Thus, we cannot discount sedimentation as an explanation for the observed streamline crossing after the bead meridian.

Attachment location and re-entrainment. All of the deposited colloids came to rest before the rear stagnation point, where the velocities of the near-surface fluid

were presumably non-zero. With the possible exception of Particle 191, which arrested near the rear stagnation point, the observed attachment locations are inconsistent with secondary minimum capture because there is no resistive component to the secondary minimum attachment that would oppose the translation of captured colloids in the presence of shear (Redman et al., 2004), and colloids would be predicted to continue moving until there is no longer shear (i.e., at the rear stagnation points of the glass beads in our micromodel). While some researchers suggest that there may be a resistive component to secondary energy minimum attraction analogous to the rolling resistance experienced by colloids attached in the primary minimum (Torkzaban et al., 2007), there is, as yet, no hypothesized mechanism to account for this force. The fact that reversible deposition of secondary minimum-captured colloids is not observed in impinging jet experiments (e.g., Redman et al., 2004, Johnson and Tong, 2006, de Kerchove et al., 2007) supports the conventional view that there is no significant resistive component associated with secondary energy minimum attraction.

In contrast, the attractive nano-domain model accounts for resistance to lateral translation via frictional forces related to the physical contact of colloids with the surface that could result in colloid attachment where the fluid velocity is non-zero (Duffadar and Davis, 2008). The attractive nano-domain model, however, predicts that colloids will come to rest as soon as advective forces (fluid shear) balance the resistive forces and, by extension, that the colloids should be easily re-entrained with even a slight increase in the flow rate. The fact that our colloids either were not re-entrained or re-entrained only after significant increases in the flow rate indicates that the colloid–surface attraction was of much greater magnitude than the fluid shear experienced at the time of attachment and, furthermore, that the attachment location was either unrelated to the local shear or related to shear but not simply by the balancing of resistive and advective forces.

Neither secondary minimum capture nor the attractive nano-domain model adequately explains the observed colloid attachment locations and the apparent discrepancy in local shear and attachment energies. Here, we briefly consider other attachment scenarios in the context of these two models as mechanisms of near-surface transport. To begin, it is useful to make explicit assumptions regarding the heterogeneity of the bead surfaces, namely, that (i) the surface comprised patches that were significantly more favorable for colloid deposition than the surface in general, and (ii) these patches were randomly and evenly distributed across the surface. Such surface heterogeneity would not be unexpected for these glass beads, given that they exist even in "pure" surfaces, as evidenced by the numerous cases of irreversible deposition in impinging jet studies (e.g., Johnson and Tong, 2006).

If the colloids translated while in continuous or intermittent contact with the surface via attractive nano-domains, they may simply have come to rest when they randomly encountered local patches whose attraction was significantly greater than the surface in general (Fig 8A). In this scenario, attachment location and energy would essentially be decoupled from the local fluid shear. Alternatively, if the colloids translated at a set distance from the surface while captured in a secondary energy minimum, they may have deposited onto locally attractive surfaces after first being drawn closer to the surface (Fig. 2.8B). Colloids passing near a local attractive surface would approach the surface, but would make contact only if fluid shear did not cause the colloids to be translated beyond the influence of the locally attractive surface (Nazemifard et al. 2005). In other words, the colloids would only attach when the shear was sufficiently low to enable the colloids to contact the attractive surface before being swept past it. In this scenario, attachment energy would be significantly greater than the local shear, while attachment location would be indirectly coupled with the local fluid shear. Finally, while it is possible that settling resulted in the initial approach of colloids to the surface, it is unlikely that it would cause the colloids to deposit onto the bead surfaces because the gravitational force

would like not be sufficient to overcome the energy to primary minimum deposition. Thus, if settling played a role here, the role was to bring the colloids to the vicinity of the surface where they would be subject to translation via another mechanism such as the attractive nano-domain interaction or capture in the secondary energy minimum.

While our observations did not offer sufficient resolution to distinguish interaction with attractive nano-domains or secondary minimum capture, they did demonstrate near-surface colloid translation under chemically unfavorable conditions and suggest a potentially important role for such translation that is not currently accounted for in classic filtration theory. Nonattachment colloid–surface interaction may cause colloids to separate from fluid streamlines in favor of traveling near collector surfaces, increasing the opportunity for captured colloids to encounter and interact with local surface anomalies, which may result in reversible or irreversible deposition. Considering that surface heterogeneity is the rule rather than the exception in natural porous media, near-surface translation, in addition to leading to colloid deposition in low-flow zones (Johnson et al., 2007a, Tong et al., 2008, Torkzaban et al., 2008), may have a significant quantitative and qualitative impact on colloid retention in porous media under unfavorable conditions.

SUMMARY AND CONCLUSIONS

The pore-scale epifluorescence-based visualization method under development by our group yields three-dimensional position (*x*, *y*, and *z*) and time (*t*) data, with colloid axial position (z) being estimated based on the location of colloid reflections on glass beads of the micromodel or by exploiting the relationship between the AD of out-of-focus colloids and their distance from the focal plane. For the system presented here, the standard deviation of *z* estimates based on reflection and AD methods is on the order of 34 μm across a range of almost 1200 μm. While this error is acceptable for studying the large-scale behavior of colloids, it is inadequate for

investigating phenomena such as colloid–surface interactions, which occur at separation distances <100 nm. System resolution can be improved by increasing the magnification, improving the resolution of the optical train components, optimizing the experimental conditions, or more accurately characterizing the AD–*z* relationship.

The results from the two mini-studies presented here illustrate the utility of three-dimensional particle tracking in pore-scale studies of colloid transport. The first study used trajectory data to demonstrate an apparent "zone of avoidance" surrounding orthogonal grain-to-grain contact points. Further studies are necessary to determine the extent to which this zone is avoided and the mechanism leading to this behavior. The second study used colloid position and velocity data to investigate the potential mechanisms of retention of eight colloids on glass beads under chemically unfavorable conditions. We observed streamline crossing of colloids as they moved rearward along the beads consistent with secondary minimum capture, transient attachment to attractive nano-domains, or sedimentation. The fact that the colloids came to rest before the rear stagnation point and that attachment in some cases was irreversible was inconsistent with secondary minimum capture. The results suggest that an essential role of secondary minimum capture or attractive nano-domain interaction, in addition to funneling colloids to low-flow zones where they may be retained, is to increase the opportunity for them to encounter and interact with local surface heterogeneities.

It is reasonable to question the utility of visualization methods if they require the use of micromodels that are not adequately representative of porous media. In this regard, criticisms of the models presented here may be twofold. First, these models did not include grains upstream and downstream of the isolated bead pair, which would impact the incoming and exiting flow and the existence of low-flow zones surrounding rear grain-to-grain contacts. These issues, however, can easily be remedied by the inclusion of contextual grains in addition to those under

observation in the micromodels and are not a limitation of the visualization method per se. Perhaps the single greatest limitation of this (and other) light-based visualization methods remains the inability to look at internal pores of a porous medium. Because it is necessary to have a direct line of sight to the object being viewed, observations are limited to the surface of the medium, where colloid behavior may significantly be affected by the boundary, which in almost all cases is a flat glass surface (cover slip or slide). The glass does not simulate the topography of internal pores and may present a surface that is chemically and physically different from that of the medium grains. The ideal visualization method would enable an investigator to look through overlying media grains to internal pores. One solution may be to use media grains made of optically transparent materials such as Nafion (DuPont Fluoroproducts, Fayetteville, NC) or CYTOP (Asahi Glass Co., Tokyo) that have refractive indices similar to water (Leis et al., 2005).

The challenge of medium penetration notwithstanding, the ability to directly visualize colloid behavior in three dimensions brings experimental capabilities closer in line with those of computer simulations, setting the backdrop for paired experimental and theoretical investigations, with mutual benefit from both approaches. Particularly for the investigation of pore-scale mechanisms governing colloids, direct observation of colloid behavior can bring to light hitherto unknown phenomena as well as serve as a means to empirically validate theory, while simulations can provide information about local hydrodynamic conditions that are not measurable in experiments but are useful for interpreting the observed colloid behavior.

ACKNOWLEDGEMENTS

This research was supported by a grant from the National Research Initiative of the USDA Cooperative State Research, Education and Extension Service, Grant no.

2006-35107-17231. We thank Celeste Jones for her skilled assistance with this project.

LITERATURE CITED

Auzerais, F., J. Dunsmuir, B. Ferreol, N. Martys, J.Olson, T. Ramakrishnan, D. Rothman, and L. Schwartz. 1996. Transport in sandstone: a study based on three dimensional microtomography. Geophys. *Res. Lett*. 23:705-708.

Bradford, S.A., S. Torkzaban, and S.L. Walker. 2007. Coupling of physical and chemical mechanisms of colloid straining in saturate porous media. *Water Res*. 41:3012-3024.

Cardenas, M.B. 2008. Three-dimensional vortices in single pores and their effects on transport. *Geophys. Res. Let.* 35:L18402.

Cushing, R.S., and D.F. Lawler. 1998. Depth filtration: fundamental investigation through three-dimensional trajectory analysis. *Environ. Sci. Technol*. 32:3793-3801.

Davis, A.M.J., M.E. O'Neill, J.M. Dorrepaal, and K.B. Ranger. 1976. Separation from the surface of two equal spheres in Stokes flow. *J. Fluid Mech.* 77:625-644.

de Kerchove, A.J., P. Weronski, and M. Elimelech. 2007. Adhesion of nonmotile *Pseudomonas aeruginosa* on "soft" polyelectrolyte layer in a radial stagnation point flow system: measurements and model predictions. *Langmuir.* 23:12301-12308.

Derjaguin, B.V., and L. Landau. 1941. Theory of the stability of strongly charged lyophobic sols and of the adhesion of strongly charged particles in solutions of electrolytes. *Acta Physicochim. URSS.* 14:633-662.

Duffadar, R.D., and J.M. Davis. 2008. Interaction of micrometer-scale particles with nanotextured surfaces in shear flow. *J. Colloid and Interface Sci.* 308:20-29.

Duffadar, R.D., and J.M. Davis. 2008. Dynamic adhesion behavior of micrometer-scale particles flowing over patchy surfaces with nanoscale electrostatic heterogeneity. *J. Colloid and Interface Sci*. 326:18-27.

Elimelech, M., M. Nagai, C. Ko, and J.N. Ryan. 2000. Relative insignificance of mineral grain zeta potential to colloid transport in geochemically heterogeneous porous media. *Environ. Sci. Technol.* 34:2143-2148.

Elimelech, M., and C.R. O'Melia. 1990. Kinetics of deposition of colloidal particles in porous media. *Environ. Sci. Technol*. 24:1528-1536.

Hahn, M.W., D. Abadzic, and C.R. O'Melia. 2004. Aquasols: on the role of secondary minima. *Environ. Sci. Technol*. 38:5915-5924.

Huber, N., T. Baumann, and R. Niessner. 2000. Assessment of colloid filtration in natural porous media by filtration theory. *Environ. Sci. Technol*. 34:3774-3779.

Johnson, W.P., X. Li, and G. Yal. 2007a. Colloid retention in porous media: mechanistic confirmation of wedging and retention in zones of flow stagnation. *Environ. Sci. Technol*. 41:1279-1287.

Johnson, W.P., and M. Tong. 2006. Observed and simulated fluid drag effects on colloids deposition in the presence of an energy barrier in an impinging jet system. *Environ. Sci. technol*. 40:5015-5021.

Johnson, W.P., M. Tong, and X. Li. 2007b. On colloid retention in saturated porous media in the presence of energy barriers: the failure of α, and opportunities to predict η. *Water Res. Res*. 43:W12813.

Keller, A.A. and M. Auset. 2007. A review of visualization techniques of biocolloid transport processes at the pore scale under saturated and unsaturated conditions. *Adv. Water Res.* 30:1392-1407.

Kline, T.R., G. Chen, and S.L. Walker. 2008. Colloidal deposition on remotely controlled charged micropatterned surfaces in a parallel-plate flow chamber. *Langmuir*. 24:9381-9385.

Kuznar, A.A. and M. Elimelech. 2007. Direct microscopic observation of particle deposition in porous media: role of the secondary energy minimum. *Colloids Surf. A: Physicochem. Eng Aspects.* 294:156-162.

Leis, A.P., S. Schlicher, H. Franke, and M. Strathmann. 2005. Optically transparent porous medium for nondestructive studies of microbial biofilm architecture and transport dynamics. *Appl. Environ. Microbiol*. 71:4801-4808.

Li, X., C. Lin, J.D. Miller, and W.P. Johnson. 2006. Pore-scale observation of microsphere deposition at grain-to-grain contacts over assemblage-scale porous media domains using x-ray microtomography. *Environ. Sci. Technol*. 40:3762-3768.

Liu, Y., M.S. Janjaroen, T.B. Kuhlenschmidt, and T.H. Nguyen. 2009. Deposition of *Cryptosporidium parvum* oocysts on natural organic matter surfaces: microscopic evidence for secondary minimum deposition in a radial stagnation point flow cell. *Langmuir*. 25:1594-1605.

Luo, R., X.Y. Yang, X.F. Peng, and Y. Sun. 2006. Three-dimensional tracking of fluorescent particles applied to micro-fluidic measurements. *J. Micromech. Microeng*. 16:1689-1699.

Manz, B., F. Volke, D. Goll, and H. Horn. 2003. Measuring local flow velocities and biofilm structure in biofilm systems with magnetic resonance imaging (MRI). *Biotechnol. Bioeng*. 84:424-432.

McDowell-Boyer, L.M. 1992. Chemical mobilization of micron-sized particles in saturated porous media under steady flow conditions. *Environ Sci. Technol*. 26:586-593.

Moschakis, T., B.S. Murray, and E. Dickinson. 2006. Particle tracking using confocal microscopy to probe the microrheology in a phase-separating emulsion containing non-adsorbing polysaccharide. *Langmuir*. 22:4710-4719.

Nazemifard, N., J.H. Masliyah, and S. Bhattacharjee. 2006. Particle deposition onto micropatterned charge heterogeneous substrates: trajectory analysis. *J. Colloid Interface Sci*. 293:1-15.

Ochiai, N., E.L. Kraft, and J.S. Selker. 2006. Methods for colloid transport visualization in pore networks. *Water Res. Res*. 42:W12S06.

Olsen, M.G. and R.J. Adrian. 2000. Out of focus effects on particle image visibility and correlation in microscopic particle image velocimetry. *Expmt Fluids*. (suppl)s166-s174.

Paraskeva, C.A., V.N. Burganos, and A.C. Payatakes. 1991. three-dimensional trajectory analysis of particle deposition in constricted tubes. *Chem. Eng. Sci*. 108:23-48.

Redman, J.A., S.L. Walker, and M. Elimelech. 2004. Bacterial adhesion and transport in porous media: role of the secondary energy minimum. *Environ. Sci. Technol*. 38:1777-1785.

Schneider, G. 2003. X-ray microscopy: methods and perspectives. *Anal. Bioanal. Chem.* 376:558-561.

Smith, J., B. Gao, H. Funabashi, T.N. Tran, D. Luo, B.A. Ahner, T.S. Steenhuis, A.G. Hay, and M.T. Walter. 2008. Pore-scale quantification of colloid transport in saturated porous media. *Environ Sci. Technol*. 42:517-523.

Snyder, L.J. and W.E. Stewart. 1966. Velocity and pressure profiles for Newtonian creeping flow in regular packed beds of shapes. *AIChE J*. 12:161-173.

Speidel, M., A. Jonas, and E.L. Florin. 2003. Three-dimensional tracking of fluorescent nano-particles with subnanometer precision by use of off-focus imaging. *Optics Letters*. 28:69-71.

Spielman, L.A. and P.M. Cukor. 1973. Deposition of non-brownian particles under colloidal forces. *J. Colloid Interface Sci*. 43:51-65.

Tong, M., H. Ma, and M.P. Johnson. 2008. Funneling of flow into grain-to-grain contacts drives colloid-colloid aggregation in the presence of an energy barrier. *Environ. Sci. Technol*. 42:2826-2832.

Torkzaban, S., S.A. Bradford, and S.L. Walker. 2007. Resolving the coupled effects of hydrodynamics and DLVO forces on colloid attachment in porous media. Langmuir. 23:9652-9660.

Torkzaban, S., S.S. Tazehkand, S.L. Walker, and S.A. Bradford. 2008. Transport and fate of bacteria in porous media: coupled effects of chemical conditions and pore space geometry. *Water Res. Res*. 44:W0403.

Tufenkji, N. and M. Elimelech. 2005. Breakdown of colloid filtration theory: role of the secondary energy minimum and surface charge heterogeneities. *Langmuir*. 21:841-852.

Verwey, E.J.W. and J.T.G. Overbeek. 1948. Theory of the stability of lyophobic colloids. Elsevier, Amsterdam.

Wu, X.L. and A. Libchaber. 2000. Particle diffusion in a quasi-two-dimensional bacterial bath. Phys. Rev. Letters. 84:3017-3020.

Yao, K.M., M.T. Habibian, and C.R. O'Melia. 1971. Water and waste water filtration: concepts and applications. *Environ. Sci. Technol*. 5:1105-1112.

Yoon, J.S., J.T. Germaine, and P.J. Culligan. 2006. Visualization of particle behavior within a porous medium: mechanisms for particle filtration and retardation during downward transport. *Water Res. Res*. 42:W06417.

FIGURES

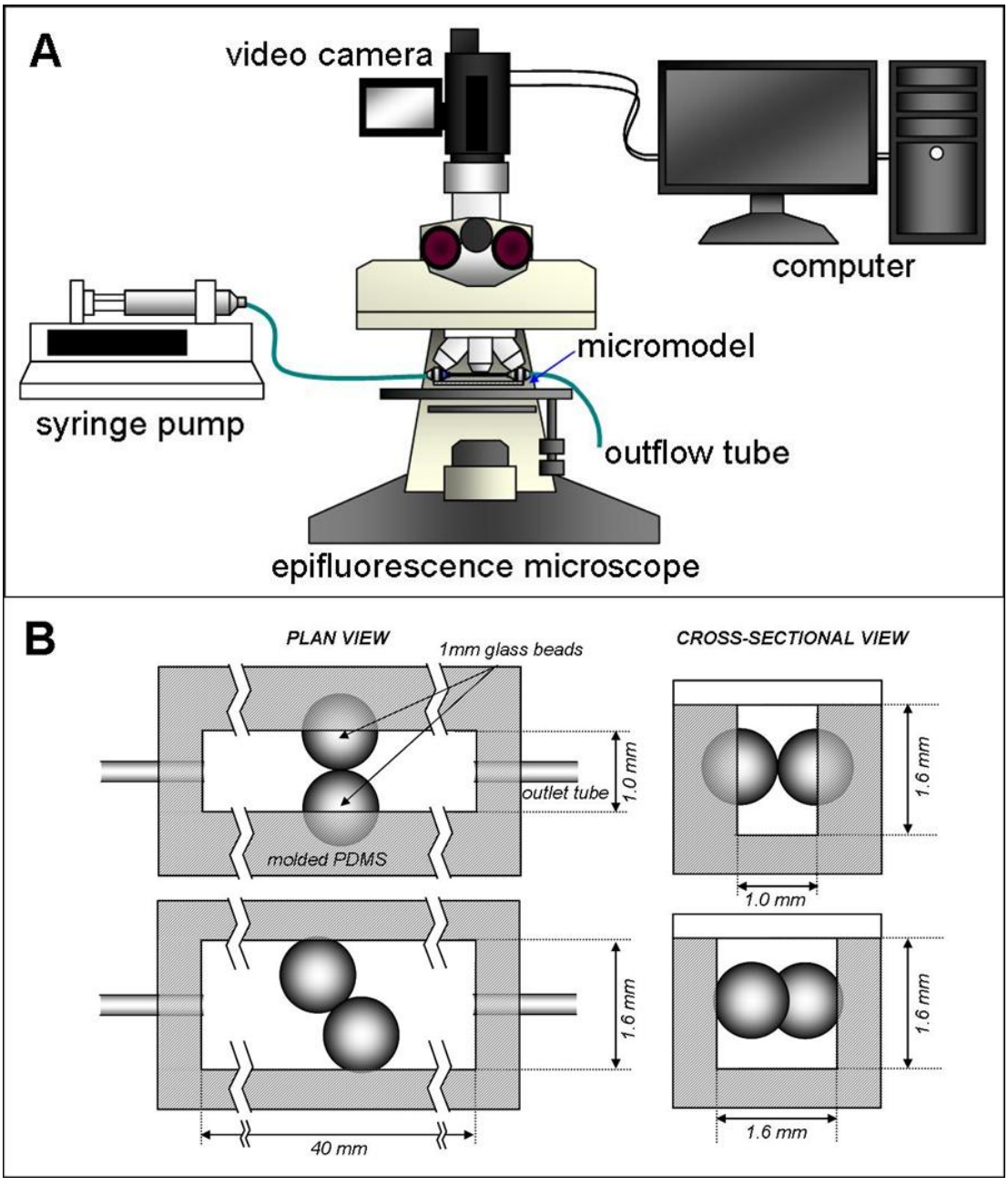

Figure 2.1. Schematic of (A) the visualization system and (B) a typical micromodel setup with a pair of touching glass beads in orthogonal and offset orientations.

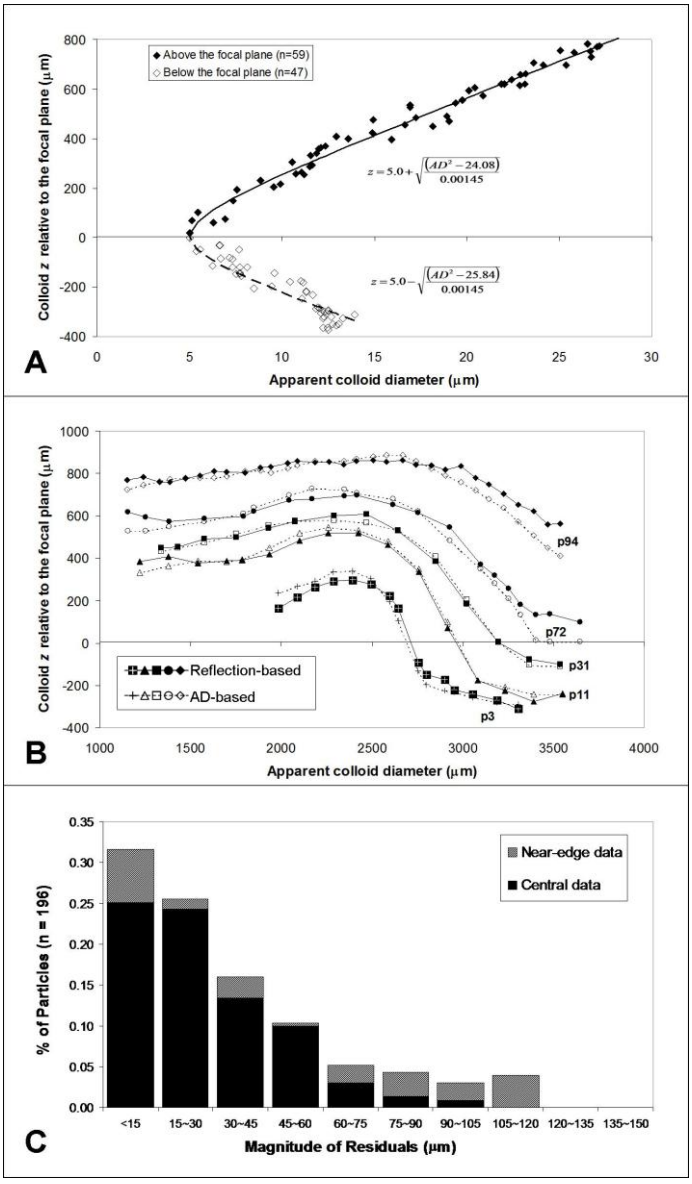

Figure 2.2. (A) Graph of apparent image diameter (AD) vs. reflection-based colloid height (*z*) estimates fo*r training* data set with best-fit correlation equations for colloids above and below the focal plane, (B) comparison of selected test trajectories using reflection-based *z* estimates (solid markers and solid lines) and the same trajectory using AD-based *z* estimates (open markers and dashed lines), and (C) histogram showing the percentage of particles in the test data set with residuals (difference in *z* estimates by reflection- and AD-based methods) falling in different magnitude ranges. Solid bars represent data for particles in the center 2000 μm of the field of view.

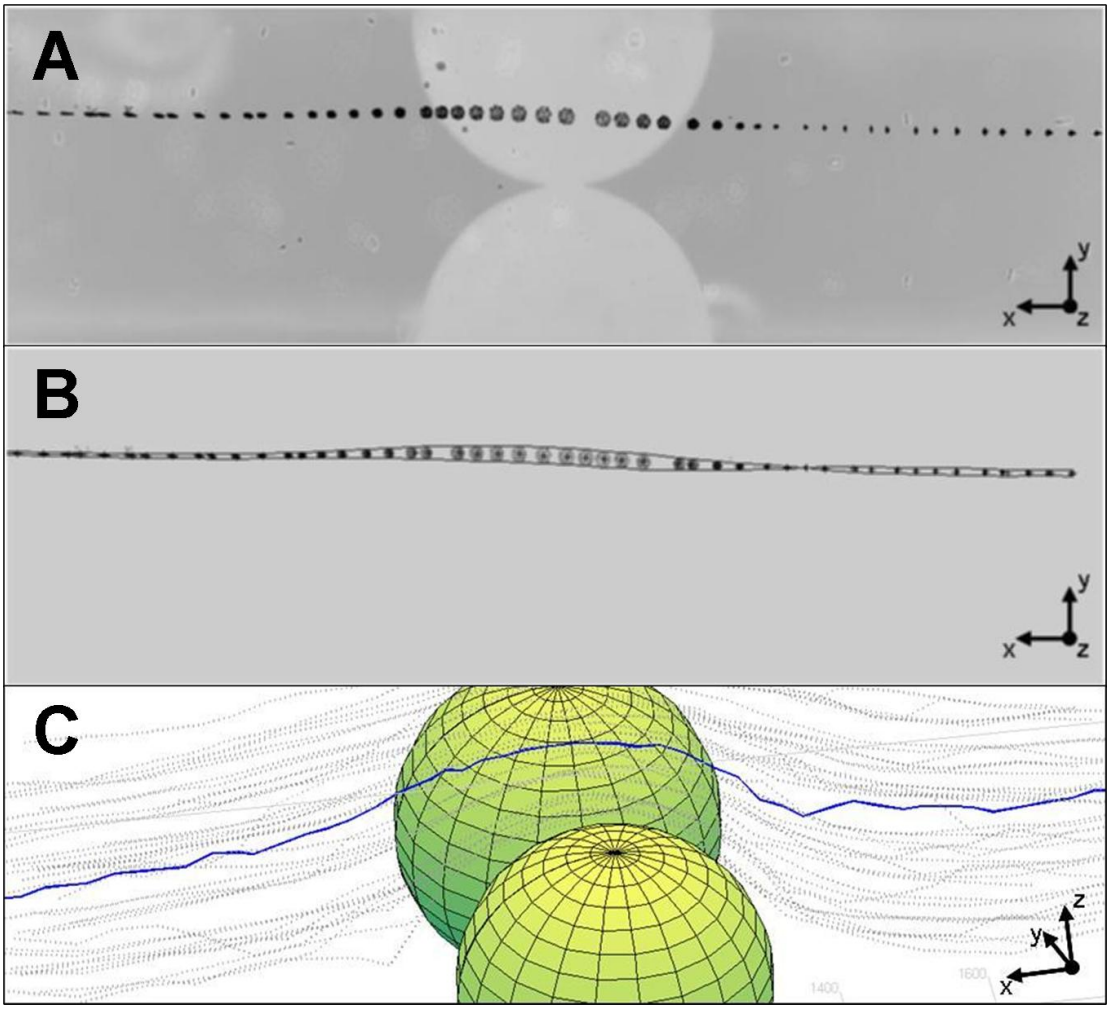

Figure 2.3. (A) Composite (negative) image of an isolated colloid trajectory, (B) with tops and bottoms of out-of-focus image edges delineated, and (C) three-dimensional trajectory using an empirical correlation equation to relate out-of-focus image diameter to colloid height (*z*).

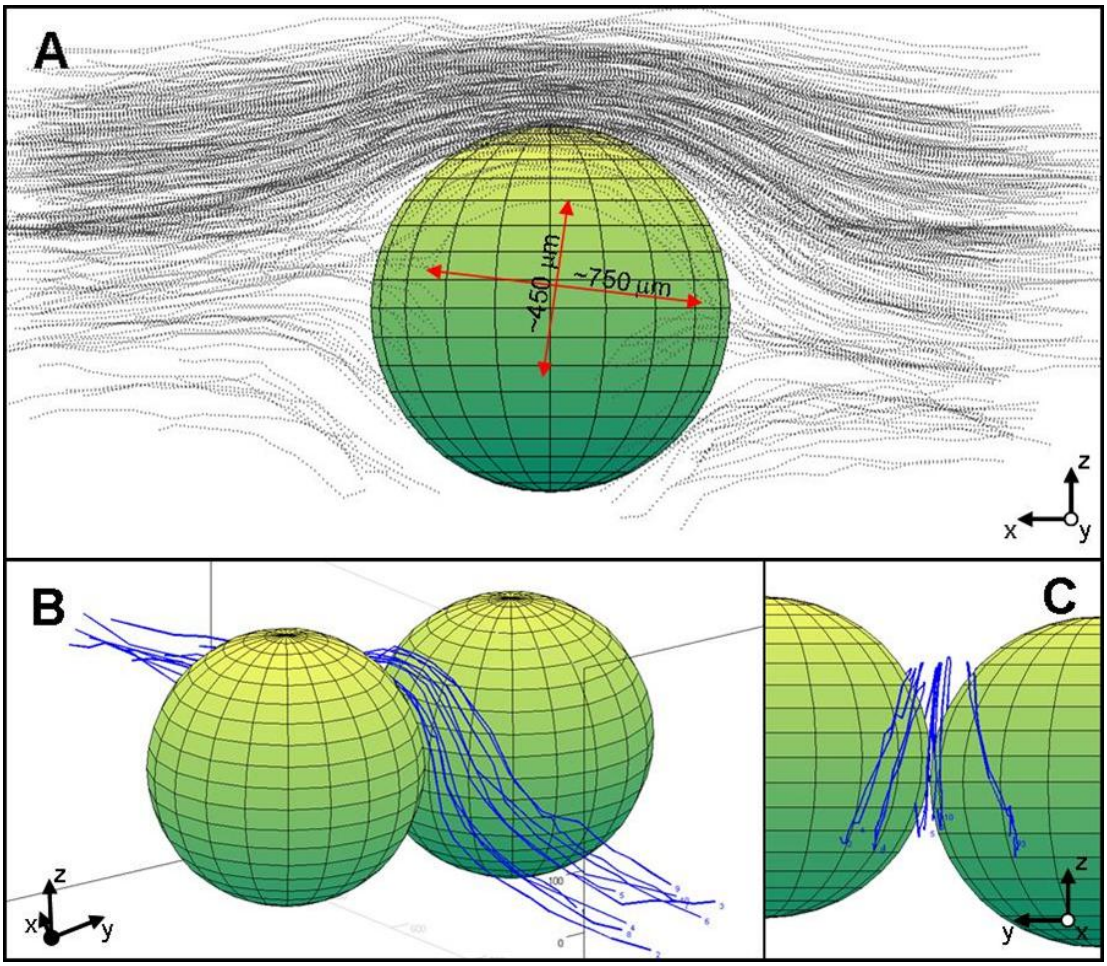

Figure 2.4. (A) Typical trajectories (*n* = 444) of colloids passing between a bead pair whose center-to-center line is orthogonal to the direction of flow (mean velocity in the open micromodel chamber ~5.7 m d^{-1}), the image of the bead closer to the viewer has been removed to permit a view of the space between beads, and only partial trajectories are available for colloids passing below the bead pair, the overlying arrows approximate the major and minor of axes of the ellipse that outlines the "avoided" zone, and (B) oblique and (C) cross-sectional views of the 10 trajectories that pass above and closest to the grain-to-grain contact.

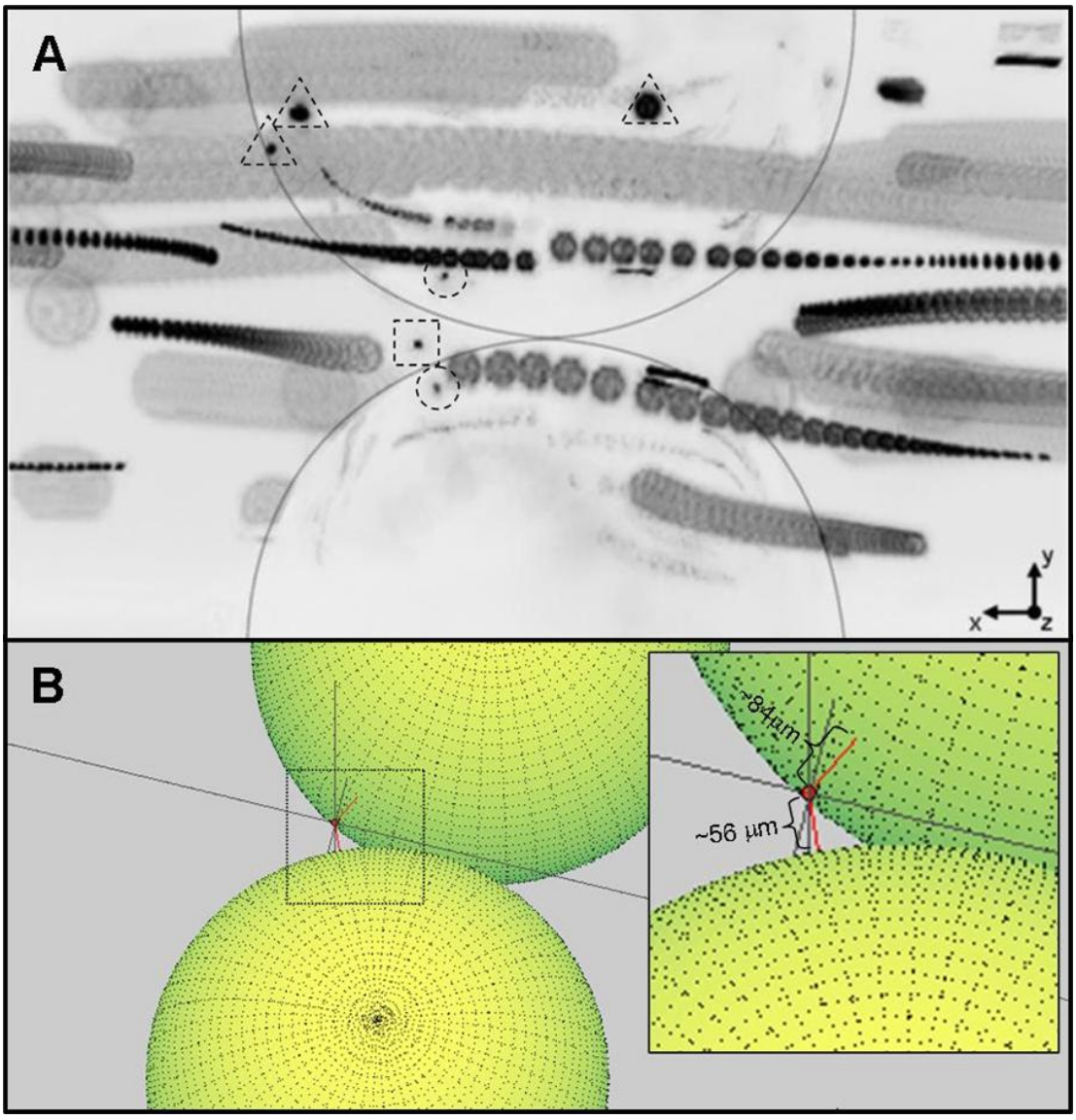

Figure 2.5. (A) Composite negative image spanning 10 s showing the lack of movement of a colloid trapped in the "avoidance" zone surrounding the orthogonal grain-to-grain contact point (the stationary colloid and its reflections on the beads are designated by the square and circles, triangles represent colloids "attached" to a glass bead), and (B) position of the stationary colloid in three-dimensional space with estimated distances to the nearest points on the glass beads.

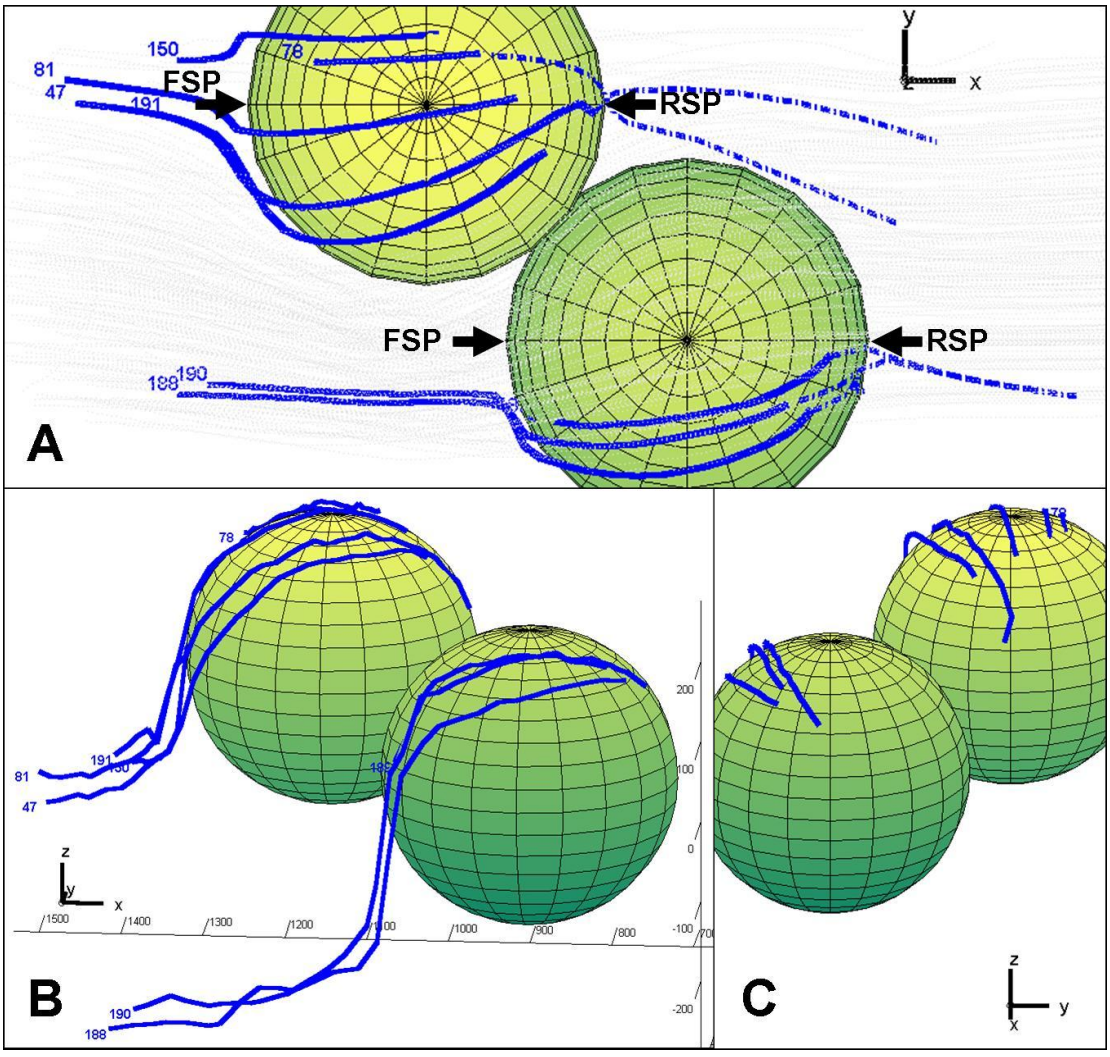

Figure 2.6. Trajectories of seven colloids that attached to the beads in the offset glass bead pair micromodel: (A) plan, (B) transverse, and (C) cross-sectional views. The arrows in (A) indicate the forward (FSP) and rear stagnation points (RSP) used to calculate the normalized location of colloids along the bead surface. The normalized distance from the FSP (L/L_{max}) is the ratio of the distance of the colloid projection onto the bead surface to the FSP (L) and half the bead perimeter (L_{max}). Dashed lines represent trajectories of reentrained colloids.

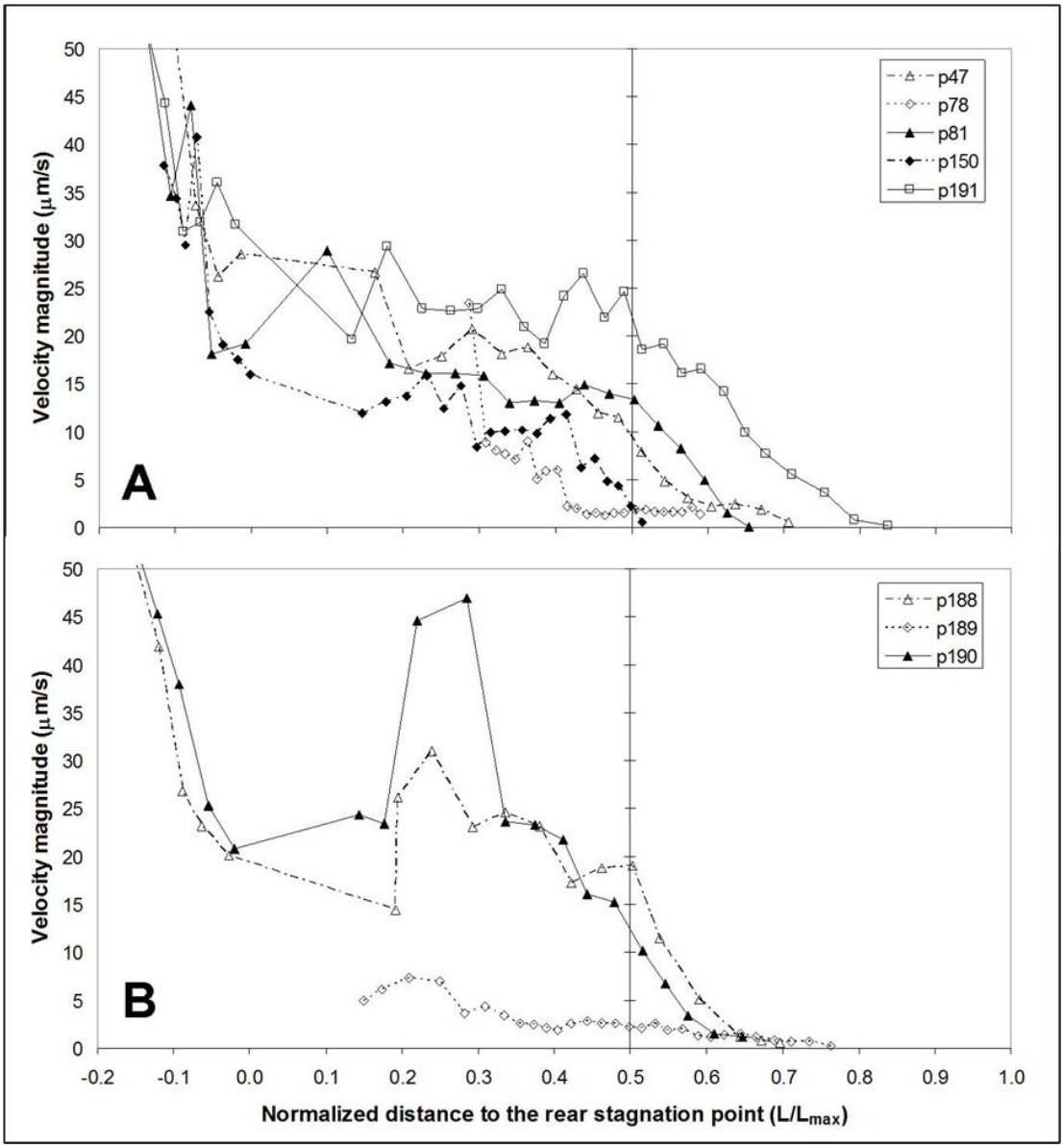

Figure 2.7. Velocity profiles of the seven colloids that attached to the beads in the offset glass bead pair micromodel (Fig. 2.6), with respect to normalized distance from the forward stagnation point (L/L_{max}) along the bead.

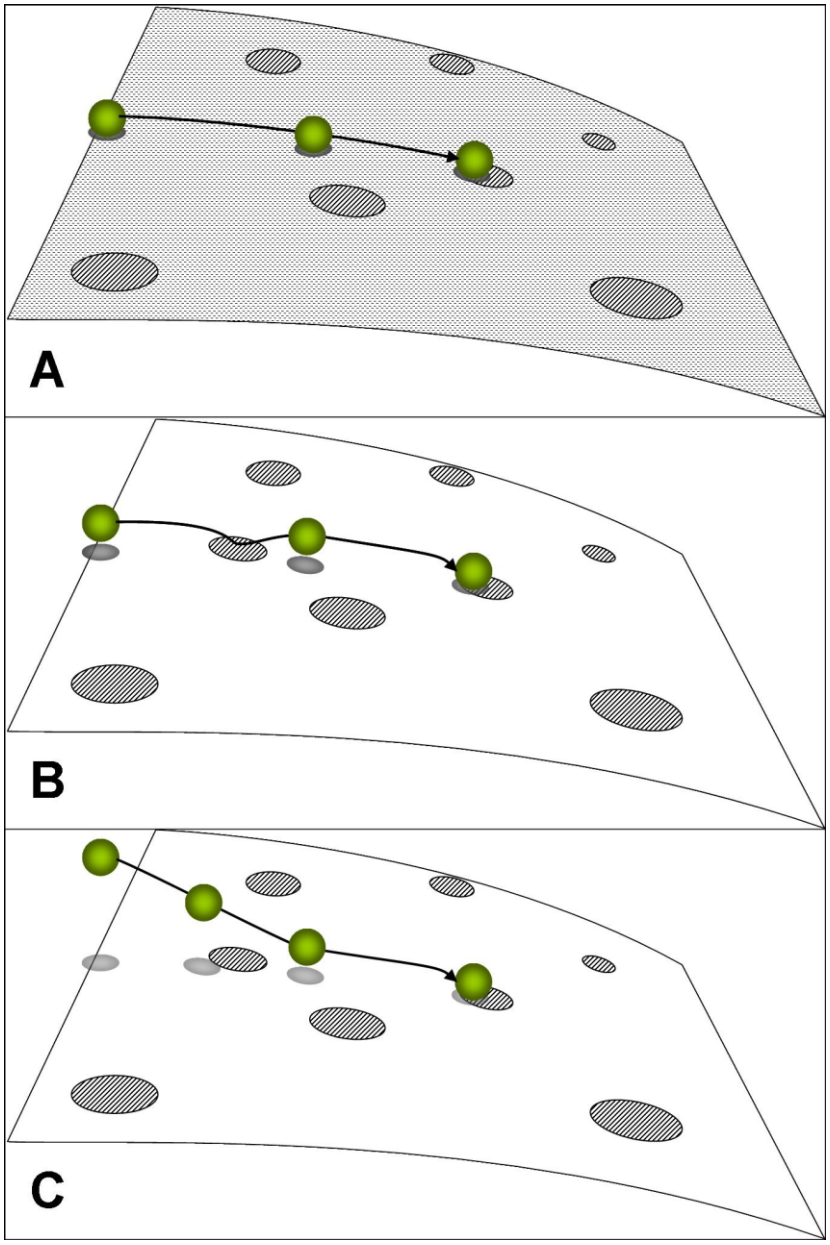

Figure 2.8. Potential scenarios for colloid attachment to local attractive surfaces designated by the striped ovals: (A) random encounter of a local attractive surface by a colloid translating while held in contact with the collector surface via attractive nano-domains, (B) transient approach and attachment to a local attractive surface by a colloid translating while captured in a secondary energy minimum at a given separation distance from the collector surface, (C) settling of a colloid into the secondary minimum before eventually approaching and attaching to a local attractive surface.

EXECUTIVE SUMMARY

We developed a method using a single epifluorescence microscope to track fluorescent colloids in three dimensions based on the out-of-focus image diameter. We also present results of two mini-studies for application of this method for measuring colloid transport in an idealized porous medium consisting of two contacting glass beads embedded in a chamber.

Exclusion of non-Brownian particles from orthogonally-oriented grain-to-grain contacts

Naoyuki Ochiai, Marshall Richmond, Maria Ines Dragila, and Jennifer L. Parke

Prepared for submission to Environmental Science and Technology
American Chemical Society Publications
1155 Sixteenth Street
N.W., Washington, DC 2003
Submission date TBD

ABSTRACT

The transport of suspended particles of biotic and abiotic origin through natural and engineered porous media is relevant to a wide range of disciplines. The failure of classic colloid filtration theory to predict the retention of suspended particles under chemical conditions unfavorable to deposition has led to development of the hypothesis that particles are retained in low-flow zones of individual pores. Because of their ubiquity and their notable impact on the flow field, grain-to-grain contacts have received particular attention as potential sites for particle retention. In the present study, we follow up on prior observations (Ochiai et al., 2010) that large, non-Brownian particles appear to 'avoid' a certain volume surrounding the grain-to-grain contact and arc a significant distance (230 μm) above or below the grain-to-grain contact. Using computational fluid dynamics to simulate flow in an isolated bead-pair flow-cell based on the physical micromodel employed by Ochiai et al. (2010), we demonstrate that entry into the low flow zone via advection requires that particles are traveling, prior to reaching the bead constriction, on streamlines that are within 1 μm of the horizontal z = 0 plane that passes through the grain-to-grain contact point. Particles traveling on streamlines further offset from the z = 0 plane arc significantly above (> 200 μm) the grain-to-grain contact point. The presence of the low flow zone with low probability of entry via advection results in reduction in the bead surface area available for particle capture relative the single-sphere collector model on the order of 5%. The emerging view of low flow zones associated with orthogonally-oriented grain-to-grain contacts suggests that they may serve as a watershed of sorts, enabling entry of small, Brownian particles via diffusion but preventing entry by large, non-Brownian particles, which are only subject to advection.

INTRODUCTION

Prediction of the transport and retention of suspended particles moving through porous media is relevant to researchers in a variety of fields including bioremediation (Loffler and Edwards, 2006), water filtration (e.g. Hijnen et al., 2007), contaminant and pathogen transport (e.g. Semenov et al., 2009). Typically, the suspended particles of interests, which can include mineral fragments, precipitates, organic macromolecules, or microorganisms, are of similar density to water and fall into the colloidal size range (< 1 μm). However, transport of somewhat larger particles (< 10 μm), most notably oospores of human pathogens *Cryptosporidium* (Tufenkji et al., 2004) or *Giardia*, are considered within the same theoretical framework due to similarities in transport behaviors. The 1 μm size criterion, while somewhat arbitrary, marks an important transition between Brownian and non-Brownian particles for which diffusion is or is not relevant.

Current colloid filtration theory (CFT) yields reasonably accurate predictions of colloid retention in porous media in cases where the chemical conditions are favorable for colloid deposition in the primary energy minimum. These conditions include relative surface charges of the colloids and media & the ionic strength, pH, of the carrying solution) However, colloids are frequently observed to be, at least partially, reversibly retained in porous media, even under chemically unfavorable conditions (Johnson et al., 2007), and at a rate exceeding estimates based on impinging jet experiments (Tong and Johnson, 2006). Such unfavorable deposition is commonly attributed to mechanisms such as retention in a secondary energy minimum (Redman et al., 2004), capture in low-flow zones (Johnson et al., 2007), or attachment to attractive nano-domains of the media surface (Duffadar and Davis, 2008). Importantly, these scenarios hypothesize that retention occurs where attractive colloid-media interactions, balance the hydrodynamic forces that would otherwise transport the colloids further. Even where the assumption can be made for uniform chemical conditions throughout a given porous media, 3-dimensional

pore topography leads to subpore-scale heterogeneity of the flow field, leading to variability throughout the porous media in the balance between hydrodynamic forces and electromagnetic-chemical colloid-media interactions.

Grain-to-grain contacts (G2G) have received particular attention as potential sites for colloid retention, since they are a common feature of granular porous media and represent regions of low velocity (Tong et al., 2008) or regions that are hydrodynamically 'disconnected' from the main flow (Torkzaban et al., 2008). A number of experimental studies have demonstrated colloid accumulation at grain-to-grain contacts under chemically unfavorable conditions (Li et al., 2006; Yoon et al., 2006; Kuznar and Elimelech, 2007; Tong et al., 2008; Johnson et al., 2010). It is hypothesized that colloids are either transported to these regions by the streamlines on which they are traveling or are translated along bead surfaces with which they have become associated via the secondary minimum (e.g. Kuznar and Elimelech, 2007) or attractive nano-domains (Duffadar and Davis, 2008).

Recognizing the potentially important role played by G2Gs in the retention of colloids under chemically unfavorable conditions, the present study was motivated by an a prior observation by our group that large particles (4.7 μm) seem to 'avoid' orthogonally oriented G2Gs and the resulting speculation that the retention potential of G2Gs may depend on their orientation relative to the direction of flow (Ochiai et al. 2010). We adopt the convection introduced in Ochiai et al., (2010) for designating the geometry of G2Gs. Orientation of grains such that the line connecting grain centers is aligned with the flow are designated as parallel grain-to-grain contacts (pG2Gs). G2Gs whose center-center lines are perpendicular to the flow are referred to as orthogonal G2Gs (oG2Gs) and G2Gs whose orientation is neither parallel nor orthogonal are referred to as oblique G2Gs (obG2Gs).

First, since the translation of 'captured' colloids along grain surfaces is a major means by which colloids are transported to G2Gs, it would seem that retention in pG2Gs is favored over other G2G orientations. By definition, pG2Gs occur at the

rears of grains. Since the majority of near-surface streamlines lead to the rear of grains, the majority of 'captured' colloids should be translated to the low flow regions associated with pG2Gs. In contrast, very few streamlines lead to the low flow regions associated with oG2Gs. Such orientation-dependent G2G accumulation is clearly demonstrated in direct observations of colloid retention in single-layer glass bead micromodels (Figure 4 in Kuznar and Elimelech, 2006). While these micromodels did not include oG2Gs, it is apparent that the colloids preferentially accumulated at the pG2Gs rather than the obG2Gs. However, orientation-dependent accumulation is not always observed (Tong, et al., 2008, Johnson et al., 2010), perhaps because G2G orientation is difficult to classify even in simple, single-layer models because of the complexity of flow.

Second, during direct observations of 4.7 μm microspheres passing between orthogonally-oriented glass bead pairs, we noted that microspheres tended to arc a significant distance (> ~230 μm) above or below oG2Gs (Ochiai et al., 2010). This included microspheres that appeared while upstream of the grains to be on trajectories aimed directly at the grain-to-grain contact point, leading to the speculation that direct transport of (large, non-Brownian) particles to low flow zones surrounding oG2Gs is rare. Taken together with the presumed low probability of deposition via surface translation discussed above, these observations suggest that oG2Gs are not as favorable to colloid retention as pG2Gs.

The last statement, if true, has important implications for predicting the location and quantity of colloids retained in porous media under chemically unfavorable conditions. Furthermore, the existence of pore regions that are essentially only accessible via diffusion may partially explain the anomalous behavior of tracers even in so-called homogeneous media (Levy and Berkowitz, 2003). There is a need to theoretically validate the existence of such zones and to investigate the mechanisms of 'avoidance' in order to begin quantify their impact on macroscale transport dynamics. Thus, this paper represents a first attempt to characterize the flow field in

the vicinity of oG2Gs and the connection of this low flow region to the upstream and downstream flow in an 'ideal pore' with the aid of computational fluid dynamics (CFD). In addition, we estimate the frequency of particle entry into this region via advection only, which represents the case of transport of neutrally buoyant non-Brownian (large) particles. These results are compared to experimental observations presented in Ochiai et al., (2010). Finally, we discuss the potential relevance, as well as the inferential limitations, of these results to macroscale colloid transport dynamics in more realistic continuous porous media.

MATERIALS AND METHODS

For simulations, measured dimensions of the physical flow cell used by Ochiai et al. (2010) were idealized to create a geometry that was symmetrical and centered in the channel. A solid geometry model was created using SolidWorks computer aided design (CAD) software (Dessault Systemes Version Professional 2009 SP0.0). The resulting micromodel flow cell geometry is shown in Fig. 3.1. A 50 μm-diameter collar was used at the grain to grain contact point to avoid creating a so-called 'pinch out point' that would be problematic for mesh generation step. The solid geometry was then imported in a computational fluid dynamics (CFD) code, starccm+ (Starccm+ version 5.04.006, starccm2010), where non-uniform trim cell type meshes were constructed. A total of 5 meshes with numbers of computational cells ranging from about 2 to 8 million were created. An example view of the computational mesh (about 5 million cells) is shown in Fig. 3.2. Note the use of variable mesh resolution to resolve regions near the grain surfaces and in the grain-to-grain contact zone.

Once the computational meshes were completed, the three-dimensional Navier-Stokes equations were solved by starccm+ using finite-volume solution methods. A uniform influx of 1.313888E-7 kg/s and an outflow boundary condition were used for all simulations. The surfaces of the microchannel walls and grains were all assigned to be no slip boundaries. Each simulation was carried out for 10,000 iterations.

Residual values for mass and momentum (x,y, and z components) were converged after 9,000 iterations and all residual values were reduced to below 1e-6 at the end of the simulation. The CFD model output was archived for later use by the post-processing software (TecPlot).

A sequence of simulations was carried out for each of the 5 meshes to test the effect of mesh refinement on the solution. Each simulation was run for 10,000 iterations. The difference in error difference in pressure drop from upstream to downstream of the spheres was less than 0.1% different from the coarsest to finest resolution mesh. A random sample (1000 points) of the velocity and its gradient field along a line starting from the contact point was also done to test mesh convergence. Velocities and velocity gradient are especially relevant since streamline and particle trajectories will be directly dependent on those simulated values. The rms error for the velocity magnitude and magnitude of the strain rate tensor as the number of mesh cells increases is shown in Table 3.1. As expected, error generally decreases as the number of cells increases. Based on these tests, mesh 4 (about 5 million cells) was selected as a good balance between error reduction and increasing computational cost.

RESULTS

We consider non-diffusive particles without mass or volume. In this simplest case, particles are expected to exclusively travel along fluid streamlines, thus we begin with an analysis of streamlines with respect to the zone surrounding the grain-to-grain contact point (G2G). Based on characteristics of the flow field in this region, we tentatively delineate a low flow zone (LFZ) associated with the G2G.

The density of streamlines along the sagittal XZ plane running between the beads is much lower in the vicinity of the bead-bead contact than further away from the G2G, indicating the lower velocity of the fluid in this region (Fig. 3.3). Perhaps of more relevance, the height of streamline arcing above the G2G region is greatest for

streamlines originating closest to the horizontal XY plane passing through the G2G at z = 0). Note that while streamlines originating at z = 0 are shown to arc above the G2G, this is an artifact caused by the inclusion of a collar at the G2G, which is necessary to avoid a sharp pinch point which is computational problematic. Streamlines originating only 1μm above the z=0 plane (at z = 1 μm) arc considerably (≈200 μm) above the G2G. Closer analysis of the relationship between streamline seed height and arc height over the G2G reveals that arc height increases rapidly for streamlines seeded between z = 0 and z ≈ 1 μm, but at a substantially slower rate for streamlines seeded at z > 1 μm (Fig. 3.4).

While there is clearly no physical boundary between the low flow associated with the G2G and main-channel flow, the inflection in streamline height above the G2G as a function of streamline height above the z = 0 plane prior to the beads for the streamline originating around z = 1 μm serves as a useful, pragmatic criterion for parsing flow zones. The stream tube defined by streamlines originating around z = 1 μm (Fig. 3.5) is similar in size and shape to the zone 'avoided' by the large particles in our previous experiments (Fig. 4 of Ochiai et al., 2010), suggesting the z = 1 μm envelope may function as a sort of natural watershed.

The presence of the low flow zone associated with the G2G would have the effect of reducing the interception of particles relative to predictions by the well-known Happel Sphere-in-Cell, since there is reduced flow to the portion of the bead surface enclosed by the LFZ (Fig. 3.6). Assuming that there is a very low probability of particle entry into the LFZ via advection, and in the absence of diffusion or sedimentation, the presence of the LFZ would reduce predicted retention by about 5%, relative to the single sphere case. Considering that the mean coordination number of grains in a disordered monodisperse porous media is around 6 (Gervois et al., 1989), the presence of multiple LFZs may significantly reduce the effective surface area available for interception.

DISCUSSION

Streamline analysis indicates the existence of a low flow zone surrounding the grain-to-grain contact of an orthogonally oriented bead pair. Streamlines originating 1 μm above or below the horizontal plane transecting the G2G (z = 0) arc significantly above and below the G2G (±200 μm), indicating that the low flow zone is narrowly connected with the upstream and downstream flow. The shape of the low flow zone appears to coincide with the zone 'avoided' by 4.7 μm particles in our earlier study (Ochiai et al., 2010).

The narrowness of the streamtube leading to the low flow zone indicates a low probability of entry via advection only. We further hypothesize that the entry probability of large particles (> 1 μm) is even lower due to steric hindrance that results in large particles shifting away from slow streamlines leading to the low flow zone. Briefly, large particles whose centers are near z = 0, experience increasing differential fluid drag across their bodies as they approach the grain-to-grain constriction (Fig. 3.6). Analogous to the case of particles moving near walls (Cherukat and McLaughlin, 1994), this shear gradient results in particle lift, i.e. a shift in streamlines, away from the low flow region. As demonstrated in our streamline analysis (Fig. 3.4), even a small shift in streamlines away from the equatorial plane results in a large shift in the trajectory above the grain-to-grain contact. Thus, for large particles, entry into the low flow zone is lower than that of small particles due to both the lack of diffusion and greater inertial lift away from streamlines leading to the low flow zone. This view of low flow zones associated with orthogonal grain-to-grain contacts may shed some light on previously-reported size-dependent differences in particle deposition/retention.

Ma et al. (2009) proposed a Hemisphere-in-Cell (HIC) model, with essentially the same geometry as our 'ideal pore', as an alternative to the Happel Sphere-in-Cell representation of pore space in colloid filtration theory. They demonstrated good agreement in contact efficiencies (η) estimated by their HIC model with those

predicted by single-collector models (Rajagopalan and Tien, 1976; Tufenkji and Elimelech, 2004) for smaller, Brownian particles (< 1 μm). However, they reported approximately two-fold lower contact efficiencies for larger non-Brownian particles (> 2 μm), which they speculated may have (i) resulted from the presence or absence of the G2G or (ii) been an artifact of their trajectory analysis or flow field implementation. As indicated by our analyses, non-Brownian particles are excluded from the low flow zones associated with G2Gs, precluding their contact with the bead surface area that is enclosed by the G2G-LFZ. As particle size decreases, increasing diffusivity increases access to the bead surface enclosed in G2G-LFZs and, as a result, increases capture potential.

Tong and Johnson (2006) observed greater retention of smaller particles (0.1 μm) in porous media than larger particles (2 μm) (p. 7730) under chemical conditions unfavorable to particle deposition. Furthermore, this size-dependent difference was only observed for the lower of two flow rates (4 $m \cdot d^{-1}$ and 8 $m \cdot d^{-1}$). The authors suggested that there was a greater probability of retention of the smaller particles in flow stagnation zones due to their smaller size (i.e. more particles able to fit in a given volume) and lower fluid drag. Based on our analyses, the probability of entry into low flow zones associated with G2Gs (G2G-LFZs) should depend on the ratio of particle diffusivity to advective velocity, i.e. the particle Peclet number. Thus, at a given advective velocity, smaller, diffusive particles should have a greater probability of entry into G2G-LFZ than larger particles. At lower fluid velocities, diffusion becomes increasingly important for small particles but remains insignificant for large particles. At higher fluid velocities, diffusion becomes decreasingly relevant for even small particles. Thus, the difference in probability of Brownian and non-Brownian particles entering low flow zones should be greatest at low velocities and least prominent at high velocities.

To assess the potential relevance of these low flow zones in continuous porous media, we make a rough estimate for the case of homogenous media (1 mm glass

beads) with a porosity of 36%. The proportion of the pore space occupied by a single low flow zone is approximately 0.9% of the pore space. Assuming a coordination number of 6, the pore space occupied by the assembly of low flow zones is on the order of 5%.

SUMMARY & CONCLUSIONS

Flow field analysis using computational fluid dynamics confirmed the existence of a region with low mass flux similar in size and shape of the zone observed to be 'avoided' by 4.7 mm particles (Ochiai et al., 2010). The narrow connection of this low flow zone to upstream and downstream flows indicates a low probability of particle entry via advection alone. We hypothesize that the entry probability of large particles (> 1 μm) is further reduced by steric hindrances that cause large particles to shift away from slow streamlines leading to the low flow zone. The resulting view of the low flow zone as essentially inaccessible to large, non-Brownian particles but accessible to smaller Brownian particles may explain previously-reported size-dependent differences in particle deposition/retention (e.g. Ma et al., 2010; Tong and Johnson, 2006). Further mechanistic elucidation of the steric exclusion of large particles from entering the low flow zone as well as additional studies to quantify particle entry due to diffusion and sedimentation are warranted.

ACKNOWLEDGEMENTS

This research was supported by a grant from the National Research Initiative of the USDA Cooperative State Research, Education and Extension Service, Grant no. 2006-35107-17231. We thank Dr. John Serkowski for his skilled assistance with the computational fluid dynamics coding.

LITERATURE CITED

Cherukat, P. and J.B. McLaughlin. 1994. The inertial lift on a rigid sphere in a linear shear flow field near a flat wall. *J. Fluid Mech*. 263:1-18.

Duffadar, R.D., and J.M. Davis. 2008. Dynamic adhesion behavior of micrometer-scale particles flowing over patchy surfaces with nanoscale electrostatic heterogeneity. *J. Colloid and Interface Sci*. 326:18-27.

Gervois, A., M. Lichtenberg, L. Oger, and E. Guyon. 1989. Coordination number of disordered packings of identical spheres. *J. Phys. A. Math. Gen*. 22:2119-2131.

Hijnen, W.A.M., Y.J. Dullemont, J.F. Shijven, A.J. Hanzens-Brower, M. Rosielle, and G. Medema. 2007. Removal and fate of *Cryptosporidium parvum*, *Clostridium perfringens* and small-sized centric diatoms (*Stephanodiscus hantzschii*) in slow sand filters. *Water Res.* 41:2151-2162.

Johnson,W.P., E. Pazmino, and H. Ma. 2010. Direct observations of colloid retention in granular media in the presence of energy barriers, and implications for inferred mechanisms from indirect observations. *Water Res*. 44:1158-1169.

Johnson, W.P., M. Tong, and X. Li. 2007b. On colloid retention in saturated porous media in the presence of energy barriers: the failure of α, and opportunities to predict η. *Water Res. Res*. 43:W12813.

Kuznar, A.A. and M. Elimelech. 2007. Direct microscopic observation of particle deposition in porous media: role of the secondary energy minimum. *Colloids Surf. A: Physicochem. Eng Aspects.* 294:156-162.

Levy, M. and B.J. Berkowitz. 2003. Measurement and analysis of non-Fickian dispersion in heterogeneous porous media. *Contamin. Hydrol.* 65:203-226.

Li, X., C. Lin, J.D. Miller, and W.P. Johnson. 2006. Pore-scale observation of microsphere deposition at grain-to-grain contacts over assemblage-scale porous media domains using x-ray microtomography. *Environ. Sci. Technol*. 40:3762-3768.

Ma, H.L., J. Pedel, P. Fife, and W.P. Johnson. 2009. Hemispheres-in-cell geometry to predict colloid deposition in porous media. *Environ. Sci. Technol*. 43:8573-8579.

Ochiai, N., M.I. Dragila, and J.L. Parke. 2010. Three-Dimensional Tracking of Colloids at the Pore Scale Using Epifluorescence Microscopy. *Vadose Zone J*. 9:576-587.

Rajagopalan, R. and C. Tien. 1976. Trajectory analysis of deep-bed filtration with sphere-in-cell porous media model. *AIChE*. 22:523-533.

Redman, J.A., S.L. Walker, and M. Elimelech. 2004. Bacterial adhesion and transport in porous media: role of the secondary energy minimum. *Environ. Sci. Technol*. 38:1777-1785.

Semenov, A.V., L. van Overbeek, and A.H.C. van Bruggen. 2009. Percolation and survival of *Escherichia coli* O157:H7 and *Salmonella enterica Serovar Typhimurium* in soil amended with contaminated dairy manure or slurry. *Appl. Environ. Microbiol*. 75:3206-3215.

Tong, M. and W.P. Johnson. 2006. Excess colloid retention in porous media as a function of colloid size, fluid velocity and grain angularity. *Environ. Sci. Technol*. 40:7725-7731.

Tong, M., H. Ma, and W.P. Johnson. 2008. Funneling of flow into grain-to-grain contacts drives colloid-colloid aggregation in the presence of an energy barrier. *Environ. Sci. Technol*. 42:2826-2832.

Torkzaban, S., S.S. Tazehkand, S.L. Walker, and S.A. Bradford. 2008. Transport and fate of bacteria in porous media: coupled effects of chemical conditions and pore space geometry. *Water Res. Res*. 44:W0403.

Tufenkji, N. and M. Elimelech. 2004. Deviation from the classical colloid filtration theory in the presence of repulsive DLVO interactions. *Langmuir*. 20:10818-10828.

Yoon, J.S., J.T. Germaine, and P.J. Culligan. 2006. Visualization of particle behavior within a porous medium: mechanisms for particle filtration and retardation during downward transport. *Water Res. Res*. 42:W06417.

TABLES AND FIGURES

Table 3.1. Effect of mesh refinement on velocity magnitude and strain rate tensor magnitude.

Grid Sizes	Mesh Refinement ratio - r	Vmag rms error(%)	StrainRate rms error (%)
MESH1 – MESH2	1.12	0.839	2.374
MESH2 – MESH3	1.23	1.479	4.804
MESH3 – MESH4	1.09	0.195	0.912
MESH4 – MESH5	1.04	0.104	0.279

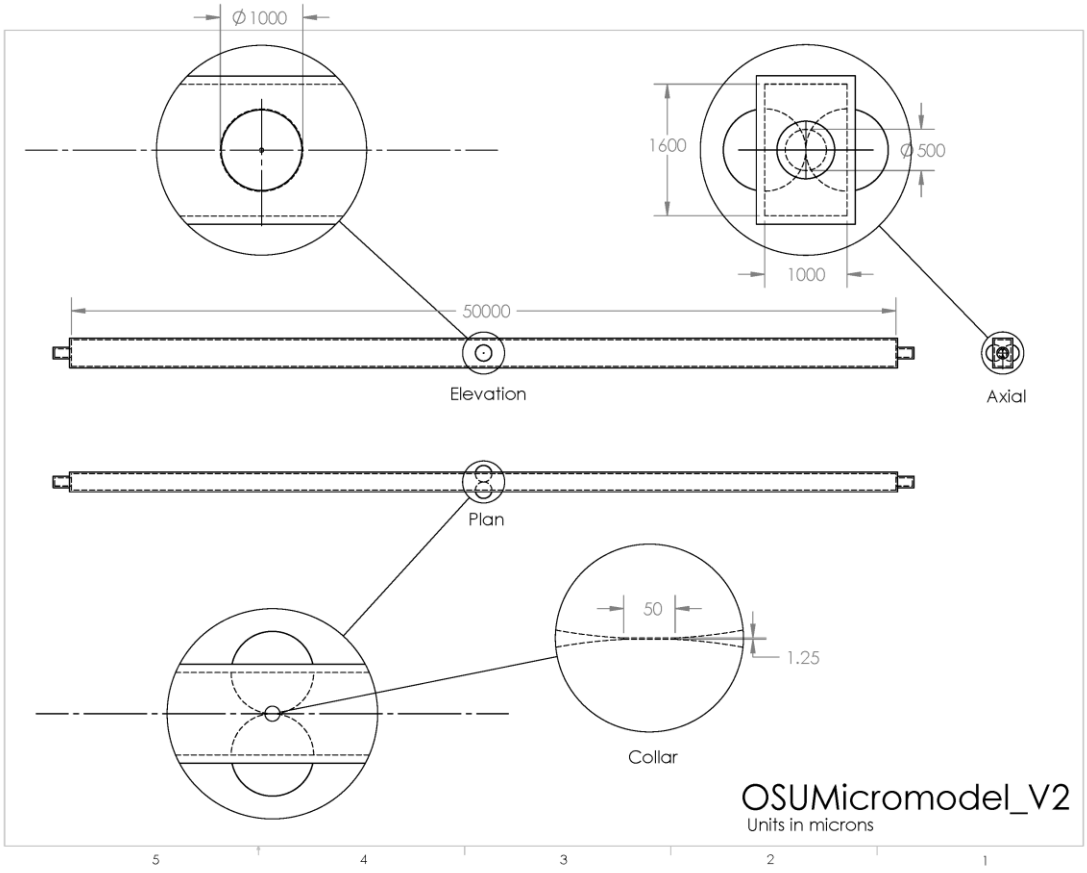

Figure 3.1. Idealized version of the orthogonal bead pair micromodel employed by Ochiai et al. (2010) used to define the solid geometry in the CFD model. Units are in microns. A 50 μm-diameter cylinder (collar) is used at the grain-to-grain contact point to improve mesh quality at this location.

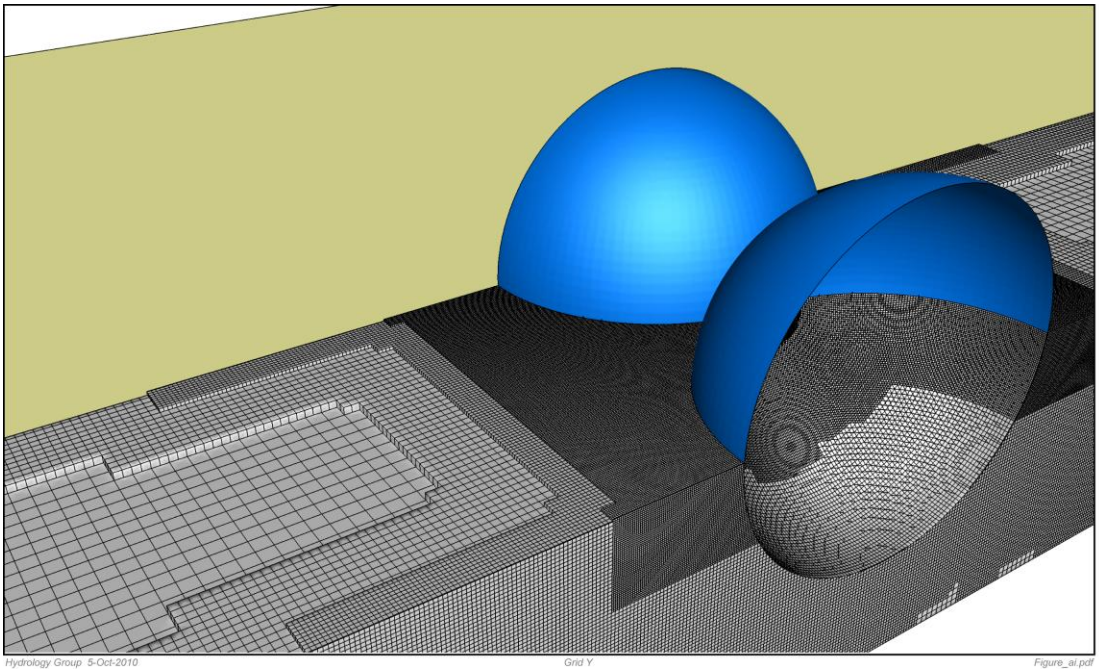

Figure 3.2. Three-dimensional computational mesh used in the CFD simulations. Note that the mesh is progressively refined near the grain surfaces.

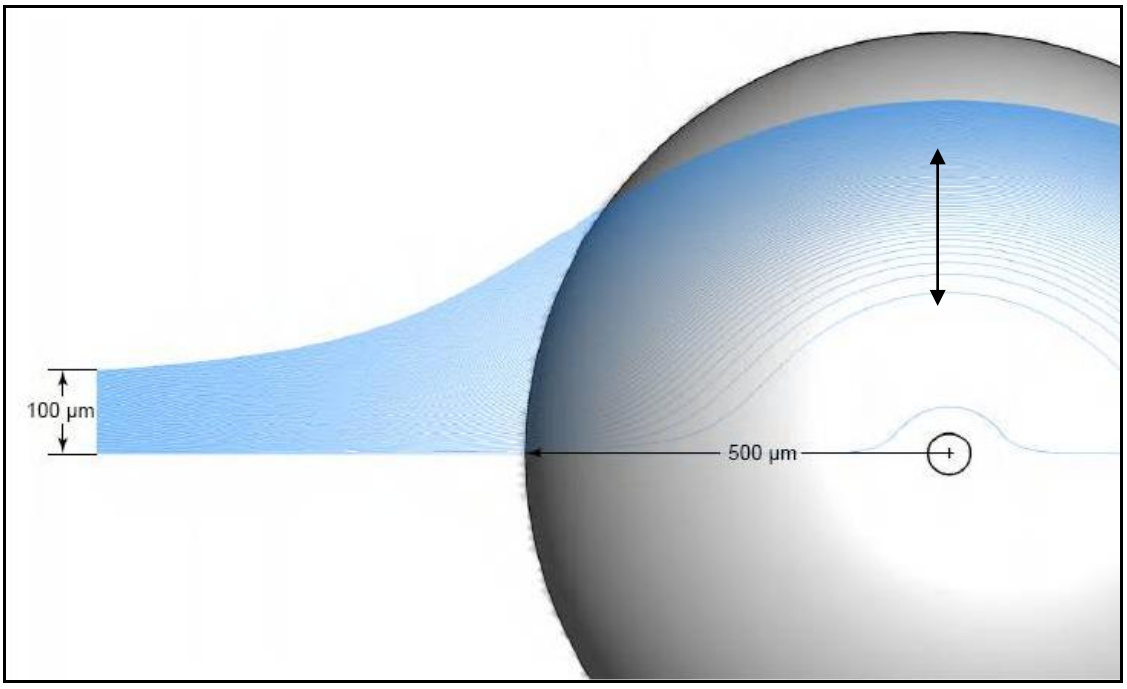

Figure 3.3. Streamlines along the XZ plane passing through grain-to-grain contact seeded at 1 µm intervals starting at the height of the bead-bead contact (z = 0) 500 µm upstream of the bead edge. The foreground bead has been removed to enable viewing of central streamlines within the bead-bead impingement.

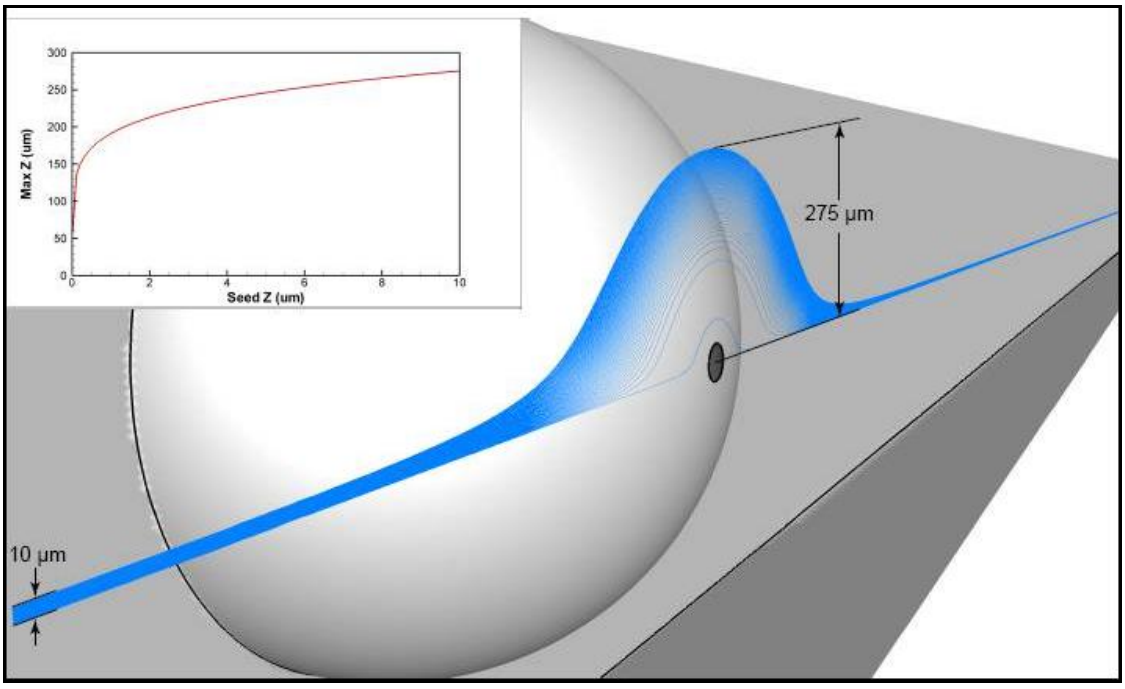

Figure 3.4. Streamlines along the XZ plane passing through the grain-to-grain contact, seeded at 0.1 mm intervals (z = 0 to 10 µm), 500 µm upstream of the bead edge. The foreground bead has been removed to enable viewing of streamlines within the bead-bead impingement. Inset shows height of streamlines passing over the bead-bead contact as a function of seed height.

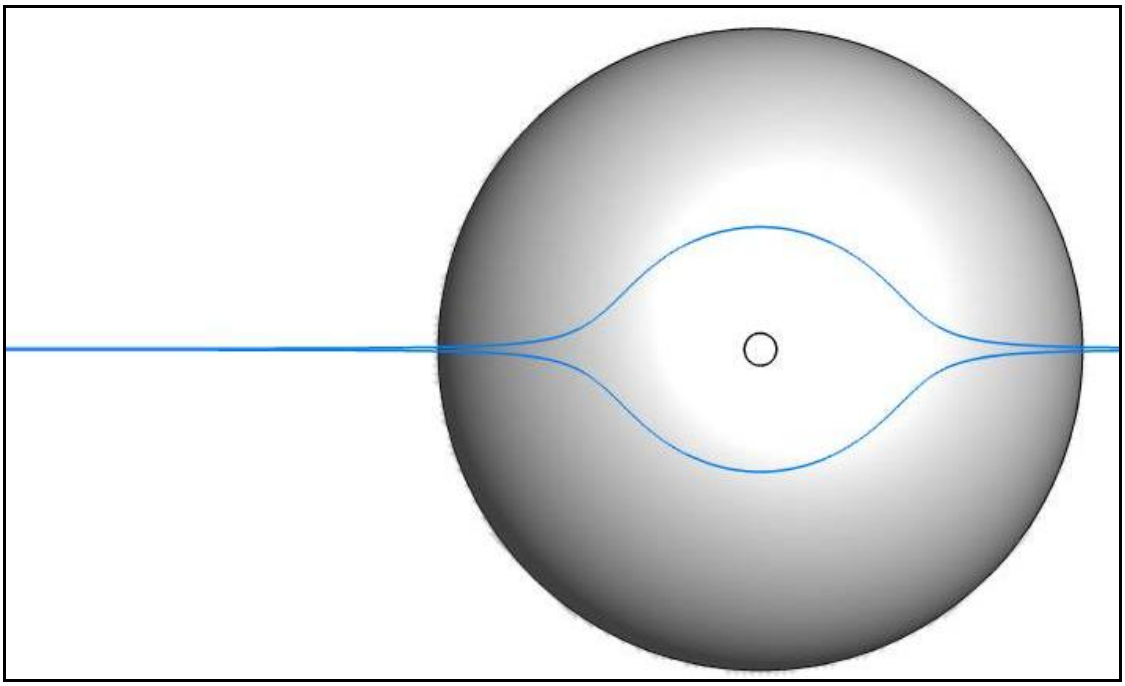

Figure 3.5. Low flow zone defined by envelope of streamlines originating at z = ± 1 μm.

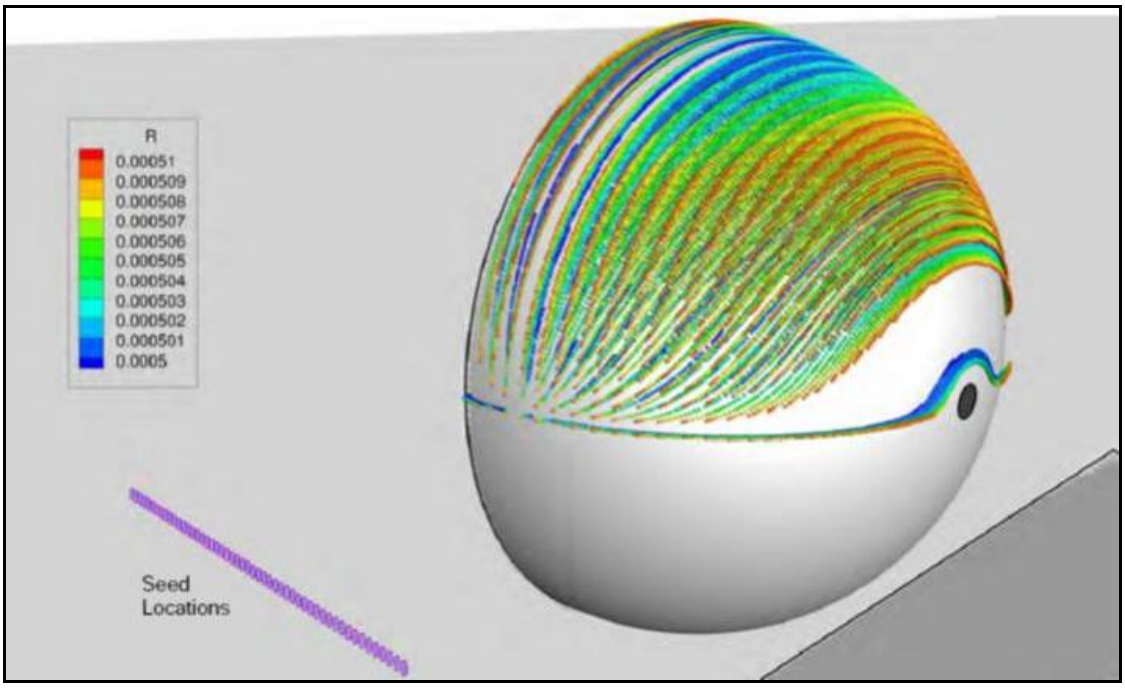

Figure 3.6. Distances from the bead surface (in cm) of streamlines seeded at z = 0 and z = 0.5 mm, 500 μm upstream of the bead. The foreground bead has been removed to enable viewing of streamlines between beads.

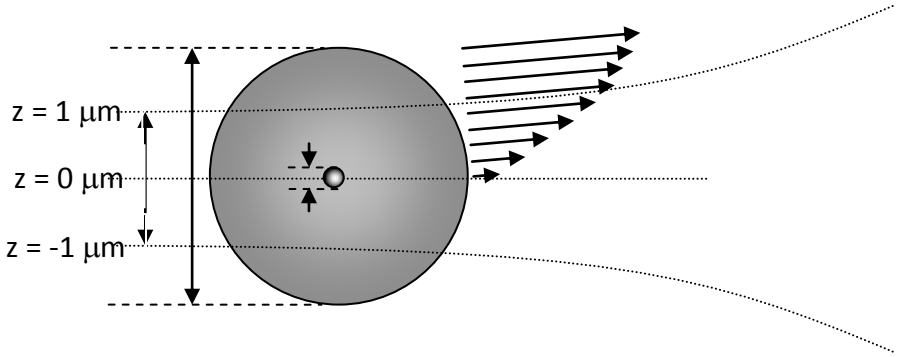

Figure 3.7. Hypothesized impact of fluid shear as a function of particle size of particles traveling on near-center streamlines leading to the LFZ. The significant difference in fluid velocity across the colloid body creates lift *away* from the center streamline similar to the case of "wall effect" lift (Cherakut and McLaughlin, 1994).

Pattern swimming of *Phytophthora citricola* zoospores: an example of microbial bioconvection

Naoyuki Ochiai, Jennifer L. Parke, and Maria Ines Dragila

Fungal Biology
Published by Elsevier on behalf of the British Mycological Society
360 Park Avenue South
New York, NY 10010
Accepted (Oct. 2010)

ABSTRACT

The genus *Phytophthora,* belonging to the class *Oomycota,* comprises a group of over fifty fungus-like plant pathogens in both managed and unmanaged ecosystems. A unique feature of the *Oomycete* life-cycle is a zoosporic stage in which motile, unicellular propagules, serving as the primary agents of dispersal, are produced and released in the presence of water. In Petri dish suspensions, zoospores frequently exhibit 'pattern swimming', whereby they spontaneously form concentrated swimming masses, visible to the naked eye, even in the absence of a chemical or electrical gradient. The nature of this behavior is unclear, but is of interest because of the potential for auto-attraction and implications for cohort recruitment during infection. Similar behavior observed in a variety of motile bacteria, algae, and protists is attributed to 'bioconvection' that results from instability in fluid density due to the organisms' upward-swimming tendency and greater-than-water density. In this investigation, we determined that *P. citricola* zoospore 'pattern swimming' is unrelated to phototaxis, surface tension-driven (Marangoni) convection, or auto-attraction and that the observed convective pattern, directional swimming, and depth- and concentration dependence are consistent with bioconvection. In addition, we speculate that such pattern swimming occurs in the natural environment and may contribute to the high degree of genetic exchange observed in nature by serving as a mechanism for bringing together zoospores of different species and, thereby, setting the stage for hybridization. (225 words)

Keywords: *Phytophthora*, *Oomycete*, zoospore, motility, pattern swimming, auto-aggregation, bioconvection, negative geotaxis

INTRODUCTION

The genus *Phytophthora* comprises a group of foliar and soil-borne plant pathogens belonging to the class *Oomycota*. Despite morphological and ecological similarities to true fungi, molecular analyses place *Oomycota* in the Kingdom Stramenopiles, alongside brown algae and diatoms, whose common characteristic is having a unicellular motile (zoosporic) life stage. The zoosporic stage, a vestige of the Oomycete's aquatic ancestry, plays a prominent role in their lifecycle, serving as the primary means of dispersal. Oomycete zoospores, produced and released only in the presence of water, are capable of propelling themselves by means of two different flagella and exhibit a variety of directional swimming behaviors including chemotaxis (e.g. Khew and Zentmeyer 1973, Zentmeyer, 1961), electrotaxis (Morris and Gow, 1993), and negative geotaxis (Cameron and Carlile, 1977) that presumably increase dispersal range and ability to locate new hosts.

'Pattern swimming' refers to a phenomenon frequently observed in *Phytophthora* and other Oomycota (Thomas and Peterson, 1990), whereby zoospores, in the absence of chemical or electrical signals, spontaneously form patterns of concentrated swimming masses (Fig. 4.1A) that are visible to the naked eye (e.g. Ko and Chase, 1973). While this tendency to swarm suggests potential self-attracting behavior, there is, as yet, no experimental evidence demonstrating that this behavior is due to zoospore-zoospore attraction. Nevertheless, it remains of interest to researchers (van West et al. 2003, Walkera and van West, 2007), since such behavior would have significant implications for cohort recruitment during infection/colonization. The current ambiguity regarding the nature of this behavior is indicated by the range of terms used to refer to it, from 'pattern swimming' (Carlile, 1983) to 'adelphotaxis' (Lounsbury, 1927) and 'auto-aggregation' (van West et al. 2003).

It has been suggested that this 'pattern swimming' is not the result of self-attraction, but rather, 'bioconvection' (Carlile, 1983). Bioconvection is a well-known

phenomenon occurring in a variety of motile microorganisms, ranging from bacteria (Kessler, 1985a), algae (Pedley and Kessler, 1992), to protists (Winet and Jahn, 1972), which share the characteristics of tending to swim upward and being denser than water. Briefly, bioconvection, as first proposed by Platt (1961) and subsequently developed by others (Bees and Hill, 1998, Childress et al. 1975, Hill et al. 1989, Plesset and Whipple, 1974), involves accumulation of a high number of denser-than-water microorganisms in a layer just below the water surface due to the organisms' upward-swimming tendency. The density of the near-surface liquid layer, from a continuum perspective, becomes greater than that of the underlying liquid. Instabilities at the interface between density layers eventually leads to the formation of 'fingers' where the denser upper layer falls through the less-dense under-layer, carrying with it a high concentration of organisms. Individual organisms, thus removed from the near-surface layer, are replaced by other upward swimming organisms, initiating a convective cycle.

Given the current uncertainty among Oomycete researchers regarding 'pattern swimming' and continued speculation of auto-attraction (eg. Walkera and van West, 2007), our objective was to clarify the nature of this phenomenon, drawing on the body of evidence and theory supporting bioconvection of similar microorganisms. In the first part of this paper, we describe the phenomenon in detail, explore conditions under which it occurs, and test a variety of potential mechanisms, including phototaxis, surface tension-driven (i.e. Marangoni) convection, and auto-aggregation. Next, we discuss *Phytophthora* 'pattern swimming' in the context of bioconvection theory. Finally, we speculate on the relevance of pattern swimming, and related behavior, in natural environments.

MATERIALS AND METHODS

P. citricola Sawada, isolate 98-517 (identified as *P. citricola* III *sensu* (Jung and Burgess, 2009)) was isolated from rhododendron and cultured on PAR agar (Jeffers

and Martin, 1986) amended with PCNB (66.7 mg·L^{-1}) and hymexazol (25 mg·L^{-1}). Multiple agar plugs were taken from the margins of an actively growing culture, transferred to clarified V8 broth (Singleton et al., 1992) and incubated statically for 2 to 3 days at room temperature (17~20˚C). After rinsing the mycelial mats with filtered (0.2 μm) tap water, the clarified V8 broth was replaced with autoclaved water from Oak Creek, Corvallis, OR and samples were incubated in Petri dishes for 10 to 14 days, allowing for production of abundant zoosporangia. Zoospore release was induced by replacing the creek water with filtered tap water, chilling the cultures for 1 h at 4˚C, and then placing cultures at room temperature for 1 to 2 h. Prior to experiments, zoospore suspensions were filtered through a 20 μm nylon mesh to remove zoosporangia and hyphal debris.

Pattern swimming experiments. A series of experiments were conducted to investigate various aspects of "pattern swimming." These included: (i) characterization of macroscopic "patterns", (ii) microscopic observation of zoospore behavior vis-à-vis macroscopic "patterns", (iii) effect of light (phototaxis), (iv) effect of surface tension, (v) effect of initial zoospore concentration, and (vi) effect of suspension depth. All tests consisted of observations of zoospore suspensions in 5 cm-diameter Petri dishes. Zoospore concentrations for all trials, with the exception of the zoospore concentration experiments, was > 5 x 10^5 zoospores·mL^{-1} to ensure formation of well-defined patterns. Petri dishes were uncovered in all tests, except in the case of surface-tension trials in which the dishes were filled to capacity and covered with an acrylic lid to eliminate the air-water interface. All experiments were carried out under darkfield illumination with the exception of phototaxis experiments that were only briefly illuminated for the purpose of image capture but otherwise were conducted in the dark. Unmagnified still images were captured using a commercial digital camera using the macro setting. Magnified observations (1.5 to 4.5X) and video-capture were conducted using a high definition commercial camcorder (HDR-SR11, Sony Electronics, San Diego, CA) attached to a zoom

inspection microscope (6000X w/ 1X adapter, Navitar Inc., Rochester, NY). Zoospore swimming behavior (direction and velocity) from microscopic observations were analyzed using time-lapse images generated from captured video using a custom program developed in MATLAB (R2008b, MathWorks Inc., Natick, MA). All trials were repeated at least 3 times.

Auto-aggregation tests. Two types of experiments (swim-in and population segregation) were conducted to test zoospore auto-attraction. Swim-in tests were conducted in a square chamber (1.5 x 1.5 x 1.0cm) fitted with pipette tips on each side, filled with filtered tap water or zoospore suspension filtrate passed through a 0.2 μm filter to remove zoospores. Approximately 10 min after introducing a low-concentration zoospore suspension to the main chamber, the concentration of zoospores in each of the tips was assessed by evacuating the tip contents and observing under magnification. Population segregation tests were conducted using custom apparatus consisting of a main chamber (4 x 3 x 1 cm) and two holding chambers (1 x 3 x 1 cm) located at each end of the main chamber and separated from the main chamber by a 5 μm mesh chosen to allow passage of diffusible chemicals but not zoospores. To ensure connectivity across the mesh barrier, both of the holding chambers were first filled with filtered water and the apparatus was maintained under tension until the liquid level in the main chamber was equilibrated with that in the holding chambers. The filtered water in one of the holding chambers was replaced with a high-concentration zoospore suspension (> 5×10^5 zoospores·mL^{-1}). A low concentration zoospore suspension (< 1×10^4 zoospores·mL^{-1}) was introduced to the main chamber and the accumulation of zoospores near the mesh barriers of both holding chambers was assessed over time. All trials were repeated three times.

RESULTS

Characteristics of macroscopic patterns. Filtered zoospore suspensions were poured into Petri dishes, homogenized by mixing, and observed over time under darkfield illumination. Although the banding pattern varied by trial, in the majority of cases, a single circular band formed at the perimeter of the dish in less than 1 minute after mixing (Fig. 1A). The circular band contracted over several minutes, eventually coalescing into a single point or line near the center of the Petri dish (Supplemental video A). In other cases, branch patterns formed creating the tessellated appearance similar to that reported elsewhere (Ko and Chan, 1974, Ko and Chase, 1973).

Zoospore movement vis-à-vis "patterns". Observation at 4.5X magnification clearly demonstrated that the bright bands (or nodes) constituted localized accumulations of zoospores relative to the darker non-band areas that contained fewer zoospores (Fig. 4.1C~F). When circular bands formed, the center of the ring often appeared to be relatively more depleted of zoospores than the area outside of the ring. Focusing at different depths within the suspension, we observed that zoospores in the upper part of the suspension tended to swim towards the bands (or nodes) and zoospores deeper in the suspension tended to swim away from the band (or node). This directional movement is demonstrated by maps of locally averaged velocity vectors (Fig. 4.2). In the vicinity of band midlines or node centers (as seen from above), zoospore movement was not obviously directional and the length of horizontal travel was relatively shorter than further away from the bands, which we interpret as indicating relatively greater vertical (z-axis) travel. Thus, it appears that zoospore 'pattern swimming' involves a convective circulation whereby the zoospores move towards bands (or nodes) in the upper layers of the suspension, downwards at the band (or node) centers, and away from bands (or nodes) deeper in the suspension (Fig. 4.3).

Phototaxis and surface-tension. Given that some brown algae, related to Oomycetes, are known to be phototactic (Kawai et al., 1991), it has been suggested, but not experimentally demonstrated, that *Phytophthora* may also be responsive to light (Petri, 1925 as reported in Carlile, 1983). We ruled out phototaxis as contributing to 'pattern swimming' by repeating the above Petri dish experiments in the dark, illuminating the sample only briefly to capture images (Fig. 4.4A). Samples left in the dark exhibited similar band patterns that evolved in a similar manner as those produced in ambient light. The tessellated pattern without a ring shown in Fig. 4A was less common but not atypical of patterns formed in the presence of light. In addition, we ruled out the possibility of surface tension-related convection by repeating trials in Petri dishes covered with a lid such that there was no air-water interface. Pattern formation and convective movement in the covered dishes were identical to those in the uncovered trials (Fig. 4.4B).

Effect of concentration. Bands formed over a significant range of initial zoospore concentrations (Fig. 4.5). Bands became progressively difficult to discern with decreasing zoospore concentrations, thus, it was not possible to determine whether pattern swimming ceased to occur in the lower concentration suspensions or was simply no longer visible to the naked eye. Elsewhere, patterns were only observed for concentrations above ~1 x 10^6 zoospores·mL^{-1} in *P. palmivora* (Ko and Chase, 1973) and ~1x10^5 zoospores·mL^{-1} in *P. capsici* (Ko and Chan, 1974). However, these authors did not elaborate on whether this was a limitation of the method of observation. Thus, while it appears that pattern swimming does not occur below a given concentration, it is a possibility that it does occur, but simply is undetectable.

Effect of sample depth. It is important to note that pattern swimming has not been observed to occur in shallow samples typical of microscopic observation. We observed band formation only in samples 3.6 mm deep and greater, but not in samples 3.1 mm or less (Table 4.1). This critical depth range is similar to that estimated from data presented in Ko and Chase (1973) for *P. palmivora* and by Ko

and Chan (1974) for *P. capsici*, and suggests that a minimum depth is required for the pattern swimming to occur.

Auto-attraction. To test for zoospore auto-attraction, two types of experiments were conducted: swim-in tests (attraction to filtrate) and population segregation tests (attraction to zoospores). In the former tests, using a similar approach to the chemotactic assay described by Zentmeyer (1961), we compared the rate of zoospore entry into pipette tips filled either with filtrate from a zoospore suspension (harvested from a concentrated band) or filtered water. In the latter tests, we compared the accumulation of zoospores in a test suspension near two holding chambers separated from the test chamber by a μm nylon mesh and filled either with filtered tap water or with a concentrated zoospore suspension. We were unable to detect preferential accumulation of zoospores in either the filtrate-filled pipette tips or near zoospore holding chambers relative to the filtered water controls, thus were unable to confirm auto-attraction.

DISCUSSION

Our investigation yielded the following observations: 'pattern swimming' of *Phytophthora citricola* zoospores constitutes (i) the accumulation of swimming zoospores in bands (or nodes) and involves a convective circulation that is (ii) not related to surface-tension, whereby (iii) zoospores move towards bands (or nodes) near the surface, downwards at band (or node) centers, and away from bands (or nodes) deeper in the suspension. Furthermore, zoospore 'pattern swimming' occurs (iv) only above a critical background concentration, (v) in samples that are deeper than approximately 3.6 mm, and (vi) is not related to attraction to either zoospore filtrate or other zoospores. These observations enable us to rule out the involvement of phototaxis, surface tension-related convection, and auto-attraction and provide data for evaluating bioconvection as an explanation for the zoospore pattern swimming.

Bioconvection (overturning instability). To begin, we provide a brief, qualitative introduction to bioconvection and highlight particular aspects that are most relevant to our observations. A more comprehensive and quantitative review of bioconvection is provided by (Hill and Pedley, 2005). The term "bioconvection" was coined by Platt (1961) to describe the pattern formation due to overturning instability in cultures of the upward-swimming protozoan *Tetrahymena pyriformis*. The phenomena has since been recognized as occurring in a variety of microorganisms ranging from bacteria (Kessler, 1985a), protists (Plesset and Whipple, 1974), and algae (Pedley and Kessler, 1990) having the common characteristics of an upward-swimming tendency and density greater than water. The upward-swimming propensity results in formation of a highly-populated near-surface liquid layer that, by virtue of the microorganisms being denser than water, is denser, from a continuum perspective, than the less-populated underlying liquid. The juxtaposition of denser liquid over less-dense liquid, a situation known as a Rayleigh-Taylor instability, is inherently unstable, and leads to the dense liquid settling through the less-dense liquid, carrying with it a high concentration of microorganism that replenishes the population of organisms in the underlying liquid. This initiates a convection whereby the near-surface population, thus removed, is quickly replaced by upwards swimming individuals from the underlying layer. Unlike the case of two liquids with differing density, for which there is a final state where the higher density liquid underlies the less-dense liquid, bioconvection leads to a steady state in which the rate of depletion of the near-surface population equals the rate of replenishment from lower layers. Furthermore, in this steady state, the locations of downward settling and upwelling are fixed at short timescales (seconds to minutes), creating the observed patterns.

Considering *Phytophthora* pattern swimming in the context of bioconvection theory, we first note that *Phytophthora* zoospores are denser than water and are known to accumulate near the surface of a liquid (e.g. Ho & Hickman, 1967).

Cameron and Carlile (1977) demonstrated that the upward movement of *Phytophthora* zoospores (*P. cactorum, P. palmivora, P. nicotianae*) was not due to aerotaxis and concluded that it was an example of negative geotaxis. We suspect that this upward swimming tendency results from the zoospore's inherent upward tilt caused by its center of gravity being offset (behind) from its center of buoyancy, as in the case of the alga *Chlamydomonas nivalis* (Kessler, 1985a, Roberts, 2006). In the context of bioconvection, the relevant consequence of this upward-swimming tendency, regardless of the mechanism, is the formation of a zoospore-enriched near-surface layer, with an approximate depth of 3 mm (Cameron and Carlile, 1977). Notably, we did not attempt to characterize the vertical gradient in zoospore concentration, as this varies significantly, both spatially and temporally, after onset of bioconvection and would necessitate a sufficiently precise sampling protocol along with significant theoretical modeling to yield meaningful data.

Second, in our experiments, swimming masses were always associated with convective zoospore movement (Fig. 4.3) whose direction was consistent with that predicted for bioconvection. We noted, in addition, that while the zoospores near the surface did not swim in straight lines towards bands (or nodes), the overall direction of individual zoospores, as well as the average direction of a group of zoospores, was towards the bands (Fig. 4.2A & C). A similar description can be applied to the net movement of zoospores deeper in the sample away from the band (Fig. 4.2B & D). Although there is mention of zoospore movement with respect to bands (or nodes) in the *Phytophthora* literature, these amount to only partial descriptions: Ko and Chase (1973) noted that the majority of zoospores, presumably near the water surface, appeared to swim towards band centers, Reid et al. (1995) observed "circulation" of *P. palmivora* zoospores that established "water currents which pulled in surrounding zoospores", and Cameron (1979), as reported by Carlile (1983), described circulation, although the direction is somewhat unclear. Taken with these previous reports, our observations suggest that the maintenance of

concentration bands results not only of the circulation of fluid (hydrodynamics) but also the zoospores' directional swimming (biology).

Given the zoospores' ellipsoid shape, it is not surprising that they would exhibit rheotaxis, i.e. preferentially swimming in the direction of flow. Although, interestingly, in the only investigation of *Phytophthora* swimming vis-à-vis shear that we are aware of, zoospores were observed to swim against, not with, the current (Katsura and Miyata, 1966). Kessler (1985a, b) proposed that, in the presence of fluid shear, negatively geotactic organisms would align with streamlines due to a combination of gravitational and viscous forces and used the term "gyrotaxis" to describe this behavior. Thus, in the case of zoospores, shear-aligned swimming may be encouraged both by soma shape and the mass-displacement which is presumably responsible for upwards swimming. In the context of bioconvection, gyrotaxis and rheotaxis are predicted to reinforce initial density-driven instabilities and to stabilize bioconvective pattens by causing individuals to swim both upwards and towards down-welling regions (Hill et al., 1989, Pedley et al. 1988). Thus, the observed movement of zoospores towards bands (or nodes), which we describe as a combination of swimming and convection, is likely an example of rheotaxis/gyrotaxis related to bioconvection.

Bioconvection theory further provides reasonable explanations for the dependence of pattern formation on sample depth and initial suspension concentration. From observations of *T. pyriformis* (Childress et al., 1975, Levandowsky et al. 1975, Winet and Jahn, 1972), it is evident that patterns do not occur if the sample depth is less than a critical depth h_c. Based on the present investigation and others (Ko and Chan, 1974, Ko and Chase, 1973), we estimate the h_c for onset of zoospore pattern swimming to be in the range of 3.1 to 3.6 mm. Bioconvection theory predicts that h_c decreases with increasing average concentration N_o of the suspension. Although we did not explicitly look at the relationship between h_c and N_o, we estimate that 3.1~3.6 mm represents the lower

end of the h_c range, based on the fact that the natural depth of the near-surface accumulation layer h_u is estimated to be 3 mm (Cameron and Carlile, 1977). It stands to reason that bioconvection will not occur in samples where $h < h_u$, since there would be no separation of fluid into density layers. Bioconvection theory also predicts that, for a given sample depth, there is a critical average concentration N_c, below which patterns will not form. However, as discussed previously, experimental determination of N_c is hindered by the fact that at lower concentrations, concentration bands become increasingly difficult to detect with the available equipment.

Several aspects of the observed zoospore pattern formation are not as readily explained by current bioconvection theory. We suspect that the variability in pattern shape was a function of the type of mixing used to homogenize suspension. Circular mixing may have resulted in residual bulk fluid motion that encouraged formation of circular bands. Alternatively circular mixing may have initially concentrated zoospore at the outer walls of the Petri dish, which would explain both the circular patterns and the apparent depletion of zoospores within circular bands (Fig. 4.1).

Ecological relevance of zoospore 'pattern swimming'. Zoospore 'pattern swimming' has not, as yet, been observed in natural environments, leading to the speculation that it is a laboratory artifact with limited ecological relevance (Carlile, 1983). While 'pattern swimming' is likely irrelevant to zoospores in soil, given the small size of soil pores (Kuznetsov and Jiang, 2003), the required conditions (>3 mm deep, quiescent water, high number density) do occur frequently in nature. Zoospores are commonly isolated from wetlands, puddles and ponds in both managed and unmanaged ecosystems, often in high concentrations.

If 'pattern swimming' does occur in nature, what function, if any, does it serve? It has been demonstrated that bioconvection, and bacterial motility in general, promotes fluid mixing and enhances diffusion of large particles (Kessler, 2000) and high molecular weight compounds (Kim and Breuer, 2004). However, bioconvection

was found to have no effect on the diffusion of oxygen (Janosi et al, 2002), perhaps because of oxygen's inherent high diffusivity. In any case, it is unclear how enhancing fluid mixing would benefit zoospores, which do not utilize external energy sources.

Rather, the benefit of "pattern swimming" and related behaviors for zoospores may lie in their concentrating effect. It has been demonstrated that a number of zoospore behaviors, including cohort recruitment during infection, are density-dependent (e.g. Galiana et al., 2008, Kong and Hong, 2010, Mitchell and Kannwischer-Mitchell, 1983). While it is speculated that bioconvection may contribute to cyst aggregate formation by funneling high numbers of zoospores to developing aggregates (Reid et al. 1995, Walkera and van West, 2007), the fact that patterns are not stationary, i.e. they move and change over fairly short time scales, suggests that they are not associated with cyst aggregates, which presumably are stationary. That said, gyrotaxis, not bioconvection *per se*, may play a role in zoospore recruitment during cyst aggregate formation or infection. As in the case of bioconvection, the mass movement of zoospores in a given direction may initiate fluid movement that "recruits" other zoospores via gyrotaxis, with the resulting feedback loop reinforcing zoospore movement in the given direction.

SUMMARY AND CONCLUSIONS

In the present investigation, we determined that the 'pattern swimming' of *P. citricola* zoospores was not due to phototaxis, Marangoni (surface tension-related) convection, or auto-attraction. Furthermore, our observations related to convective pattern, directional swimming, and depth- and concentration-dependence, suggest that the zoospore swarming behavior is an example of bioconvection involving both density instability due to the upward swimming tendency of the zoospores and rheotaxis/gyrotaxis.

It is important to note that the scope of conclusions to be drawn from this investigation is limited to the pattern swimming of *Phytophthora* zoospores in the absence of chemical or electrical signals. It has been demonstrated in numerous instances that zoospores exhibit taxis in the presence of chemical or electrical gradients. On this point, it is especially important to distinguish between 'pattern swimming', which has been shown here not to be due to auto-attraction, and cyst aggregate formation, for which there is growing evidence of auto-taxis (Gallana et al. 2008, Reid et al. 1995, Thomas and Peterson, 1990).

While the ecological significance of bioconvection remains uncertain, "pattern swimming" provides insight into aspects of zoospore behavior, particularly the interaction of biology and physics, which may be useful in understanding other phenomena in nature. These aspects include: (i) the concentrating effect of negative geotaxis (either mechanically or biologically induced) in the presence of an upper boundary (air-water or solid-water interface), (ii) the effects on fluid density of localized high concentrations of zoospores, (iii) the hydrodynamic focusing of zoospores due to gyrotaxis/rheotaxis in the presence of shear, and (iv) the feedback loop in which coordinated movements of zoospores create water currents which lead to further recruitment of zoospores.

ACKNOWLEDGEMENTS

This research was supported by a grant from the National Research Initiative of the USDA Cooperative State Research, Education, and Extension Service, Grant no. 1006-35107-17231.

LITERATURE CITED

Bees, M.A. and N.A. Hill. 1998. Linear bioconvection in a suspension of randomly swimming, gyrotactic micro-organisms. *Phys. Fluids.* 10:1864-1881.

Brasier, C.M., D.E.L. Cooke, and J.M. Duncan. 1999. Origin of a new *Phytophthora* pathogen through interspecific hybridization. *PNAS.* 96:5878-5883.

Brasier, C.M., D.E.L. Cooke, J.M. Duncan, and E.M. Hansen. 2003. Multiple new phenotypic taxa from trees and riparian ecosystems in *Phytophthora gonapodyides*-*P. megasperma* ITS Clade 6, which tend to be high-temperature tolerant and either inbreeding or sterile. *Mycol. Res.* 107: 277-290.

Brasier, C.M., S.A. Kirk, J. Delcan, D.E.L. Cooke, T. Jung, and W.A.M. In't Veld. 2004. *Phytophthora alni* sp. nov. and its variants: designation of emerging heteroploid hybrid pathogens spreading on *Alnus* trees. *Mycol. Res.* 108:1172-1184.

Burgess, T.I., M. Stukely, T. Jung, D. White, D. Huberli, and G.E. Hardy. 2010. Molecular characterization of a *Phytophthora* hybrid swarm in native ecosystems and waterways in Western Australia. *5th IUFRO Phytophthoras in Forests and Natural Ecosystems, Rotorua, New Zealand. Mar.* 7-12, 2010. (Abstr.)

Cameron J.N. 1979. Taxes of zoospores of the fungus Phytophthora. *Ph.D. thesis*, University of London. 169 pp.

Cameron, J.N., and M.J. Carlile. 1980. Negative chemotaxis of zoospores of the fungus Phytophthora palmivora*. J. Gen. Microbiol*. 120:347-353.

Carlile, M.J. 1983. Motility, taxis and tropism in *Phytophthora*. Pages 95-107 in: *Phytophthora*, Its Biology, Taxonomy, Ecology and Pathology. Erwin D.C., S. Bartniki-Garcia, P.H. Tsao, eds. American Phytopathological Society, St. Paul, Minnesota.

Childress, S., M. Levandowsky, E.A. Spiegel. 1975. Pattern formation in suspension of swimming micro-organisms. *J. Fluid Mech.* 69:595-613.

Galiana, E., S. Fourre, and G. Engler. 2008. *Phytophthora parasitica* biofilm formation: installation and organization of microcolonies on the surface of a host plant. *Environ. Microbiol.* 10:2164-2171.

Hill, N.A., and T.J. Pedley. 2005. Bioconvection. *Fluid Dynamics Res.* 37:1-20.

Hill, N.A., T.J. Pedley, and J.O. Kessler. 1989. The growth of bioconvection patterns in a suspension of gyrotactic micro-organisms in a layer of finite depth. *J. Fluid Mech.* 208:509-543.

Ho, H.H. and C.J. Hickman. 1967. Factors governing zoospore response of *Phytophthora megasperma* (*var. sojae*) to plant roots. *Can. J. Bot.* 45:1983-1994.

Janosi, I.M., A. Czirok, D. Silhavy, and A. Holczinger. 2002. Is bioconvection enhancing bacterial growth in quiescent environments? *Environ. Microbiol.* 4:525-531.

Jeffers, S.N., and S.B. Martin. 1986. Comparison of two media selective for *Phytophthora* and *Pythium* species. *Plant dis.* 70:1038-1043.

Jung, T. and T.I. Burgess. 2009. Re-evaluation of *Phytophthora citricola* isolates from multiple woody hosts in Europe and North America reveals a new species, *Phytophthora plurivora sp. nov*. *Persoonia*. 22:95-110.

Katsura, K. and Y. Miyata. 1966. Movements of zoospores of *Phytopthoracapsici* III: rheotaxis. *The scientific reports of Kyoto Prefectural University.*18:51-56.

Kawai, H., M. Kubota, T. Kondo, and M. Watanabe. 1991. Action spectra for phototaxis in zoospores of the brown alga *Pseudochorda gracilis*. *Protoplasma.* 161:17-22.

Kessler, J.O. 1985a. Co-operative and concentrative phenomena of swimming micro-organisms. *Contemp. Phys.* 26:147

Kessler, J.O. 1985b. Hydrodynamic focusing of motile algal cells. *Nature* (London). 313:218-220.

Kessler, J.O. 2000. Dynamics of swimming bacteria at low and high volume fractions. Pages 1284-1287 in: *"Differential equations"*. Fiedler, B., K. Groege, and J. Sprekels, eds. World Scientific, Singapore.

Khew, K.L. and G.A. Zentmyer. 1973. Chemotactic response of zoospores of five species of *Phytophthora*. *Phytopath.* 63:1511-1517.

Kim, M.J. and K.S. Breuer. 2004. Enhanced diffusion due to motile bacteria. *Phys. Fluids*. 16:L78-L81.

Ko, W.H. and M.J. Chan. 1974. Aggregation of *Phytophthora capsici* zoospores and their interaction with zoospores of *P. palmivora*. *J. Gen. Microbiol.* 80:549-551.

Ko, W.H. and L.L. Chase. 1973. Aggregation of zoospores of *Phytophthora palmivora*. *J. Gen. Microbiol.* 78:79-82.

Kong, P. and C. Hong. 2010. Zoospore density-dependent behaviors of *Phytophthora nicotianae* are autoregulated by extracellular products. *Phytopath*. 100:632-637.

Kuznetsov, A.V. and N. Jiang. 2003. Bioconvection of negatively geotactic microorganisms in a porous medium: the effect of cell deposition and declogging. *International Journal of Numerical Methods for Heat & Fluid Flow*. 13:341-364

Levandowsky, M., W.S. Childress, E.A. Spiegel, and S.H. Hunter. 1975. A mathematical model of pattern formation by swimming micro-organisms*. J. Protozool.* 22:296-306.

Lounsbury, J.A. 1927. A case of phenomenal zoospore behavior of an apparently sterile *Isoachlya* and a description of the plant. *Trans. of the Wisconsin Academy* 23:539-549.

Mitchell, D.J. and M.E. Kannwischer-Mitchell. 1983. Relationship of inoculum density of Phytophthora disease incidence in various hosts. Pages 259-269 in: *Phytophthora*, Its Biology, Taxonomy, Ecology and Pathology. Erwin D.C., S. Bartniki-Garcia, P.H. Tsao, eds. American Phytopathological Society, St. Paul, Minnesota.

Pedley, T.J. and J.O. Kessler. 1992. Hydrodynamic phenomena in suspensions of swimming microorganisms. *Ann. Rev. Fluid Mech.* 24:313-358.

Pedley, T.J., N.A. Hill, and J.O. Kessler. 1988. The growth of bioconvection patterns in a uniform suspension of gyrotactic micro-organisms. *J. Fluid Mech.* 195:223-237.

Petri, 1925.Osservazioni biologiche sulla '*Blepharospora cambivora*.' Reprinted from Ann R Ist Sup Agario e Forestale Ser. 2A in the *Review of Applied Mycology* 10:122-123 (1931).

Platt, J.R. 1961. "Bioconvection patterns" in cultures of free-swimming organisms. *Science.* 133:1766-1767.

Plesset , M.S. and C.G. Whipple. 1974. Viscous effects in Rayleigh-Taylor instability. *Phys. Fluids.* 17:1-7.

Plesset, M.S., and H. Winet. 1974. Bioconvection patterns in swimming microorganism cultures as an example of Rayleigh-Taylor instability. *Nature.* 248:441-443.

Reid, B., B.M. Morris, and N.A.R. Gow. 1995. Calcium-dependent, genus-specific, autoaggregation of zoospores of phytopathogenic fungi. *Experimental Mycol.* 19:202-213.

Roberts, A.M. 2006. Mechanisms of gravitaxis in Chlamydomonas. *Biological Bulletin* 210:78-80.

Singleton, L.L., J.D. Mihail, and C.M. Rush. 1992. Methods for research on soil borne phytopathogenic fungi. APS Press, St. Paul, Minn. 265 pp.

Thomas, D.D. and A.P. Peterson. 1990. Chemotactic auto-aggregation in the water mould *Achlya*. *J. Gen. Microbiol.* 136:847-853.

van West, P., A.A. Appiah, N.A.R. Gow. 2003. Advances in research on oomycete root pathogens. *Physiol. Molec. Plant Pathol.* **62:**99-113.

Walkera, C.A. and P. van West. 2007. Zoospore development in the oomycetes. *Fungal Biol. Rev.* 21:10-18.

Winet, H. and T.L. Jahn. 1972. On the origin of bioconvective fluid instabilities in *Tetrahymena* culture systems. *Biorheol*. 9:87-104.

Zentmeyer, G.A. 1961. Chemotaxis of zoospores for root exudates. *Science.* 133:1595-1596.

TABLES AND FIGURES

Table 4.1. Effect of sample depth on presence or absence of 'pattern swimming' of *Phytophthora citricola* zoospores.

Aliquot (mL)	Depth (mm)	Patterns?
3	1.5	No
5	2.5	No
6[a]	3.1	No
7	3.6	Yes
8	4.1	Yes
9	4.6	Yes
10	5.1	Yes

[a]Samples were subsequently transferred to smaller chambers (resulting sample depth = 5.0 mm) whereupon swimming patterns formed immediately.

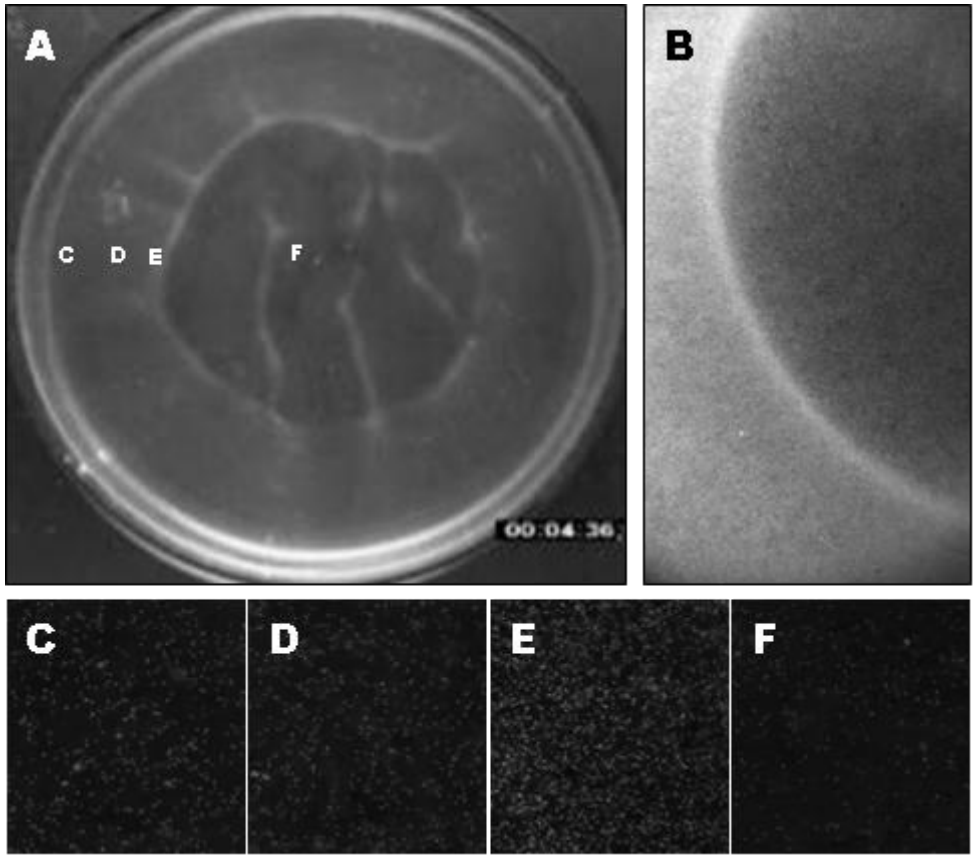

Figure 4.1. Formation of (A) macroscopic swimming 'patterns' by *Phytophthora citricola* zoospores, involving (B) the concentrating of zoospores in bands or nodes. Magnified images of zoospore suspension along a transect from (C) the outer edge of the petri dish, (D) near a concentration band, (E) within a concentration band, and (F) to the zoospore-depleted center of the suspension.

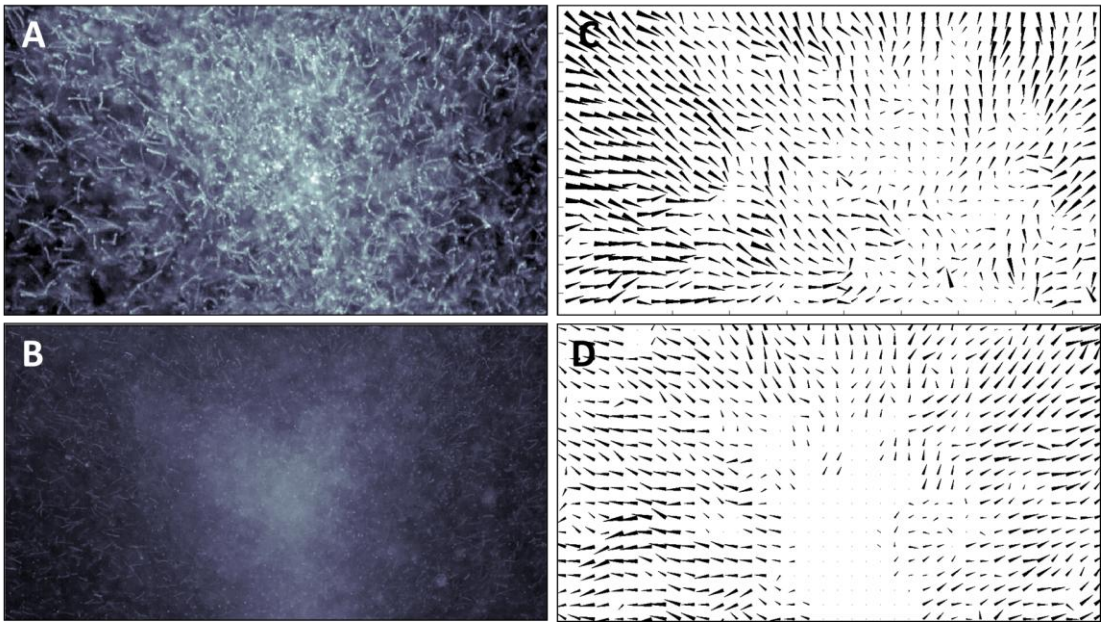

Figure 4.2. Time-lapse images of *Phytophthora citricola* zoospores in the vicinity of a concentration node (central white hazy area) captured (A) at the surface and (B) near the bottom of a suspension (image contrast has been adjusted to facilitate zoospore tracking). Locally averaged velocity vectors indicating the average swimming direction and velocity of zoospores (C) at the surface and (D) near the bottom of the zoospore suspension.

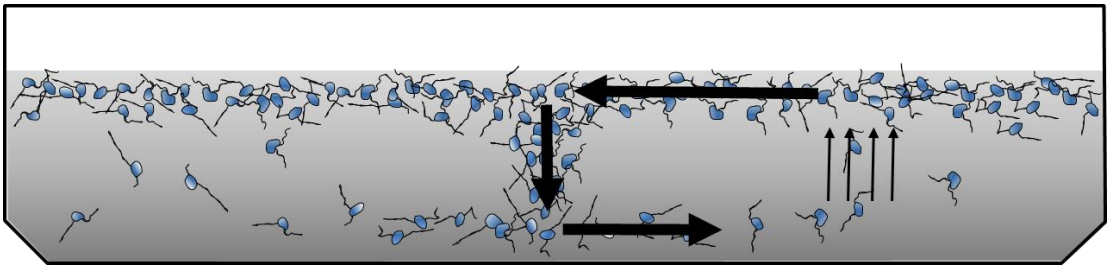

Figure 4.3. Convection pattern involving swarming of zoospores towards the concentration band (or node) at the surface of the suspension, downward movement of zoospores at the concentration band (or node), movement away from the concentration band deeper in the sample, and return of zoospores to the surface via negative geotaxis.

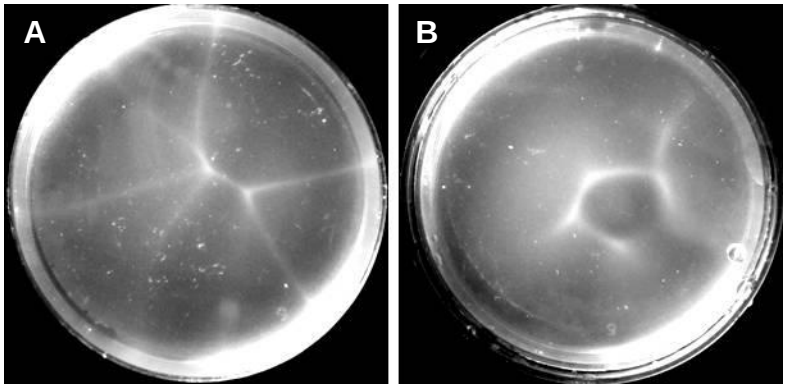

Figure 4.4. Pattern formation of Phytophthora citricola zoospores (A) in the absence of light and (B) in the Peri dishes covered with an acrylic lid to eliminate the air-water interface.

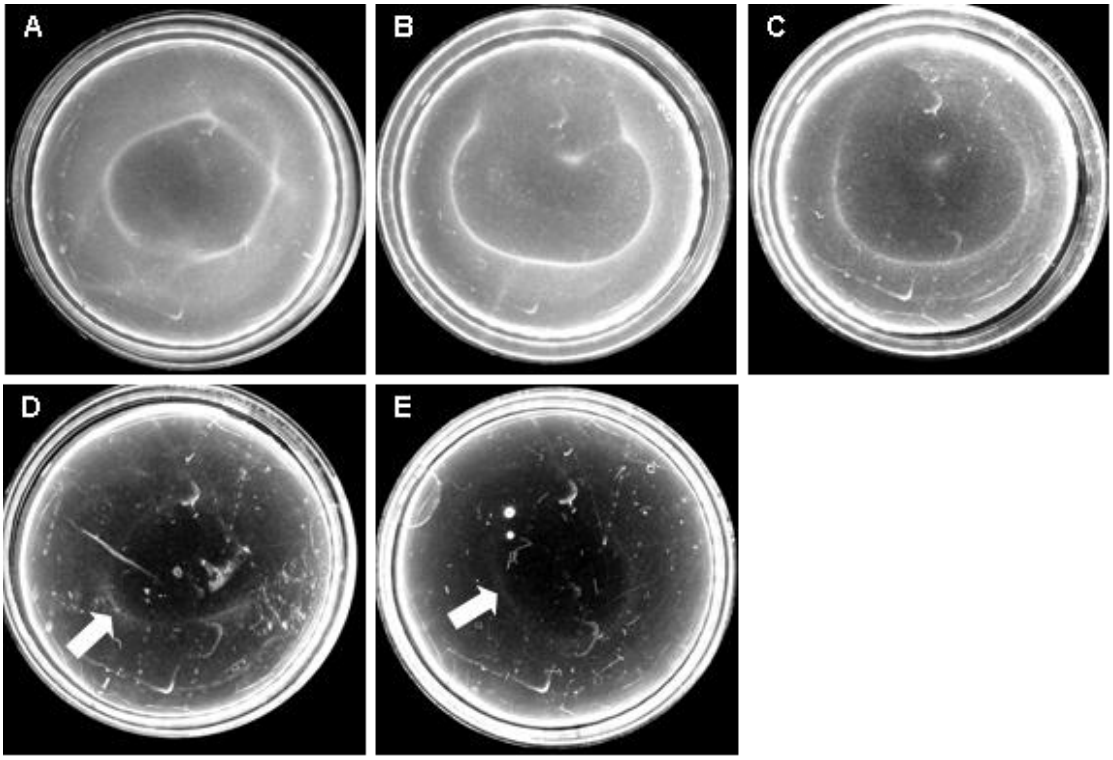

Figure 4.5. Pattern formation of *Phytophthora citricola* zoospore suspensions with initial (homogenized) concentrations of approximately (A) 3 x 10^5, (B) 1.5 x 10^5, (C) 3 x 10^4, (D) 6 x 10^3, (E) 3 x 10^3, and (F) 1.5 x 10^3 zoospores mL^{-1}. Arrows indicate location of concentration band.

Anomalous peak convergence of negatively geotactic *Phytophthora zoospores* during transport through saturated porous media

Naoyuki Ochiai, Jennifer L. Parke, and Maria Ines Dragila

Prepared for submission to Environmental Science and Technology
American Chemical Society Publications
1155 Sixteenth Street
N.W., Washington, DC 2003
Submission date TBD

ABSTRACT

The genus *Phytophthora* comprises over 50 plant pathogenic species with worldwide significance in both managed and unmanaged ecosystems. The dispersal of root-infecting *Phytophthora* spp. in soil, achieved by specialized motile propagules (zoospores) and involving both advection with infiltrating water and self-movement, remains poorly understood. Rather than dispersing as expected, zoospore plumes passed through a saturated 'ideal' soil exhibited 'convergence' characterized by plume narrowing, increase in peak concentration to above the input concentration, and a shift in the arrival time of the plume center relative to the fluid. Longitudinal zoospore velocity distributions generated from direct observations of zoospores in the presence of flow indicated that, at any point time, a certain portion of the zoospores were turned and swimming upstream, while the remainder were moving downstream. The proportion of upstream-turned zoospores declined from approximately 55% in the absence of flow to approximately 9% at an ambient fluid velocity of 275 $\mu m \cdot s^{-1}$. To explain plume convergence we propose that zoospores within a plume are relatively more able to turn and swim upwards, against a current, than zoospores at the plume edge. This plume position-dependent upward-swimming ability results in accumulation of zoospores at the trailing edge of a plume. Random walk simulations based on this conceptual model replicated, to a large degree, the observed plume convergence and flowrate-dependence of plume shape but systematically resulted in delayed plume arrival time. We conclude by discussing implications of this conceptual model for zoospore dispersal under realistic environmental conditions as well as for the coupled advection/swimming of other motile microorganisms in soil water.

Keywords: *Phytophthora*, zoospore, microbial transport, porous media, convergence

INTRODUCTION

The genus *Phytophthora* comprises over 50 foliar and root-infecting plant pathogenic species with significance worldwide in both managed and unmanaged ecosystems (Erwin and Ribeiro, 1996). Despite morphological and ecological similarities to fungi, *Phytophthora,* along with other Oomycetes, are placed in the Kingdom Stramenopiles, alongside aquatic brown algae and diatoms. The *Phytophthora* lifecycle features a water-requiring dispersive stage during which specialized unicellular motile spores (zoospores) are produced and released. For the majority of *Phytophthora spp*., which are root-infecting, this dispersal takes place in the soil and involves the combination of advective transport with the infiltrating water as well as active swimming. Despite the ecological importance of soil dispersal, the biological and physico-chemical processes governing zoospore movement in soil and other porous media remain relatively poorly understood. This is because the majority of research on zoospore motility has focused on specific aspects of zoospore behavior, including chemotaxis (e.g. Zentmeyer, 1961, Khew and Zentmeyer 1973), electrotaxis (Morris and Gow, 1993), negative geotaxis (Cameron and Carlile, 1977), and rheotaxis (Katsura and Miyata, 1966) in free-swimming zoospore suspensions or dispersal (Duniway, 1976, Newhook et al., 1981), early encystment (Ho and Hickman, 1967, Bimpong and Clerk, 1970, Young et al., 1979, Benjamin and Newhook, 1982), and chemotaxis (Allen and Newhook, 1973, Young et al., 1979) of zoospores confined in porous media, but in the absence of flow. Few studies have attempted to investigate zoospore behavior in porous media in the presence of flow (Young et al., 1979, Newhook et al., 1981) and little effort has been made to place these results in a broader theoretical context of porous media transport.

In contrast to the scarcity of information regarding zoospore transport, there is a growing body of research on the transport of protozoa, bacteria, viruses in porous media, motivated by the relevance of these processes to a broad range of disciplines

including bioremediation (Loffler and Edwards, 2006), water filtration (e.g. Hijnen et al., 2007), contaminant and pathogen transport (e.g. Semenov et al., 2009). Currently, our theoretical understanding of regarding macro-scale microbial transport, i.e. the spatio-temporal change in distribution of a population of microbes as they pass through a porous medium, borrows heavily from colloid filtration theory (CFT), which describes the retention, release, and transport of particles in porous media (Harvey and Garabedian, 1991). CFT, in turn, builds on the Advection Dispersion Equation (ADE) generally used to model transport of solutes through porous media. The ADE-CFT approach has been applied to microbial transport with limited success (Tufenkji, 2007). The morphology and metabolism of microorganisms pose numerous challenges to transport theory, including heterogeneity of microbe-grain interaction energies (e.g. Foppen et al., 2010), modification of porosity by biofilm formation (e.g. Hand et al., 2008), growth and decay of populations (e.g. Mercer et al., 1993), and enhanced diffusion or chemotaxis (e.g. Ford and Harvey, 2007), etc. (reviewed by Ginn et al., 2002). Some of these complications, such as variability of microbe-grain interaction energies (Tufenkji et al. 2003), may be dealt with within the ADE-CFT framework as long as they do not lead to violation of the assumption Fickian dispersion that underlies the ADE-CFT approach, however, other behaviors such as chemotaxis may result in non-Fickian plume dispersion and require alternative modeling techniques (Tufenkji, 2007).

Random walk models have been frequently employed to model the dispersal of a variety of biological agents, including microorganisms. A comprehensive review of the theory and application of random walk models in biological systems is provided by Codling et al. (2008). In the case of microorganisms, the random walk approach has been most commonly been employed to model bacterial chemotaxis in unrestricted space, either in the absence (e.g. D'Orsogna et al., 2003 , Nicolau et al., 2009) or presence of flow (e.g. Bearon, 2003 , Locsei and Pedley, 2009). Random walks have also been limitedly employed to simulate transport of bacteria through

porous media (Duffy et al., 1995) or in restricted pore-space (Kusy and Ford 2007). The Kusy and Ford (2007) investigation aptly illustrates a strength of the random walk approach, it inherent 'up-scaling', which enables researchers to simulate the behavior of populations, which is generally the scale of interest in transport studies, by specifying behaviors of individuals and characteristics of the micro-scale environment, which is typically the scale at which quantitative data is available.

In this study, we present an example of non-Fickian transport of *Phytophthora citricola* zoospores through saturated sand columns characterized by peak-narrowing (negative dispersion) and non-Gaussian distribution. The non-Fickian dispersion precludes the use of ADE-CFT-based analysis. We develop a 1-D, conditionally-biased random walk model to attempt to simulate the anomalous plume development, basing the behavior of individual zoospores on a novel conceptual model involving flow rate- and plume location-dependent upstream swimming of zoospores. Estimates for swimming parameters (upstream turning probabilities and swimming velocities) of within-plume zoospores are obtained by direction observations of zoospores in flow-cells. We evaluate the success of the random walk model as well as its inability to account for dispersion of the trailing tail. Finally, we consider the potential ecological implications of the behavior described by the conceptual model for *Phytophthora* zoospores, as well as for other motile microorganisms.

MATERIALS AND METHODS

Preparation of zoospore suspensions. *P. citricola Sawada*, isolate 98-517 (identified as *P. citricola III sensu* (Jung and Burgess, 2009) was isolated from rhododendron and cultured on PAR agar (Jeffers and Martin, 1986) amended with PCNB (66.7 $mg \cdot L^{-1}$) and hymexazol (25 $mg \cdot L^{-1}$). Multiple agar plugs were taken from the margins of an actively growing culture, transferred to clarified V8 broth (Singleton et al., 1992) and incubated statically for 2 to 3 days at room temperature

(17~20˚C). After rinsing the mycelial mats with filtered (0. μm) tap water, the clarified V8 broth was replaced with autoclaved water from Oak Creek, Corvallis, OR and samples were incubated in Petri dishes for 10 to 14 days, allowing for production of abundant zoosporangia. Zoospore release was induced by replacing the creek water with filtered tap water, chilling the cultures for 1 h at 4˚C, and then placing cultures at room temperature for 1 to 2 h. Prior to experiments, zoospore suspensions were filtered through a 20 μm nylon mesh to remove zoosporangia and hyphal debris. Final zoospores concentrations ranged between 5 x 10^5 and 1.5 x 10^6 mL^{-1}, with zoospores occupying between approximately 0.055 and 0.16% of the suspension volume.

Immotile particles, sand columns, and carrying solutions. Carboxylate-coated latex microspheres (10 μm Fluoresbrite, Polysciences Inc., Warrington, PA) similar in size to *P. citricola* zoospores were used to compare zoospore transport behavior with that of comparable immotile particles. Characteristics of the latex microspheres relevant to their transport are presented in comparison to those of zoospores in table 1. Columns consisted of acrylic tubes (5 cm inner diameter x 15 cm long) wet-packed with cleaned 40/50 Accusand™ (Unimin Corp., Canaan, CT) (Schroth et al, 1996). Sand cleaning involved removal of iron oxides by soaking sand in hot (~80°C) sodium diothionite solution, followed by removal of organic matter with 25% sodium hypochlorite solution (pH 9 ~ 10), and removal of residual contaminants with 6M HCl. After each step, the sand was thoroughly rinsed with distilled water. Sand was oven dried and stored in a covered container until packed into columns. The particle-free electrolyte- and carrying solution for zoospores and colloids in all experiments consisted of 2mM NaCl (1.6mM NaCl + 0.4 mM NaCO3) (pH ~ 9.0).

Column experiments. Before each trial, consisting of a bromide tracer run followed by a particle suspension run, at least 25 pore volumes (PV) of particle-free electrolyte solution was passed through the newly-packed column to ensure equilibrium conditions were reached. In addition, at least 10 PV of particle-free

electrolyte solution was run through columns between bromide tracer and particle suspension runs to ensure complete removal of tracer solution. Effluent from columns was collected using an automated fraction collector (Model 100, Amersham corp, GE Healthcare, Piscataway, NJ). A diluent containing concentrated $NaNO_3$ was added to bromide samples prior to bromide analysis using an ion-selective probe (NexSens Technology, Inc., Beaver Creek, OH). Concentrations of zoospore and microspheres in effluent fractions were analyzed with coulter counter (dual threshold model Z1, Beckman-Coulter Inc., Brea, CA) using a 50 μm aperture and measuring window between 7.5 and 12.5 μm. In order to prevent the lysis or encystment of zoospores after their collection, glutaraldehyde was first added to zoospore fractions prior to addition of Isoton II solution (Beckman Coulter), yielding a final glutaraldehyde concentration of 2%. Only Isoton II was added to latex particle fractions.

Visualization studies. Flow cells used in the visualization studies consisted of a chamber with a rectangular 4.0 x 1.6 mm cross-section, constructed by sandwiching a 1.6 mm-thick rubber gasket with inner open dimensions of 4.0 x 50 mm between a custom-made glass slide with inlet and outlet ports and a 50 x 25 mm glass cover slip. Particle-free solution and zoospore suspensions were introduced into the chamber via 1/16 in inner diameter Teflon tubing connected to a syringe pump (MicroCSP-3000, FIAlab Instruments, Bellevue, WA) fitted with a 1 mL syringe. Chambers were positioned vertically so that flow was downward. High definition digital video (1920 x 1080 pixels, 29.7 fps) was captured using a commercial video camera (HDR- Sony Corp USA, San Jose, CA) attached to a horizontally-mounted inspection microscope (Zoom 6000, Navitar Inc., Rochester, NY). Consecutive still images (10 to 15 frames) rendered from the videos were composited to enable semi-manual particle tracking and trajectory analysis using a custom Matlab program (Mathworks Inc., Natick, MA).

RESULTS

Bromide tracer and latex microsphere breakthrough. To establish baseline solute and particle transport characteristics of our columns, we first examined the breakthrough of bromide tracer and latex microspheres. Mass balance calculations indicated approximately 100% recovery of bromide for all trials and visual comparison of bromide breakthrough for all trials indicated a high degree of similarity in the dispersivity (~ $m^2 \cdot s^{-1}$) of each column.

A significant proportion of the latex microspheres were retained in the column (45%) even at the highest flow rate (43 $m \cdot d^{-1}$) (Fig. 5.1A). Retention of colloids in porous media under unfavorable chemical conditions is frequently observed (e.g. Johnson et al., 2007) and is attributed to a variety of mechanisms including straining (Bradford et al., 2002), retention in the secondary energy minimum (e.g. McDowell-Boyer, 1992, Hahn et al, 2004, Tufenkji and Elimelech, 2005), retention at grain-to-grain contacts (Tong et al., 2008, Torkzaban et al., 2008), or attachment to heterogeneous nanodomains of grain surfaces (Duffadar and Davis, 2007 and 2008). Given that the particle-to-grain ratio in our experiments was on the order of 0.01, it is likely that some microspheres were physically removed from the bulk fluid via straining (Bradford et al., 2004). The correlation of retention and flow rate, however, suggests that at least some portion of retention was also due to one or more of the three latter mechanisms, which are tied to flow rate via their dependence on local hydrodynamic shear (Johnson et al., 2007, Torkzaban et al., 2008).

For all flow rates greater than 10.8 $m \cdot d^{-1}$ (125 $\mu m \cdot s^{-1}$), the mean transport velocity of microspheres, as indicated by the arrival time of the center mass of the plume, exceeded that of the conservative tracer by approximately 10%. “Early breakthrough” or “enhanced transport” of particles is a commonly observed in porous media transport studies, and is generally attributed to the size-dependent exclusion of particles from low-velocity regions near pore walls (Small, 1974), migration of particles away from pore walls towards faster, central streamlines due

to counterbalancing effects of particle rolling and hydrodynamic lift (Grindrod, et al., 1996, DiCarlo et al., 2007) and from low-velocity pathways having narrow entrances (Sirivithayapakorn and Keller, 2003). An alternative explanation is that velocity enhancement is an artifact of particle retention and results from the preferential removal of particles sampling low-velocity regions from the suspended particle population, leaving only the faster-traveling particles to exit the medium (Zhang et al., 2001). Visual inspection of the shape of the breakthrough curves confirms that dispersion of the microspheres is approximately Fickian and similar to that of the conservative tracer (Fig 5.1A).

Zoospore breakthrough. At all flow rates other than 5.4 $m \cdot d^{-1}$ (63 $\mu m \cdot s^{-1}$), recovery of zoospores was significantly higher than for latex microspheres (Fig 5.1B). This higher recovery can be attributed to the ability of zoospores to avoid the low-flow regions and straining sites that normally serve as retention sites for passively-transported particles. Similar reduction in retention rate has been observed for motile bacteria with, however, the opposite dependence of retention rate on flow rate (Camesano and Logan, 1998). In our study, the high rate of zoospore retention at the lowest flow rate may be due to zoospore encystment. During the process of encysting, zoospores develop a 'sticky' outer surface that greatly enhances their likelihood of attachment. Zoospores typically encyst in presence of a chemical stimulant, but also encyst spontaneously in the absence of such signals over a time scale of hours to days (Bimpong and Clerk, 1970). Zoospores of some *Phytophthora spp*. (Ho and Hickman, 1967, Bimpong and Clerk, 1970) but not others (Young et al., 1979, Benjamin and Newhook, 1982) encyst more rapidly when confined in porous media, presumably due to the 'contact stimulus' from repeated colloids with grain walls. Our observations are not inconsistent with early encystment due to 'contact stimulus', as the lower flow rate results in longer confinement of zoospores in the column and greater opportunity for collisions with pore walls. However, the drastic

difference in ‘retention’ between the two lowest flow rates casts some doubt on the validity of this interpretation.

In contrast to the microspheres, the mean transport velocity of the zoospores appeared to be sensitive to flowrate. For all but the highest flow rate, the mean velocity of the zoospore plume was slightly less than that of the conservative tracer (Fig. 5.1B). Flowrate-dependent retardation is also observed in the transport of solutes and colloids and is commonly attributed to the transient sorption of the solute or particles to media surfaces. However, two observations suggest that a different mechanism is involved in the zoospore case. First, as evidenced by the breakthrough curves at the three slowest flow rates (5.4, 10.8, 21.5 $m \cdot d^{-1}$) in Fig. 5.1B, the last arrival of the zoospore plume seems to coincide with the last arrival of the tracer plume. Retardation due to transient sorption should result in a consistent rearward shift (delay) of the entire plume, including the slowest elements, with decreasing flow rate. Second, at the highest flow rate, the mean arrival time of the zoospore plume is earlier than that of the tracer plume. Assuming that the same mechanism responsible for the plume ‘retardation’ is responsible for plume ‘acceleration’, this cannot be transient sorption. The terms ‘acceleration’ or ‘retardation’ may be inappropriate here, since the shift in the arrival time of the zoospore plume center perhaps does not reflect a global acceleration or retardation of the plume, but rather is a consequence of the change in the distribution of zoospores within the plume.

The most notable features of the zoospore breakthrough curves are the plume narrowing and increase in peak concentration and anisotropic dispersion. For lack of a better term, we will subsequently refer to the peak narrowing/concentrating as ‘plume convergence’. As far as we know, this is the first report of plume convergence, i.e. negative dispersion, in the microbial transport literature. As previously discussed, such non-Fickian dispersion is not readily handled within an ADE-CFT framework. Furthermore, there is no recognized mechanism that might

account for this type of anomalous transport. At first glance, the plume convergence suggests the involvement of an *anti*-entropic biological mechanism. Bacteria have been demonstrated to auto-aggregate due to chemical signaling (e.g. Ben-Jacob, et al., 2000). Zoospores in free swimming suspensions have been observed to spontaneously form concentrated swimming masses (Ko and Chan, 1974), however, this has been demonstrated to be an example of bioconvection resulting from zoospore morphology, swimming behavior, and hydrodynamics rather than auto-attraction (Ochiai et al. submitted). Having failed to identify a mechanism to explain plume convergence elsewhere, we endeavored to develop a simple conceptual model based on the behavior of individual zoospores that, when summed over a population, would be capable of explaining the observed anomalous plume behavior.

Direct observations of zoospore movement in the presence of flow. As a first step to developing our conceptual model, we directly observed zoospores in downward flow over a range of ambient fluid velocities, focusing on longitudinal swimming velocities and the ability to turn and swim upstream. Longitudinal velocity distributions typically appeared to consist of two overlapping velocity peaks, which we interpreted to represent the subpopulations of zoospores swimming upstream and downstream at the time of sampling (Fig. 5.2). In the absence of flow, the proportion of upstream-turned zoospores slightly exceeded that of downstream-turned zoospores (Fig. 5.2A), However, the proportion of upstream-turned zoospores declined with increasing ambient fluid velocity (Fig 5.2B to E). Mean downstream zoospore velocity exceeded mean fluid velocity at all but the highest (275 $\mu m \cdot s^{-1}$) ambient fluid velocity, although the magnitude of velocity excess declined with increasing ambient fluid velocity (Fig. 5.2 and 5.3A). In contrast, mean upstream zoospore velocity appeared to increase slightly with ambient fluid velocity (Fig 5.2 & 5.3B). Overall mean zoospore velocity was consistently lower than the mean fluid velocity.

The above results indicate that the longitudinal velocity of zoospores in moving fluid is not simply the sum of fluid and swimming velocities. In the downstream case, it appears that the relative contribution of zoospore swimming to downstream translocation decreases with increasing fluid velocity and may become inconsequential above a threshold velocity. Interpretation of the upstream results is less clear cut. The apparent increase in upstream swimming velocity is concomitant with a decrease in the proportion of upstream turning zoospores. Kessler's (1985a) analysis of the swimming orientation of negatively geotactic algae in a non-uniform flow field provides a plausible mechanistic explanation for the decline in upstream-turning zoospores in shear flow. Briefly, let us assume that the center of gravity of zoospores is offset from the center of rotation/buoyancy (as represented in Fig. 5.4A) and that the flagella are unimportant to this behavior. In the absence of flow, a tilted zoospore will tend to reorientate upwards, due to the gravitational torque on the zoospore body (Fig. 5.4A). A similar reorientation will occur in the presence of uniform flow (Fig. 5.4B). Viscous flow generates drag on the zoospore body, but because the flow is uniform, the torque on anterior and posterior portions of the zoospore cancel each out leaving gravitational torque as the single determinant of orientation. However, if flow is non-uniform, a zoospore may experience a torque due to differential drag on anterior and posterior portions of the body. Below a critical shear, the torque due to differential drag will be insufficient to overcome the gravitational torque and zoospores will assume the preferred, upstream-pointing orientation (Fig. 5.4C). However, above a critical shear, the torque due to differential drag will exceed the gravitational torque, causing zoospores to rotate in the direction of higher drag (Fig. 5.4D). Eventually, a zoospore's center of gravity will lie above its center of geometry. At this point, the gravitational torque and the torque due to differential drag act in the same direction, causing the zoospore to rapidly flip back to the upstream-pointing orientation. This tumbling disrupts the zoospores' ability to keep pointed and to swim upstream. At higher fluid velocities, then, a

larger portion of the flow will have sufficient shear to initiate zoospore tumbling and hinder upstream swimming and thus fewer zoospores will be pointed upstream.

Modeling longitudinal zoospore velocity distributions based on the observed relationship between mean downstream swimming velocity and mean fluid velocity (Fig. 5.3A) and the reorientation mechanism described above, whereby zoospores on fluid streamlines above a critical velocity (150 $\mu m \cdot s^{-1}$) are prevented from swimming upstream, yields reasonably good fits to the data (dashed lines in Fig. 5.2A to E). This critical fluid velocity was chosen based on its proximity to the average free-swimming velocity of zoospores used in this study as well as the velocity above which zoospores appeared to be unable to swim upstream (Katsura and Miyata, 1966). Importantly, the best fit was achieved when zoopores on streamlines above the critical velocity were simply reoriented downstream and not to set to 'tumble.' Also, best fit of the peak representing the upstream-turned subpopulation was achieved when the contribution of advection to longitudinaly translocation was reduced by a factor of 0.25.

CONCEPTUAL MODEL

The direct observations provide critical information regarding zoospore behavior in the presence of flow but do not, in themselves, explain the macro-scale plume convergence observed in the column breakthrough experiments. The shape of the breakthrough curves suggests that zoospores accumulated at the trailing edge of the plume (Fig. 5.1B). Zoospores are negatively geotactic and, thus, have been demonstrted to accumulate at a physical upper boundary such as an air-water interface (Ho and Hickman, 1967, Cameron and Carlile, 1977). However, in our transport experiments there is obviously no physically boundary separating the zoospore plume from the pursuant fluid. Our direct observations suggest a shear-based mechanism by which zoospores are prevented or hindered from turning upstream or swimming upstream. Thus, to explain the apparent accumulation of

zoospore at the trailing edge of the plume, we propose that zoospores at the plume edge (henceforth 'edge zoospores' or 'eZsp') are more susceptible, for whatever reason, to shear-induced reorientation than zoospores within the plume ('internal zoospores' or 'iZsp') (Fig. 5.5). We speculate that this is due to a reduction in shear resulting from disruption of fluid organization by the presence of high numbers of zoospores within the plume.

Traditional analysis of the potential influence of individual zoospores on fluid organization based on the particle Reynolds number (in this case $Re_p << 1$) indicates that the presence of zoospores should have negligible impact on fluid structure and that flow should remain laminar within a plume. Recent research, however, brings into question the assumption that motile organisms do not impact the fluid around them. There is growing evidence that, unlike passive particles, motile microorganisms, have some influence on the surrounding fluid through motion of their cilia, flagella, or bodies. In concentrated suspensions, the cumulative action of individuals can influence macroscopic properties of the suspending fluid. This influence ranges from enhanced mixing (Wu and Libchaber, 2000, Kim and Breuer, 2004, Saintillan & Shelley, 2008), to changes in fluid viscosity (Sokolov & Aronson, 2009, Rafai et al., 2010) or development of turbulence (Cisneros et al., 2007, Wolgemuth, 2008). These effects are just now being recognized and are still poorly understood. In the context of our conceptual model, we simply point to these results as evidence of the general principle that concentrated populations of motile microorganisms may alter their fluid environment. It is possible that such changes could lead to the postulated difference in swimming abilities of edge and internal zoospores.

RANDOM WALK SIMULATIONS

In order to investigate whether and under what conditions differences in upstream turning or swimming velocity of edge and internal zoospores would be expected to result in peak convergence, we developed a 1-D uncorrelated random walk algorithm, with behavioral rules based on the conceptual model presented above. We tracked the development of zoospore plumes, consisting of 10,000 individuals, initially distributed as a step input. At each time step, the position of each zoospore was assessed relative to the trailing edge of the plume, defined as the location of the slowest zoospore. The probability of turning upstream ($0 \leq P_{up} \leq 1$) was calculated for each zoospore based on its position, such that the turning probability increased linearly from the user-defined P_e for zoospores at the trailing edge to the model-defined P_i for zoospores 10 or more length units ahead of the trailing edge. For each upstream-turned zoospore, step length was calculated as a linear combination of advection (positive) and swimming (negative) velocities, both drawn from model-defined normal distributions. The relative influence of advection ($0 \leq \alpha \leq 1$) was calculated for each zoospore based on its position, such that the influence decreased linearly from the user-defined α_e for zoospores at the trailing edge to the model-defined α_e for zoospores 10 or more length units ahead of the trailing edge. For each downstream-turned zoospore, regardless of position within the plume, step length was drawn from a model-defined normal distribution. The model-defined parameters (P_i, α_i, μ_{up}, μ_{down}) were obtained from direct observations of zoospores.

In the first set of simulations, the turning probability of trailing edge zoospores was set equal to that of internal zoospores ($P_e = P_i = 0.21$), while we introduced a position-dependent bias in the influence of advection of trailing edge zoospores (α_e = 1, 0.75, 0.5, 0.25) (Fig. 5.6A). Physically, this represents the case where zoospores near the trailing edge experience no additional resistance to turning upstream compared to the internal zoospores, however, encounter relatively greater difficulty

moving against the current. As is evident from the results, alteration of α_e does not result in plume convergence, but does influence the plume arrival time.

In the second set of simulations, the influence of advection on trailing edge zoospores was set equal to that of internal zoospores ($\alpha_e = \alpha_i = 0.25$), while we introduced a position-dependent bias in the turning probability of trailing edge zoospores (P_e = 0.0, 0.01, 0.02, 0.03, 0.04, 0.05) (Fig. 5.6B). Physically, this represents the case where zoospores near the trailing edge experience relatively greater difficulty in turning upstream. Once turned upstream, however, trailing edge zoospores are able to swim as effectively as internal zoospores. Plume convergence occurs when the upstream turning probability of trailing edge zoospores is less than or equal to 0.02. Plume skewing, without increase in peak concentration to above the input concentration, is apparent when P_e = 0.03 and 0.05 (Fig. 5.6B).

In the third series of simulations we simultaneously examined the impacts of α_e and P_e on generation of anomalous behavior (Fig. 5.7). As indicated in the previous simulations, it is apparent that plume convergence occurs only when P_e is 0.01 or less. Interestingly, plume convergence only occurs when the influence of advection on edge zoospores is minimal ($\alpha_e \leq 0.4$).

In the final set of simulations, we examined whether the conceptual model could account for changes in characteristics of zoospores breakthrough with respect to flow rate observed in our column experiments. we identified the following trends with respect to flow rate in the column experiments (Fig. 5.1B): (i) substantial retardation of the plume at the lowest flow rate (5.4 $m \cdot d^{-1} \approx 65\ \mu m \cdot s^{-1}$), (ii) plume arrival times similar to that of the bromide tracer at higher flow rates (125, 250, 375, and 500 $\mu m \cdot s^{-1}$), (iii) shifting peak arrival time, from slightly delayed (125, 250, and 375 $\mu m \cdot s^{-1}$) to slightly accelerated (500 $\mu m \cdot s^{-1}$) relative to the arrival of the bromide peak, (iv) maximum peak height at middle flow rate (250 $\mu m \cdot s^{-1}$), (v) decreasing skewness at two highest superficial velocities (375 & 500 $\mu m \cdot s^{-1}$). Next, using the

model of zoospore swimming parameters as a function of ambient fluid velocity developed from direct visualizations, we estimated the turning probability and longitudinal velocities (for both upstream- and downstream-turned zoospores) of internal zoospores for ambient fluid velocities ranging between 25 and 300 $\mu m \cdot s^{-1}$**.** Lastly, we performed a series of simulations over the same range of fluid velocities with the turning probability (P_e) influence of advection (α_e) set to 0.0 and 0.25, respectively, for edge zoospores.

Plumes at the two lowest ambient fluid velocities (50 and 75 $\mu m \cdot s^{-1}$) exhibited significant retardation (Fig. 5.8). Similar plume arrival times were observed for higher fluid velocities (≥ 100 $\mu m \cdot s^{-1}$). At these ambient fluid velocities, peak arrival time shifted slightly with increasing fluid velocity. Interestingly, remarkably similar peak arrival time was observed in the case of several fluid velocities (100, 125 125, and 175 $\mu m \cdot s^{-1}$). Significant peak convergence (marked by a peak height greater than 1 and significant rightward skewness) was observed for fluid intermediate velocities ranging from 75 to 175 $\mu m \cdot s^{-1}$. At higher velocities (≥ 200 $\mu m \cdot s^{-1}$), plumes exhibited decreasing skewness and lowered peak height. These trends are qualitatively consistent with the trends observed in the column breakthrough data (Fig. 5.1B).

SUMMARY AND CONCLUSIONS

The plumes of negatively geotactic *Phytophthora* zoospores developed the following anomalous characteristics as they passed through saturated sand columns: (i) significantly less retention than similar-sized latex microspheres, (ii) flow-rate-dependent shift of the plume centroid relative to the conservative tracer, (iii) increase in plume concentration (negative dispersion), and (iv) apparent anistropic dispersion exhibiting a steeply falling trailing tail. To explain this anomalous breakthrough, we proposed that zoospores at the trailing edge of a plume encounter greater resistance to turning or swimming upstream than zoospores within the plume. This effectively prevents the zoospore plume from mixing with the

pursuant fluid. Monte Carlo simulations demonstrated that reduction in either turning probability or upstream swimming velocity of trailing eZsp could result in retardation, concentration, and non-Gaussian distribution of a plume similar to that observed in experiments.

We recognize that the mere fact that our model could simulate experimental results does not validate the underlying conceptual model. It is entirely possible that the underlying premise of our model is incorrect, or that it is phenotypically correct but involves an altogether different mechanism. While this paper appears to be the first report of plume-concentrating transport, the phenomenon may not be unique to *Phytophthora* zoospores and may simply be as-yet-unrecognized in other negatively geotactic organisms. Thus, further experimental investigation is necessary to gain a better understanding of not only this phenomenon but the ensemble of motility-related phenomena that can influence macro-scale transport behavior. The inability of our model to correctly simulate development of the trailing tail, which may be the result of pore- and network-scale velocity heterogeneity, highlights the importance of understanding and accounting for the multiple scales of heterogeneity inherent in porous media.

Finally, a word on the significance of these findings specifically for *Phytophthora* spp. It has long been suspected that motility enables zoospores to more effectively disperse and find new infection sites or new hosts. Motility clearly reduces removal of zoospores by the porous media via straining or capture in low-flow zones, to which immotile particles are susceptible. This presumably allows zoospores more time to discover potential host tissues. Our results indicate that if the mean velocity of the infiltrating water is greater than the zoospore swimming speed (120 $\mu m \cdot s^{-1}$), a zoospore plume will be advected downstream at approximately the fluid velocity. However, if the mean velocity of the infiltrating water is less than the zoospore swimming speed, a zoospore plume will be advected at a significantly slower speed or not advected at all. An infiltration rate of 120 $\mu m \cdot s^{-1}$ is predicted for well-sorted

fine sands. Zoospores, then, would not be expected to be advected rapidly through finer-textured soils, unless they contain significant macropores. Retarded or negligible advection would enable zoospores to remain near the soil surface, i.e. in the root zone, as suspected (Carlile, 1983).If there is standing water, zoospores may largely remain in the free surface water, where they can be transported significant distances across the soil surface (Neher and Duniway, 1992: Roberts et al., 2005). The same negative geotaxis that enables zoospores to remain near the soil surface also results in a biophysical concentrating of zoospore populations, both in the presence and absence (Ochiai et al., (bioconvection paper)) of flow. Such concentrating may be ecologically important, given that some zoospore behaviors, including cohort recruitment during infection, have been demonstrated to be density-dependent (e.g. Mitchell and Kannwischer-Mitchell, 1983, Galiana et al., 2008, Kong and Hong, 2010).

ACKNOWLEDGEMENTS

This research was supported by a grant from the National Research Initiative of the USDA Cooperative State Research, Education, and Extension Service, Grant no. 1006-35107-17231.

LITERATURE CITED

Allen, R.N. and J.D. Harvey. 1973. Negative chemotaxis of zoospores of *Phytopthora cinnamomi*. *J. Gen. Microbiol*. 84:28-38.

Bearon, R.N. 2003. An extension of generalized Taylor dispersion in unbounded homogeneous shear flows to run-and-tumble chemotactic bacteria. *Phys. Fluids*. 15:1552-1563.

Ben-Jacob, E., I. Cohen, and H. Levine, H. 2000. Cooperative self-organization of microorganisms. *Adv. Phys*. 49:96-554.

Benjamin, M. and F.J. Newhook. 1982. Effect of glass microbeads on *Phytophthora* zoospore motility. *Trans. Br. Mycol. Soc.* 78:43-46.

Bimpong, C.E. and G.C. Clerk. 1970. Motility and chemotaxis in zoospores of *Phytophthora palmivora* (Butl.) Butl. *Ann Bot London*. 34:617-624.

Bradford, S.A., M. Bettahar, J. Simunek, and M.T. van Genuchten. 2004. Straining and attachment of colloids in physically heterogeneous porous media. *Vadose Zone J*. 3**:**384-394.

Bradford, S.A., S.R. Yates, M. Bettahar, and J. Simunek. 2002. Physical factors affecting the transport and fate of colloids in saturated porous media. *Water Res. Res.* 38(12):1327.

Cameron, J.N., and M.J. Carlile. 1980. Negative chemotaxis of zoospores of the fungus Phytophthora palmivora*. J. Gen. Microbiol*. 120:347-353.

Camesano, T. and B.E. Logan. 1998. Influence of fluid velocity and cell concentration on the transport of motile and nonmotile bacteria in porous media. *Environ. Sci. Technol*. 32:1699-1708

Carlile, M.J. 1983. Motility, taxis and tropism in *Phytophthora*. Pages 95-107 in: *Phytophthora*, Its Biology, Taxonomy, Ecology and Pathology. Erwin D.C., S. Bartniki-Garcia, P.H. Tsao, eds. American Phytopathological Society, St. Paul, Minnesota.

Cisneros, L.H., R. Cortex, C. Dombrowski, and R.E. Goldstein. 2007. Fluid dynamics of self-propelled microorganisms, from individual to concentrated populations. *Exp. Fluids.* 43:737-753.

Codling, E.A., M.J. Plank, and S. Behamou. 2008. Random walk models in biology. *J. R. Soc. Interface*. 5:813-834.

Di Carlo, D., D. Irimia R.G. Tompkins, and M. Toner. 2007. Continuous inertial focusing, ordering, and separation of particles in microchannels. *PNAS*. 104:18892-18897.

D'Orsogna, M.R., M.A. Suchard, and T. Chou. 2003. Interplay of chemotaxis and chemokinesis mechanisms in bacterial dynamics. *Phys. Rev. E*. 68:021925.

Duffadar, R.D., and J.M. Davis. 2008. Interaction of micrometer-scale particles with nanotextured surfaces in shear flow. *J. Colloid and Interface Sci.* 308:20-29.

Duffadar, R.D., and J.M. Davis. 2008. Dynamic adhesion behavior of micrometer-scale particles flowing over patchy surfaces with nanoscale electrostatic heterogeneity. *J. Colloid and Interface Sci*. 326:18-27.

Duffy, K.J., R.M. Ford, and P.T. Cummings. 1997. Residence time calculation for chemotactic bacteria within porous media. *Biophys. J*. 73:2930-2936.

Duniway, J.M. 1976. Movement of zoospores of *Phytophthora cryptogea* in soils of various textures and matric potentials. *Phytopathol*. 66:877-882.

Erwin, D.C. and O.K. Ribeiro. 1996. Phytophthora diseases worldwide. APS Press, St. Paul, Minn. 562 pp.

Foppen, J.W., G. Lutterodt, and W.F.M. Roling. 2010. Towards understanding inter-strain attachment variations of *Eshcerichia coli* during transport in saturated quartz sand. *Water Res*. 44:1202-1212.

Ford, R.M. and R.W. Harvey. 2007. Role of chemotaxis in the transport of bacteria through saturated porous media. *Adv. Water Res*. 30:1608-1617.

Galiana, E., S. Fourre, and G. Engler. 2008. *Phytophthora parasitica* biofilm formation: installation and organization of microcolonies on the surface of a host plant. *Environ. Microbiol.* 10:2164-2171.

Ginn, T.R., B.D. Wood, K.E. Nelson, T.D. Scheibe, E.M. Murphy, and T.P. Clement. 2002. Processes in microbial transport in the natural subsurface. *Adv. Water Res*. 25:1017-1042.

Grindrod, P., M.S. Edwards, J.J.W. Higgo, and G.M. Williams. 1996. Analysis of colloids and tracer breakthrough curves. *J. Contamin. Hydrol*. 21:243-253.

Hahn, M.W., D. Abadzic, and C.R. O'Melia. 2004. Aquasols: on the role of secondary minima. *Environ. Sci. Technol*. 38:5915-5924.

Hand, V.L., J.R. Lloyd, D.J. Vaughan, M.J. Wilkins, and S. Boult. 2008. Experimental studies of the influence of grain size, oxygen availability and organic carbon availability on bioclogging in porous media. *Environ. Sci. Technol*. 42:1485-1491.

Harvey, R.W. and S.P. Garabedian. 1991. Use of colloid filtration theory in modeling movement of bacteria through a contaminated sandy aquifer. *Environ. Sci. Technol*. 25:178-185.

Hijnen, W.A.M., Y.J. Dullemont, J.F. Shijven, A.J. Hanzens-Brower, M. Rosielle, and G. Medema. 2007. Removal and fate of *Cryptosporidium parvum*, *Clostridium perfringens* and small-sized centric diatoms (*Stephanodiscus hantzschii*) in slow sand filters. *Water Res.* 41:2151-2162.

Ho, H.H. and C.J. Hickman. 1967. Factors governing zoospore response of *Phytophthora megasperma* (*var. sojae*) to plant roots. *Can. J. Bot.* 45:1983-1994.

Jeffers, S.N., and S.B. Martin. 1986. Comparison of two media selective for *Phytophthora* and *Pythium* species. *Plant dis.* 70:1038-1043.

Johnson, W.P., M. Tong, and X. Li. 2007. On colloid retention in saturated porous media in the presence of energy barriers: the failure of α, and opportunities to predict η. *Water Res. Res*. 43:W12813.

Jung, T. and T.I. Burgess. 2009. Re-evaluation of *Phytophthora citricola* isolates from multiple woody hosts in Europe and North America reveals a new species, *Phytophthora plurivora sp. nov*. *Persoonia*. 22:95-110.

Katsura, K. and Y. Miyata. 1966. Movements of zoospores of *Phytopthoracapsici* III: rheotaxis. *The scientific reports of Kyoto Prefectural University.*18:51-56.

Khew, K.L. and G.A. Zentmyer. 1973. Chemotactic response of zoospores of five species of *Phytophthora*. *Phytopath.* 63:1511-1517.

Kim, M.J. and K.S. Breuer. 2004. Enhanced diffusion due to motile bacteria. *Phys. Fluids*. 16:L78-L81.

Ko, W.H. and M.J. Chan. 1974. Aggregation of *Phytophthora capsici* zoospores and their interaction with zoospores of *P. palmivora*. *J. Gen. Microbiol.* 80:549-551.

Kong, P. and C. Hong. 2010. Zoospore density-dependent behaviors of *Phytophthora nicotianae* are autoregulated by extracellular products. *Phytopath*. 100:632-637.

Kusy, K. and R.T. Ford. 2007. Monte Carlo simulations derived from direct observations of individual bacteria inform macroscopic migration models at granular porous media interfaces. *Environ.Sci. Technol*. 41:6403-6409.

Locesi, J.T. and T.J. Pedley. 2009. Run and tumble chemotaxis in a shear flow: the effect of temporal comparisons, persistence, rotational diffusion, and cell shape. *Bull. Math. Biol*. 71:1089-1116.

Loffler, F.E. and E.A. Edwards. 2006. Harnessing microbial activities for environmental cleanup. *Curr. Opin. Biotechnol.* 17:274-284.

McDowell-Boyer, L.M. 1992. Chemical mobilization of micron-sized particles in saturated porous media under steady flow conditions. *Environ Sci. Technol*. 26:586-593.

Mercer, J.R., R.M. Ford, J.L. Stitz, and C. Bradbeer. 1993. Growth rate effects on fundamental transport properties of bacterial populations. *Biotechnol. Bioeng*. 42:1277–86.

Mitchell, D.J. and M.E. Kannwischer-Mitchell. 1983. Relationship of inoculum density of Phytophthora disease incidence in various hosts. Pages 259-269 in: *Phytophthora*, Its Biology, Taxonomy, Ecology and Pathology. Erwin D.C., S. Bartniki-Garcia, P.H. Tsao, eds. American Phytopathological Society, St. Paul, Minnesota.

Morris, B.M. and N.A.R. Gow. 1993. Mechanism of electrotaxis of zoospores of phytopathogenic fungi. *Phytopathol*. 83:77:882.

Neher, D. and J.M. Duniway. 1992. Dispersal of *Phytophthora parasitica* in tomato fields by furrow irrigation. *Plant Dis*. 76:582-586.

Newhook, F.J., B.R. Young, S.D. Allen, and R.N. Allen. 1981. Zoospore motility of *Phytophthora cinnamomi* in particulate substrates. *Phtyopathol. Z.* 101:202-209.

Nicolau, D.V., J.P. Armitage, and P.K. Maini. 2009. Directional persistence and the optimality of run-and-tumble chemotaxis. *Comp. Biol. Chem*. 33:269-274.

Ochiai, N., Parke, J.L., Dragila, M.I. Pattern swimming of Phytophthora citricola zoospores: an example of microbial bioconvection. Fung. Biol. (accepted).

Rafai, S., L. Jibuti, and P. Peyla. 2010. Effective viscosity of microswimmer suspensions. *Phys. Rev. Letters.* 104:098102.

Roberts, P.D., R.R. Urs, R.D. French-Monar, M.S. Hoffine, T.E. Sijo, and R.J. McGovern. 2005. Survival and recovery of *Phytophthora capsici* and oomycetes in tailwater and soil from vegetables fields in Florida. *Annals of Appl. Biol.* 146:351-359.

Saintillan, D. and M.J. Shelley. 2008. Instabilities and pattern formation in active particle suspensions: Kinetic theory and continuum simulations. *Phys. Rev. Letters*. 100:178103.

Schroth, M.H., S.J. Ahearn, J.S. Selker, and J.D. Istok. 1995. Characterization of miller-similar silica sands for laboratory studies. *Soil Sci. Soc. Amer. J*. 60:1331-1339.

Semenov, A.V., L. van Overbeek, and A.H.C. van Bruggen. 2009. Percolation and survival of Escherichia coli O157:H7 and Salmonella enterica Serovar Typhimurium in soil amended with contaminated dairy manure or slurry. *Appl. Environ. Microbiol*. 75:3206-3215.

Singleton, L.L., J.D. Mihail, and C.M. Rush. 1992. Methods for research on soil borne phytopathogenic fungi. APS Press, St. Paul, Minn. 265 pp.

Sirivithayapakorn, S. and A. Keller. 2003. Transport of colloids in saturated porous media: A pore-scale observation of the size exclusion effect and colloid acceleration. *Water Res. Res*. 39:1109.

Small, H. Hydrodynamic chromatography - technique for size analysis of colloidal particles. *J. Colloid Interface. Sci*. 48:147-161.

Sokolov, A. and I.S. Aranson. 2009. Reduction of viscosity in suspension of swimming bacteria. *Phys. Rev. Letters*. 103:148101.

Tong, M., H. Ma, and M.P. Johnson. 2008. Funneling of flow into grain-to-grain contacts drives colloid-colloid aggregation in the presence of an energy barrier. *Environ. Sci. Technol*. 42:2826-2832.

Torkzaban, S., S.S. Tazehkand, S.L. Walker, and S.A. Bradford. 2008. Transport and fate of bacteria in porous media: coupled effects of chemical conditions and pore space geometry. *Water Res. Res*. 44:W0403.

Tufenkji, N. 2007. Modeling microbial transport in porous media: Traditional approaches and recent developments. *Adv. Water Res*. 30:1455-1469.

Tufenkji, N. and M. Elimelech. 2005. Breakdown of colloid filtration theory: role of the secondary energy minimum and surface charge heterogeneities. *Langmuir*. 21:841-852.

Tufenkji, N., J.A. Redman, and M. Elimelech. 2003. Interpreting deposition patterns of microbial particles in laboratory-scale column experiments. *Environ. Sci. Technol*. 37:616-623.

Wolgemuth, C.W. 2008. Collective swimming and dynamics of bacterial turbulence. *Biophys. J*. 95:1564-1574.

Wu, M., J.W. Roberts, S.Kim, D.L. Koch, and M.P. DeLisa. 2006. Collective bacterial dynamics revealed using a three-dimensional population-scale defocused particle tracking technique. *Appl. Environ. Microbiol*. 72:4987-4994.

Young, B.R., F.J. Newhook, and R.N. Allen. 1979. Motility and chemotactic response of *Phytophthora cinnnamomi* zoospores in 'ideal soils.' *Trans. Br. Mycol. Soc.* 72:395-401.

Zentmeyer, G.A. 1961. Chemotaxis of zoospores for root exudates. *Science.* 133:1595-1596.

Zhang, P.F., W.P. Johnson, M.J. Piana, C.C. Fuller, D.L. Naftz. 2001. Potential artifacts in interpretation of differential breakthrough of colloids and dissolved tracers in the context of transport in zero-valent iron permeable reactive barrier. *Ground Water*. 39:831-840.

TABLES AND FIGURES

Table 5.1. Comparison of zoospore and microsphere characteristics

	zoospores	microspheres
dimensions	7.5 x 12.0 μm[1]	9.5 μm (diameter)
density	>1.00 g cm^{-3}†	1.05 g cm^{-3}
surface properties	HARDHAM[2]	carboxylate coating, negative charge
appendages	2 flagella (15~25 μm)[3]	N/A
swimming speed	~150 μm s^{-1}[4]	N/A
diffusion coefficient	4 x 10^{-9} m^2 s^{-1}[5]	4 x 10^{-14} m^2 s^{-1}‡
tactic behaviors	Chemotaxis[6], electrotaxis[7], negative geotaxis[8], rheotaxis[9], gyrotaxis[10]	N/A

† the density is known to greater than that of water[8]

‡ calculated using the well-known Einstein-Stokes equation

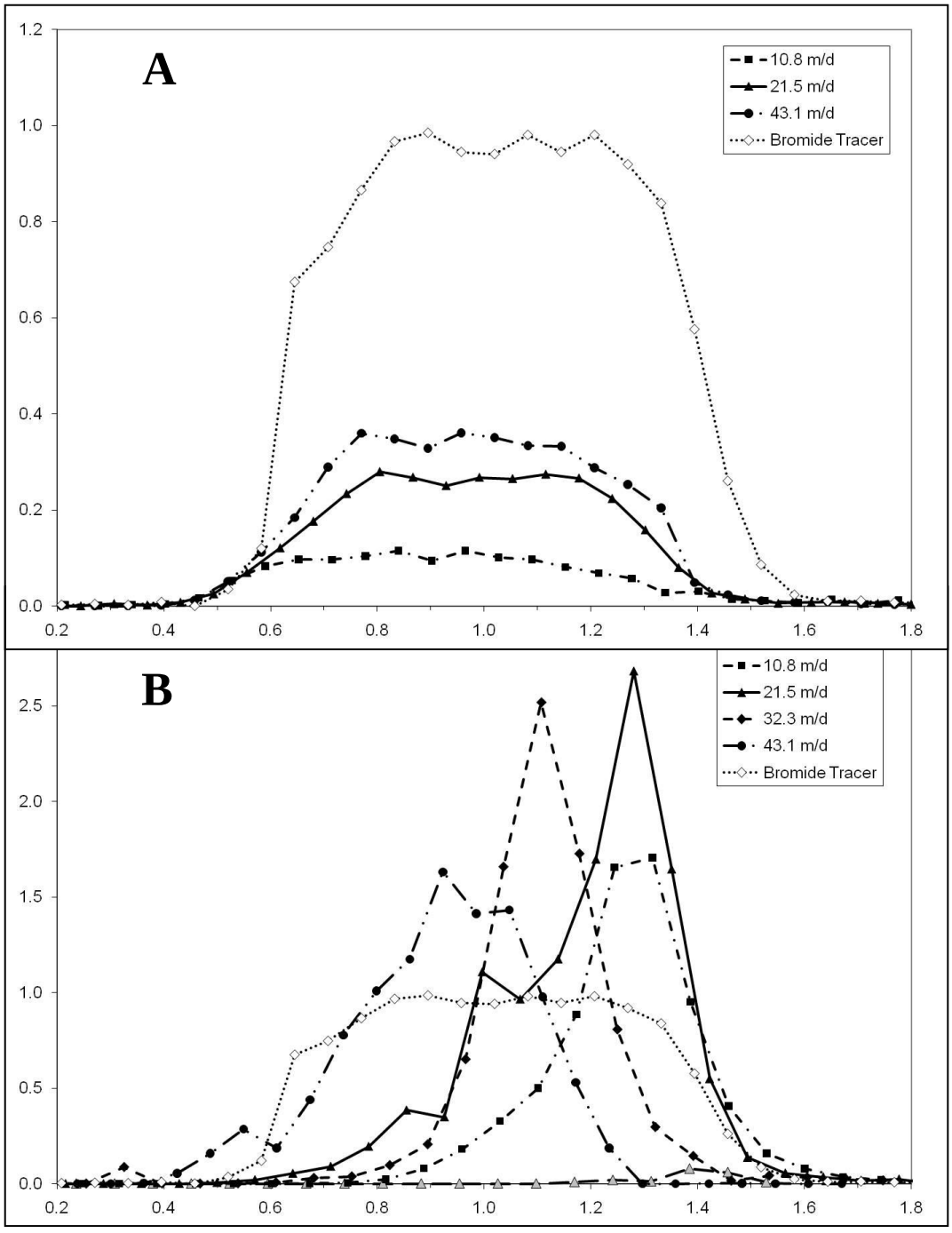

Figure 5.1. Typical breakthrough curves of (A) 9.5 μm latex microspheres and (B) zoospores. Note that the bromide curve in panels (A) and (B) are the same, but that the scale of Y-axes differ.

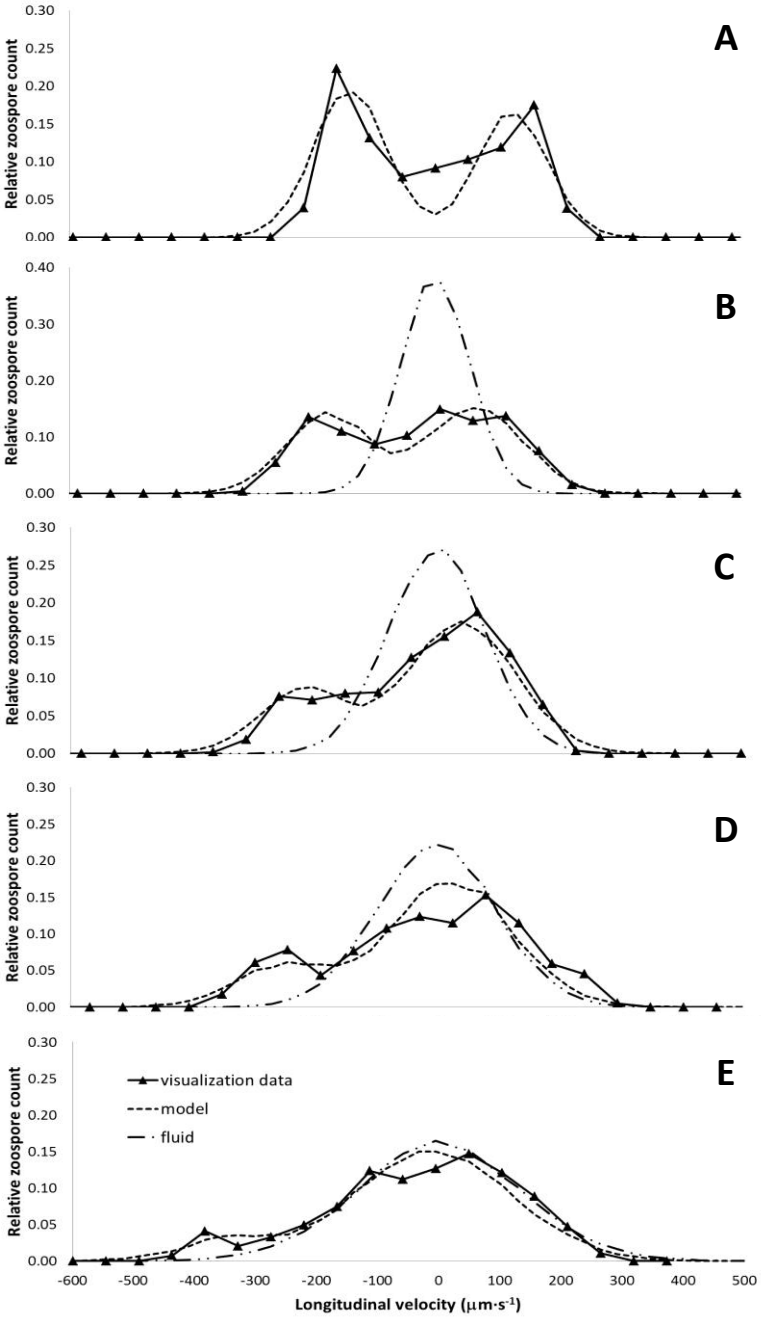

Figure 5.2. Longitudinal velocity distributions of zoospores as directly observed in the presence of downward flow at (A) 0.0, (B) 100, (C) 150, (D) 190, and (E) 275 μm s^{-1}. Solid triangles and solid lines (▲) represent visualization data, dashed lines (---) represent modeled velocity distributions, and mixed dashed lines (– ·· –) represent estimated fluid velocity distributions.

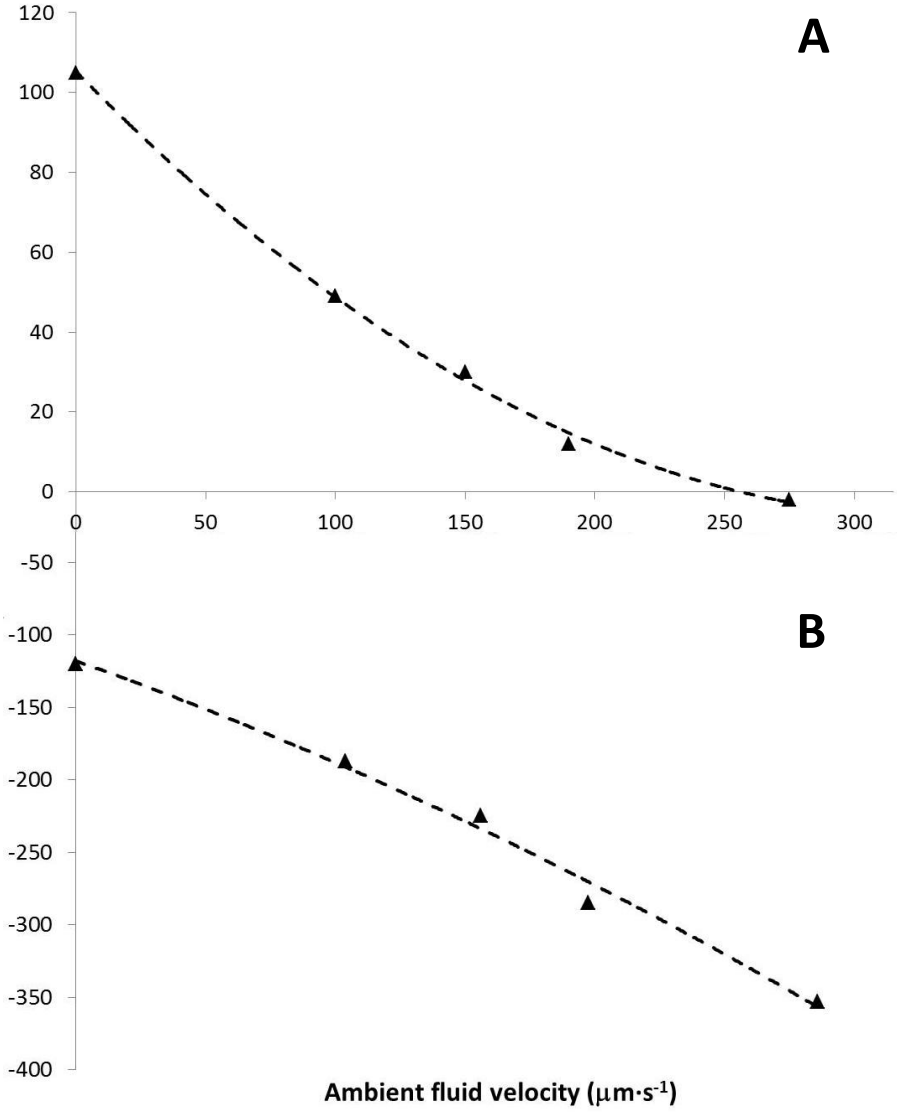

Figure 5.3. Mean (A) downstream and (B) upstream velocities of zoospores as a function of ambient fluid velocity. Negative velocities indicate movement against the direction of fluid flow.

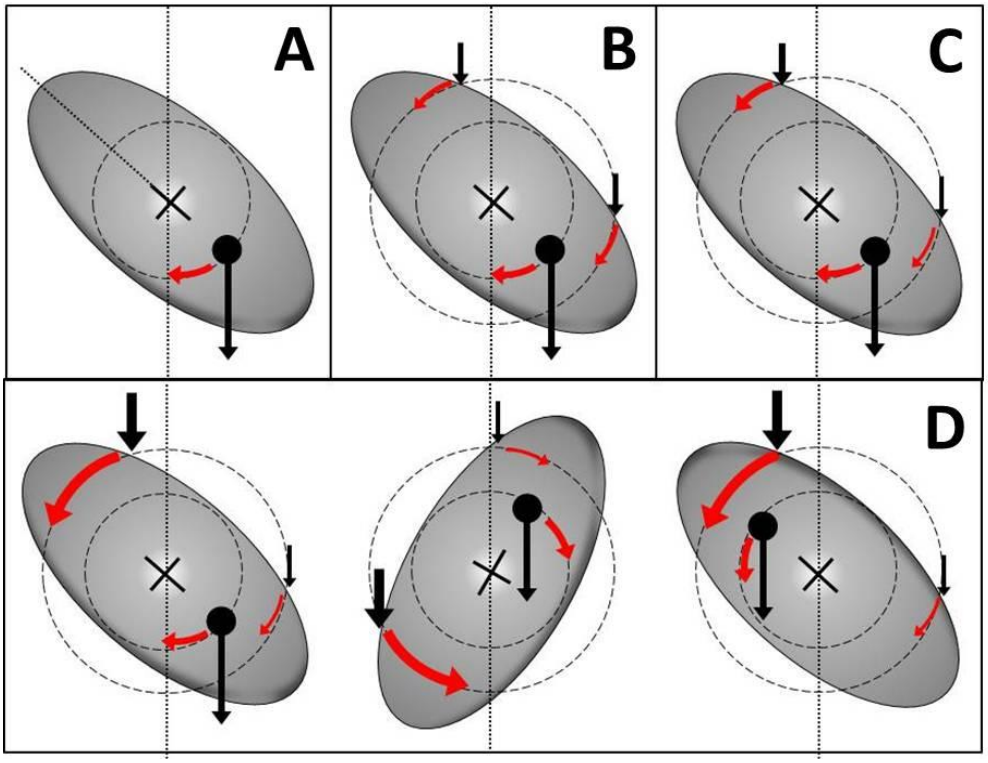

Figure 5.4. Schematic of impact of fluid shear on orientation of idealized ellipsoidal zoospore for the following cases: (A) no fluid motion, (B) no shear, i.e. flow is uniform across the zoospore body, (C) low shear, i.e. flow is non-uniform but resulting torque is insufficient to overcome gravitational torque in the opposite direction, and (D) high shear, i.e. torque to differential drag across the zoospore body is sufficient to overcome gravitational torque in the opposite direction and leads to zoospore "tumbling".

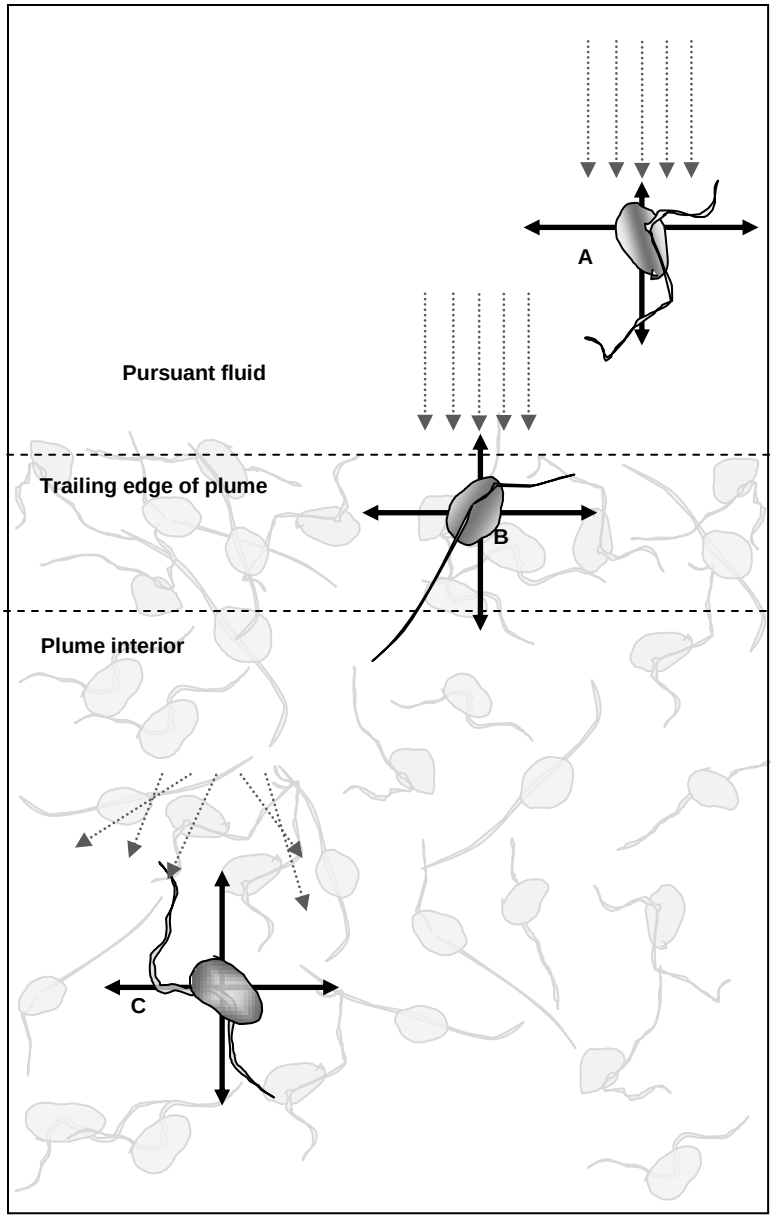

Figure 5.5. Conceptual model of plume position-dependent zoospore upstream swimming. Zoospores outside (A) and at the trailing edge (B) of a plume are more susceptible to forced turning, or "tumbling", due to shear of the pursuant fluid. Zoospores within a plume (C) are relatively less susceptible to forced downstream turning because of reduced shear effects within the plume.

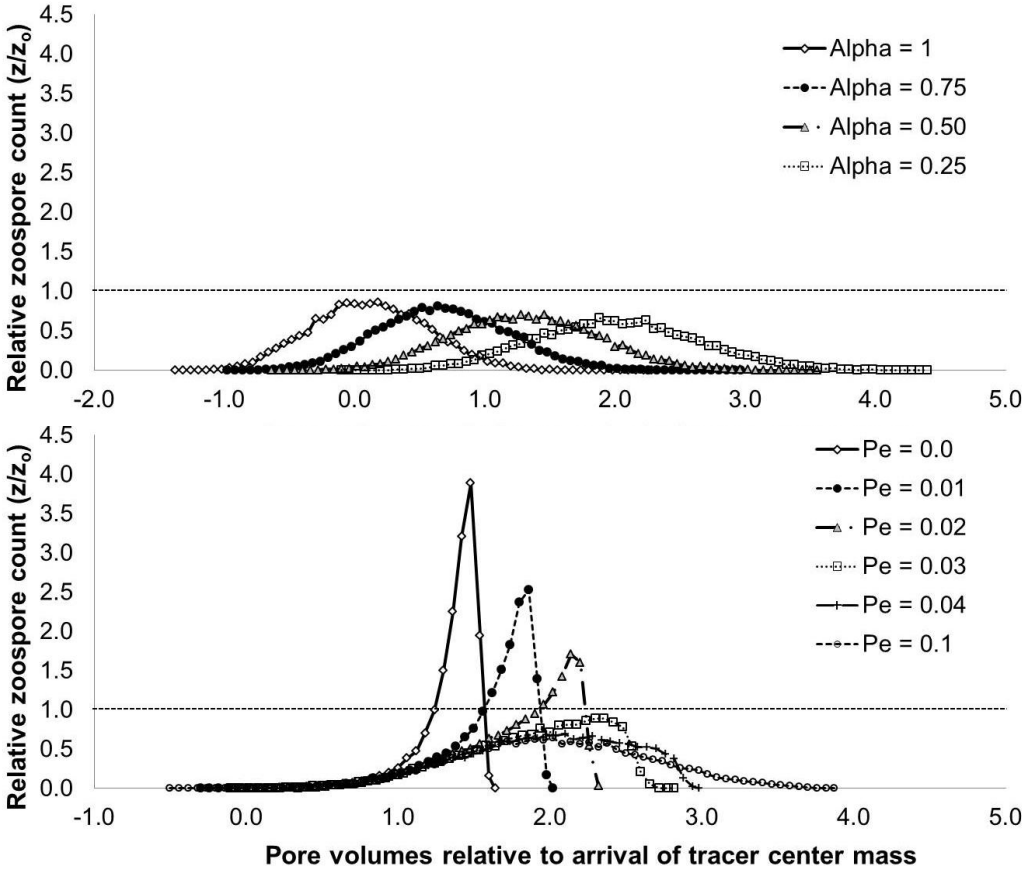

Figure 5.6. Simulated plume breakthrough (n = 10,000) for the case where (A) upstream turning probability of edge zoospores (P_e) is set equal to that of internal zoospores and influence of advection on edge zoospores (α_e) is allowed is varied between 1 and 0.25, and (B) influence of advection on edge zoospores is set equal to that of internal zoospores (α_e = α_i = 0.25) and upstream turning probability of edge zoospores (P_e) is varied between 0.0 and 0.1. The dashed horizontal line indicates peak height of the input plume.

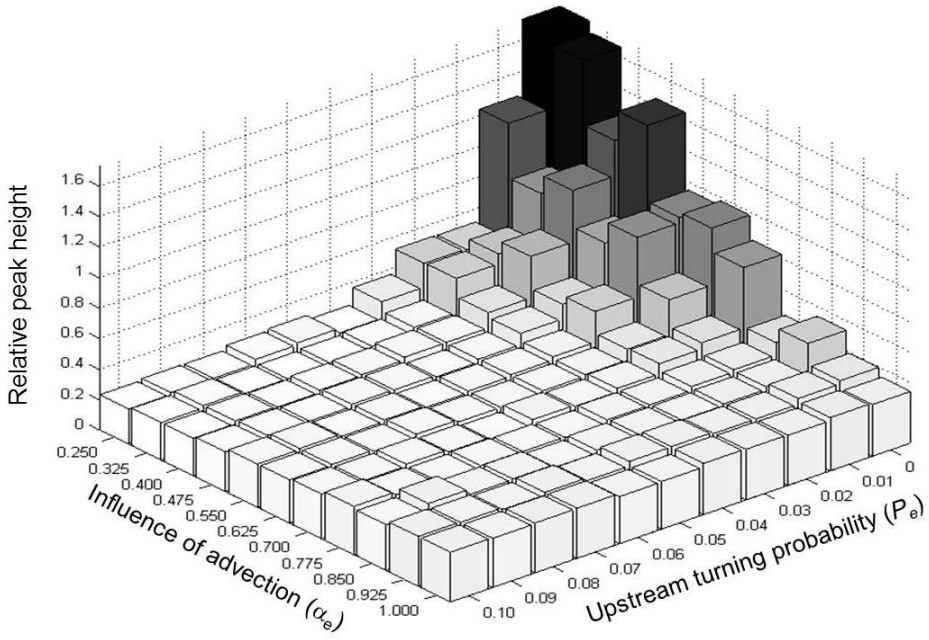

Figure 5.7. Matrix of simulated peak heights for combinations of upstream turning probability (P_e) and influence of advection (α_e) of edge zoospores. Turning probability of internal zoospores are set to 0.21 and 0.25, respectively.

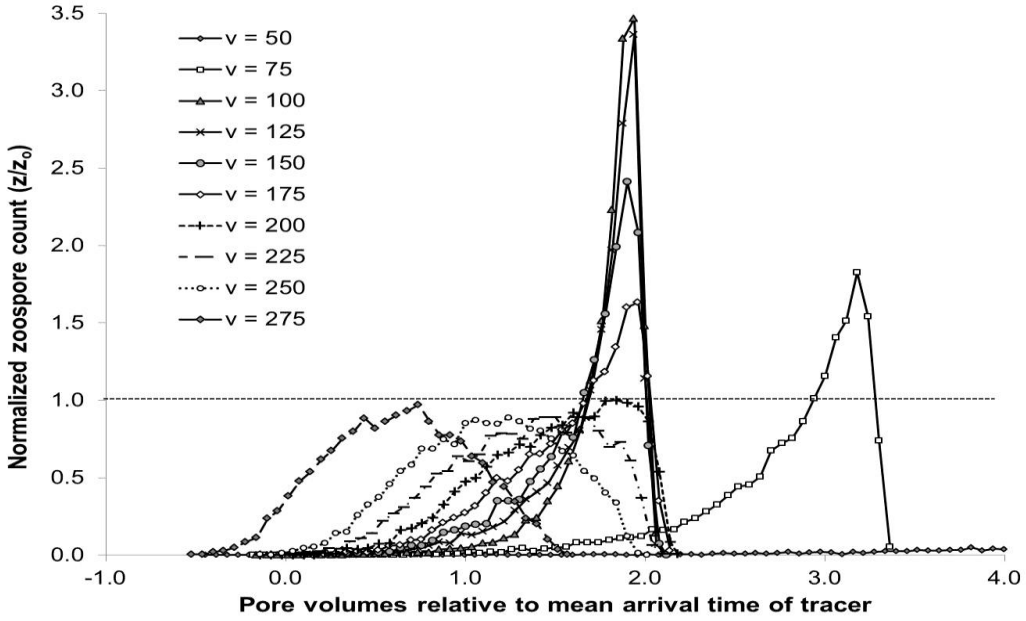

Figure 5.8. Simulated breakthrough of zoospore plumes for a range of ambient fluid velocities between 50 and 275 $\mu m \cdot s^{-1}$. Dashed horizontal line indicates the peak height of the input plume.

Chapter 6: General Conclusions

The goal of this research, represented by the four manuscripts of this dissertation, was to address the knowledge gaps identified in Chapter 1: (i) the nature of the low flow zones associated with orthogonal grain-to-grain contacts and (ii) the combined effects of passive (convective) transport and active swimming on zoospore movement through soil.

SUMMARY OF RESULTS

Chapter 2 introduced a novel visualization method to track the movement of fluorescent microspheres in 3 dimensions using a single camera attached to an epifluorescent micrcoscope. In the first of two mini-studies using this method, particles were observed to 'avoid' a certain volume associated with orthogonally-oriented grain-to-grain contacts, arcing above or below the grain-to-grain contact at a significant distance. This observation provides a contrast to the prevailing understanding of grain-to-grain contacts as regions of potential colloid retention (e.g. Tong et al., 2008) and suggests that grain-to-grain contacts may differ in quality and function depending on their orientation. The second mini-study explored the retention of latex microspheres in an offset glass bead-pair micromodel under chemical conditions unfavorable to deposition. The retained microspheres appeared to first become 'associated' with the beads and then were translated rearward along the bead surfaces, suggesting that the microspheres were either captured in the secondary energy minimum or were interacting with the bead surfaces via attractive nano-domains as proposed by other researchers (e.g. Kuznar and Elimelech, 2006, Duffadar and Davis, 2007). The microspheres finally came to rest near the rear stagnation points of the beads, where, presumably, local hydrodynamic drag was low. Chapter 3 expanded on the first study in Chapter 2 and further explored the nature of the 'avoided' zone with the aid of computational fluid dynamics. It was

demonstrated that the 'avoided' zone coincided with a low flow zone associated with the impinging walls of the adjacent beads near the grain-to-grain contact. It is minimally connected to the upstream and downstream flows by only a narrow streamtube. For this reason, the probability of colloid entry into this region by advection alone is quite low. The presence of the low flow zone with reduced entry results in a reduction on the order of 5% of the bead surface area available for particle capture relative to the Happel Sphere-in-Cell model. The emerging view of low flow zones associated with orthogonally-oriented grain-to-grain contacts indicates that they may serve as a watershed of sorts, permitting entry of Brownian particles or solutes via diffusion but preventing entry by large, non-Brownian particles.

Taken together, Chapters 2 and 3 provide an initial view into the complex hydrodynamic environment of 3-dimensional pores. In addition, they illustrate the dependence of particle behavior on the local hydrodynamic features and conditions. While it is certain that the hydrodynamic environment in natural porous media is much more complicated than in the 'idealized' pores used in these studies, the visualizations provide a starting point for developing novel conceptualizations of the pore space. This is a particularly timely endeavor given the recent calls to replace the Happel Sphere-in-Cell model that has served as the primary physical model in classic colloid tiltration theory (CFT) with one that better captures *sub*pore-scale hydrodynamic features (e.g. Cushing and Lawler, 1998, Johnson et al., 2007a, Ma et al. 2009). Specifically, the tentative conclusion that low flow zones associated with orthogonal grain-to-grain contacts are poorer candidates for colloid retention than those associated with parallel grain-to-grain contacts calls into question the sufficiency of the Hemispheres-in-Cell model proposed by Ma et al. (2009). In a larger context, insight into *sub*pore-scale hydrodynamics and its effect on particle transport lays the groundwork for understanding the transport and autonomous movement of Phytophthora zoospores (and other motile microorganisms).

In saturated transport experiments using repacked uniform sand, zoospore plumes exhibited markedly different behavior compared to latex microsphere plumes used as immotile proxies for zoospores. These differences included (i) higher recovery of zoospores in the effluent, i.e. less retention within the column, (ii) flow-rate-dependent shift of the plume centroid relative to the conservative tracer, (iii) 'plume convergence' marked by an increase in plume concentration and narrowing of plume width, and (iv) anistropic dispersion exhibiting a steeply falling trailing tail. Chapter 4 explored the nature of the 'pattern swimming' phenomenon frequently observed in free-swimming zoospores suspensions, whereby zoospores spontaneously form concentrated swimming masses, to assess the possibility of zoospore auto-attraction driving the observed 'plume convergence'. It was demonstrated that this pattern swimming phenomenon was not due to zoospore auto-attraction, but, rather, was an example of bioconvection (Hill and Pedley, 2005) observed in a wide range of denser-than-water, negatively geotactic (upward swimming) microorganisms. In addition to presenting results of the saturated column experiments described above, Chapter 5 introduced a novel conceptual model to explain the observed anomalous zoospore plume behavior. Briefly, the model posited that zoospores at the trailing edge of the plume are less able to turn or swim upstream again an opposing current than zoospores within the plume. This is because zoospores within the plume are 'protected', to a degree, from the hydrodynamic influence (advection and shear) of the pursuant fluid. This model was informed by a study on the upstream swimming ability of *Phytophthora* zoospores in the present of fluid flow (Katsura and Miyata, 1966) and a growing body of evidence, contrary to the prevailing view, that concentrated suspensions of motile microorganisms may alter macroscopic properties of the suspending fluid (Wu and Libchaber, 2000, Kim and Breuer, 2004, Cisneros et al., 2007, Saintillan & Shelley, 2008, Wolgemuth, 2008, Sokolov & Aronson, 2009, Rafai et al., 2010). One-dimensional conditionally-biased random walk simulations based on the conceptual

model were able to replicate, to a large degree, the 'peak convergence' as well as the ambient flowrate-dependent shift in peak arrival. However, the simulations did a poorer job at replicating the anisotropic dispersion, and particularly the rearward dispersion.

While recognizing that the ability to simulate the observed zoospore plume behavior does not validate the underlying conceptual model, it does provide a preliminary assessment of the model's potential. The experiments indicate that zoospores plumes will be advected at approximately the ambient fluid velocity for infiltration rates above 10 m d^{-1}, which might be expected for well-sorted fine sands or macropores. During their advection, however, zoospores plumes will converge and increase in concentration. Such concentrating, which is also demonstrated to occur in free-standing suspensions via bioconvection, may be ecologically important, given that numerous zoospore behaviors, including cohort recruitment during infection, have been shown to be density-dependent (e.g. Mitchell, and Kannwischer-Mitchell, 1983, Galiana et al., 2008, Kong and Hong, 2010). The conceptual model predicts that zoospore plumes will be advected a significantly lower speeds or not advected at all at lower infiltration rates. In other words, that the majority of zoospores will remain near the surface, i.e. in the root zone, or in the standing water above the surface, if such water is present. This has significant implications for the zoospores' opportunity to find host tissue or to be moved laterally across the soil surface (Neher and Duniway, 1992: Roberts et al., 2005).

UNRESOLVED ISSUES AND DIRECTIONS FOR FUTURE RESEARCH

As stated above, the ability to simulate experimental results clearly does not validate the underlying conceptual model. Thus, validation of the model through experimental testing of hypotheses remains as a priority for future research. Furthermore, the inability of the simulations to replicate the anisotropic dispersion patterns point to the need to further refine the conceptual model. As a first step,

this should entail accounting for the pore- and network-scale distribution in velocities, which ties in with conceptualization of pore space examined in the first phase of this research. In addition, rigorous theoretical analysis and experimental investigation of the influence of zoospore swimming and zoospore concentration on properties of the suspending fluid are necessary. If some hydrodynamic or energetic benefit is indeed gained from plume membership, this may significantly influence the behavior of both individual zoospores and zoospore populations in a wide variety of contexts, not only transport.

Overall Bibliography

Auzerais, F., J. Dunsmuir, B. Ferreol, N. Martys, J.Olson, T. Ramakrishnan, D. Rothman, and L. Schwartz. 1996. Transport in sandstone: a study based on three dimensional microtomography. Geophys. *Res. Lett*. 23:705-708.

Allen, R.N. and J.D. Harvey. 1973. Negative chemotaxis of zoospores of *Phytopthora cinnamomi*. *J. Gen. Microbiol*. 84:28-38.

Bearon, R.N. 2003. An extension of generalized Taylor dispersion in unbounded homogeneous shear flows to run-and-tumble chemotactic bacteria. *Phys. Fluids*. 15:1552-1563.

Bees, M.A. and N.A. Hill. 1998. Linear bioconvection in a suspension of randomly swimming, gyrotactic micro-organisms. *Phys. Fluids.* 10:1864-1881.

Ben-Jacob, E., I. Cohen, and H. Levine, H. 2000. Cooperative self-organization of microorganisms. *Adv. Phys*. 49:96-554.

Benjamin, M. and F.J. Newhook. 1982. Effect of glass microbeads on *Phytophthora* zoospore motility. *Trans. Br. Mycol. Soc.* 78:43-46.

Bimpong, C.E. and G.C. Clerk. 1970. Motility and chemotaxis in zoospores of *Phytophthora palmivora* (Butl.) Butl. *Ann Bot London*. 34:617-624.

Bradford, S.A., M. Bettahar, J. Simunek, and M.T. van Genuchten. 2004. Straining and attachment of colloids in physically heterogeneous porous media. *Vadose Zone J*. 3:384-394.

Bradford, S.A., J. Simunek, M. Bettahar, M.T. van Genuchten, and S.R. Yates. 2006. Significance of straining in colloid deposition: evidence and implications. *Water Res. Res*. 42(12):W12S15.

Bradford, S.A., S. Torkzaban, and S.L. Walker. 2007. Coupling of physical and chemical mechanisms of colloid straining in saturate porous media. *Water Res*. 41:3012-3024.

Bradford, S.A., S.R. Yates, M. Bettahar, and J. Simunek. 2002. Physical factors affecting the transport and fate of colloids in saturated porous media. *Water Res. Res.* 38(12):1327.

Brasier, C.M., D.E.L. Cooke, and J.M. Duncan. 1999. Origin of a new *Phytophthora* pathogen through interspecific hybridization. *PNAS.* 96:5878-5883.

Brasier, C.M., D.E.L. Cooke, J.M. Duncan, and E.M. Hansen. 2003. Multiple new phenotypic taxa from trees and riparian ecosystems in *Phytophthora gonapodyides*-*P. megasperma* ITS Clade 6, which tend to be high-temperature tolerant and either inbreeding or sterile. *Mycol. Res.* 107: 277-290.

Brasier, C.M., S.A. Kirk, J. Delcan, D.E.L. Cooke, T. Jung, and W.A.M. In't Veld. 2004. *Phytophthora alni* sp. nov. and its variants: designation of emerging heteroploid hybrid pathogens spreading on *Alnus* trees. *Mycol. Res.* 108:1172-1184.

Burgess, T.I., M. Stukely, T. Jung, D. White, D. Huberli, and G.E. Hardy. 2010. Molecular characterization of a *Phytophthora* hybrid swarm in native ecosystems and waterways in Western Australia. *5th IUFRO Phytophthoras in Forests and Natural Ecosystems, Rotorua, New Zealand. Mar.* 7-12, 2010. (Abstr.)

Cameron J.N. 1979. Taxes of zoospores of the fungus Phytophthora. *Ph.D. thesis*, University of London. 169 pp.

Cameron, J.N., and M.J. Carlile. 1980. Negative chemotaxis of zoospores of the fungus Phytophthora palmivora*. J. Gen. Microbiol*. 120:347-353.

Camesano, T. and B.E. Logan. 1998. Influence of fluid velocity and cell concentration on the transport of motile and nonmotile bacteria in porous media. *Environ. Sci. Technol*. 32:1699-1708

Cardenas, M.B. 2008. Three-dimensional vortices in single pores and their effects on transport. *Geophys. Res. Let.* 35:L18402.

Carlile, M.J. 1983. Motility, taxis and tropism in *Phytophthora*. Pages 95-107 in: *Phytophthora*, Its Biology, Taxonomy, Ecology and Pathology. Erwin D.C., S. Bartniki-Garcia, P.H. Tsao, eds. American Phytopathological Society, St. Paul, Minnesota.

cd-adapco. 2010. User Guide, STAR-CCM+ Version 5.04.006. CD-Adapco, http://www.cd- adapco.com.

Chang-ho, Y., and C.J. Hickman. 1970. Some factors involved in the accumulation of phycomycete zoospores on plant roots. Pages 103 – 108 In: Root diseases and soil-borne pathogen. T.A. Toussoun, R.V. Bega, and P.E. Nelson, eds. Uiv. Clif. Press, Berkeley.

Cherukat, P. and J.B. McLaughlin. 1994. The inertial lift on a rigid sphere in a linear shear flow field near a flat wall. *J. Fluid Mech*. 263:1-18.

Childress, S., M. Levandowsky, E.A. Spiegel. 1975. Pattern formation in suspension of swimming micro-organisms. *J. Fluid Mech.* 69:595-613.

Cisneros, L.H., R. Cortex, C. Dombrowski, and R.E. Goldstein. 2007. Fluid dynamics of self-propelled microorganisms, from individual to concentrated populations. *Exp. Fluids.* 43:737-753.

Codling, E.A., M.J. Plank, and S. Behamou. 2008. Random walk models in biology. *J. R. Soc. Interface*. 5:813-834.

Cushing, R.S., and D.F. Lawler. 1998. Depth filtration: fundamental investigation through three-dimensional trajectory analysis. *Environ. Sci. Technol*. 32:3793-3801.

Davis, A.M.J., M.E. O'Neill, J.M. Dorrepaal, and K.B. Ranger. 1976. Separation from the surface of two equal spheres in Stokes flow. *J. Fluid Mech.* 77:625-644.

de Kerchove, A.J., P. Weronski, and M. Elimelech. 2007. Adhesion of nonmotile *Pseudomonas aeruginosa* on "soft" polyelectrolyte layer in a radial stagnation point flow system: measurements and model predictions. *Langmuir.* 23:12301-12308.

Derjaguin, B.V., and L. Landau. 1941. Theory of the stability of strongly charged lyophobic sols and of the adhesion of strongly charged particles in solutions of electrolytes. *Acta Physicochim. URSS.* 14:633-662.

Di Carlo, D., D. Irimia R.G. Tompkins, and M. Toner. 2007. Continuous inertial focusing, ordering, and separation of particles in microchannels. *PNAS*. 104:18892-18897.

D'Orsogna, M.R., M.A. Suchard, and T. Chou. 2003. Interplay of chemotaxis and chemokinesis mechanisms in bacterial dynamics. *Phys. Rev. E*. 68:021925.

Duffadar, R.D., and J.M. Davis. 2008. Interaction of micrometer-scale particles with nanotextured surfaces in shear flow. *J. Colloid and Interface Sci.* 308:20-29.

Duffadar, R.D., and J.M. Davis. 2008. Dynamic adhesion behavior of micrometer-scale particles flowing over patchy surfaces with nanoscale electrostatic heterogeneity. *J. Colloid and Interface Sci*. 326:18-27.

Duffy, K.J., R.M. Ford, and P.T. Cummings. 1997. Residence time calculation for chemotactic bacteria within porous media. *Biophys. J*. 73:2930-2936.

Duniway, J.M. 1976. Movement of zoospores of *Phytophthora cryptogea* in soils of various textures and matric potentials. *Phytopathol*. 66:877-882.

Duniway, J.M. and C.D. Mckeen. 1987. Dispersal of *Phytophthora cryptogea* zoospores in soils and glass microbeads by water flow. *Phytopathol*. 77: 1744-1744.

Edwards, A.G., and W.C. Byrnes. 2007. Aerodynamic characteristics as determinants of the drafting effect in cycling. *Medicine and Science in Sports and Exercise*. 39:170-176.

Elimelech, M., M. Nagai, C. Ko, and J.N. Ryan. 2000. Relative insignificance of mineral grain zeta potential to colloid transport in geochemically heterogeneous porous media. *Environ. Sci. Technol.* 34:2143-2148.

Elimelech, M., and C.R. O'Melia. 1990. Kinetics of deposition of colloidal particles in porous media. *Environ. Sci. Technol*. 24:1528-1536.

Erwin, D.C. and O.K. Ribeiro. 1996. Phytophthora diseases worldwide. APS Press, St. Paul, Minn. 562 pp.

Foppen, J.W., G. Lutterodt, and W.F.M. Roling. 2010. Towards understanding inter-strain attachment variations of *Eshcerichia coli* during transport in saturated quartz sand. *Water Res*. 44:1202-1212.

Ford, R.M. and R.W. Harvey. 2007. Role of chemotaxis in the transport of bacteria through saturated porous media. *Adv. Water Res*. 30:1608-1617.

Galiana, E., S. Fourre, and G. Engler. 2008. *Phytophthora parasitica* biofilm formation: installation and organization of microcolonies on the surface of a host plant. *Environ. Microbiol.* 10:2164-2171.

Gervois, A., M. Lichtenberg, L. Oger, and E. Guyon. 1989. Coordination number of disordered packings of identical spheres. *J. Phys. A. Math. Gen*. 22:2119-2131.

Ginn, T.R., B.D. Wood, K.E. Nelson, T.D. Scheibe, E.M. Murphy, and T.P. Clement. 2002. Processes in microbial transport in the natural subsurface. *Adv. Water Res*. 25:1017-1042.

Grindrod, P., M.S. Edwards, J.J.W. Higgo, and G.M. Williams. 1996. Analysis of colloids and tracer breakthrough curves. *J. Contamin. Hydrol*. 21:243-253.

Hahn, M.W., D. Abadzic, and C.R. O'Melia. 2004. Aquasols: on the role of secondary minima. *Environ. Sci. Technol*. 38:5915-5924.

Hand, V.L., J.R. Lloyd, D.J. Vaughan, M.J. Wilkins, and S. Boult. 2008. Experimental studies of the influence of grain size, oxygen availability and organic carbon availability on bioclogging in porous media. *Environ. Sci. Technol*. 42:1485-1491.

Harvey, R.W. and S.P. Garabedian. 1991. Use of colloid filtration theory in modeling movement of bacteria through a contaminated sandy aquifer. *Environ. Sci. Technol*. 25:178-185.

Herskin, J. and J.F. Steffensen. 1998. Energy savings in sea bass swimming in a school: measurements of tail beat frequency and oxygen consumption at different swimming speeds. *J. Fish Biol*. 53:366-376.

Hijnen, W.A.M., Y.J. Dullemont, J.F. Shijven, A.J. Hanzens-Brower, M. Rosielle, and G. Medema. 2007. Removal and fate of *Cryptosporidium parvum*, *Clostridium perfringens* and small-sized centric diatoms (*Stephanodiscus hantzschii*) in slow sand filters. *Water Res.* 41:2151-2162.

Hill, N.A., and T.J. Pedley. 2005. Bioconvection. *Fluid Dynamics Res.* 37:1-20.

Hill, N.A., T.J. Pedley, and J.O. Kessler. 1989. The growth of bioconvection patterns in a suspension of gyrotactic micro-organisms in a layer of finite depth. *J. Fluid Mech.* 208:509-543.

Ho, H.H. and C.J. Hickman. 1967. Factors governing zoospore response of *Phytophthora megasperma* (*var. sojae*) to plant roots. *Can. J. Bot.* 45:1983-1994.

Huber, N., T. Baumann, and R. Niessner. 2000. Assessment of colloid filtration in natural porous media by filtration theory. *Environ. Sci. Technol*. 34:3774-3779.

Ishikawa, T. 2009. Suspension biomechanics of swimming microbes. *J. R. Soc. Interface*. **6:**815-834.

Janosi, I.M., A. Czirok, D. Silhavy, and A. Holczinger. 2002. Is bioconvection enhancing bacterial growth in quiescent environments? *Environ. Microbiol.* 4:525-531.

Jeffers, S.N., and S.B. Martin. 1986. Comparison of two media selective for *Phytophthora* and *Pythium* species. *Plant dis.* 70:1038-1043.

Johnson, W.P., X. Li, and G. Yal. 2007a. Colloid retention in porous media: mechanistic confirmation of wedging and retention in zones of flow stagnation. *Environ. Sci. Technol*. 41:1279-1287.

Johnson,W.P., E. Pazmino, and H. Ma. 2010. Direct observations of colloid retention in granular media in the presence of energy barriers, and implications for inferred mechanisms from indirect observations. *Water Res*. 44:1158-1169.

Johnson, W.P., and M. Tong. 2006. Observed and simulated fluid drag effects on colloids deposition in the presence of an energy barrier in an impinging jet system. *Environ. Sci. technol*. 40:5015-5021.

Johnson, W.P., M. Tong, and X. Li. 2007b. On colloid retention in saturated porous media in the presence of energy barriers: the failure of α, and opportunities to predict η. *Water Res. Res*. 43:W12813.

Jung, T. and T.I. Burgess. 2009. Re-evaluation of *Phytophthora citricola* isolates from multiple woody hosts in Europe and North America reveals a new species, *Phytophthora plurivora sp. nov*. *Persoonia*. 22:95-110.

Katsura, K. and Y. Miyata. 1966. Movements of zoospores of *Phytopthoracapsici* III: rheotaxis. *The scientific reports of Kyoto Prefectural University.*18:51-56.

Kawai, H., M. Kubota, T. Kondo, and M. Watanabe. 1991. Action spectra for phototaxis in zoospores of the brown alga *Pseudochorda gracilis*. *Protoplasma.* 161:17-22.

Keller, A.A. and M. Auset. 2007. A review of visualization techniques of biocolloid transport processes at the pore scale under saturated and unsaturated conditions. *Adv. Water Res.* 30:1392-1407.

Kessler, J.O. 1985a. Co-operative and concentrative phenomena of swimming micro-organisms. *Contemp. Phys.* 26:147

Kessler, J.O. 1985b. Hydrodynamic focusing of motile algal cells. *Nature* (London). 313:218-220.

Kessler, J.O. 2000. Dynamics of swimming bacteria at low and high volume fractions. Pages 1284-1287 in: *"Differential equations"*. Fiedler, B., K. Groege, and J. Sprekels, eds. World Scientific, Singapore.

Khew, K.L. and G.A. Zentmyer. 1973. Chemotactic response of zoospores of five species of *Phytophthora*. *Phytopath.* 63:1511-1517.

Kim, M.J. and K.S. Breuer. 2004. Enhanced diffusion due to motile bacteria. *Phys. Fluids*. 16:L78-L81.

Kline, T.R., G. Chen, and S.L. Walker. 2008. Colloidal deposition on remotely controlled charged micropatterned surfaces in a parallel-plate flow chamber. *Langmuir*. 24:9381-9385.

Ko, W.H. and M.J. Chan. 1974. Aggregation of *Phytophthora capsici* zoospores and their interaction with zoospores of *P. palmivora*. *J. Gen. Microbiol.* 80:549-551.

Ko, W.H. and L.L. Chase. 1973. Aggregation of zoospores of *Phytophthora palmivora*. *J. Gen. Microbiol.* 78:79-82.

Kong, P. and C. Hong. 2010. Zoospore density-dependent behaviors of *Phytophthora nicotianae* are autoregulated by extracellular products. *Phytopath*. 100:632-637.

Kusy, K. and R.T. Ford. 2007. Monte Carlo simulations derived from direct observations of individual bacteria inform macroscopic migration models at granular porous media interfaces. *Environ.Sci. Technol*. 41:6403-6409.

Kuznar, A.A. and M. Elimelech. 2007. Direct microscopic observation of particle deposition in porous media: role of the secondary energy minimum. *Colloids Surf. A: Physicochem. Eng Aspects.* 294:156-162.

Kuznetsov, A.V. and N. Jiang. 2003. Bioconvection of negatively geotactic microorganisms in a porous medium: the effect of cell deposition and declogging. *International Journal of Numerical Methods for Heat & Fluid Flow*. 13:341-364

Levy, M. and B.J. Berkowitz. 2003. Measurement and analysis of non-Fickian dispersion in heterogeneous porous media. *Contamin. Hydrol.* 65:203-226.

Leis, A.P., S. Schlicher, H. Franke, and M. Strathmann. 2005. Optically transparent porous medium for nondestructive studies of microbial biofilm architecture and transport dynamics. *Appl. Environ. Microbiol*. 71:4801-4808.

Levandowsky, M., W.S. Childress, E.A. Spiegel, and S.H. Hunter. 1975. A mathematical model of pattern formation by swimming micro-organisms*. J. Protozool.* 22:296-306.

Li, X., C. Lin, J.D. Miller, and W.P. Johnson. 2006. Pore-scale observation of microsphere deposition at grain-to-grain contacts over assemblage-scale porous media domains using x-ray microtomography. *Environ. Sci. Technol*. 40:3762-3768.

Liu, Y., M.S. Janjaroen, T.B. Kuhlenschmidt, and T.H. Nguyen. 2009. Deposition of *Cryptosporidium parvum* oocysts on natural organic matter surfaces: microscopic evidence for secondary minimum deposition in a radial stagnation point flow cell. *Langmuir*. 25:1594-1605.

Locesi, J.T. and T.J. Pedley. 2009. Run and tumble chemotaxis in a shear flow: the effect of temporal comparisons, persistence, rotational diffusion, and cell shape. *Bull. Math. Biol*. 71:1089-1116.

Loffler, F.E. and E.A. Edwards. 2006. Harnessing microbial activities for environmental cleanup. *Curr. Opin. Biotechnol.* 17:274-284.

Lounsbury, J.A. 1927. A case of phenomenal zoospore behavior of an apparently sterile *Isoachlya* and a description of the plant. *Trans. of the Wisconsin Academy* 23:539-549.

Luo, R., X.Y. Yang, X.F. Peng, and Y. Sun. 2006. Three-dimensional tracking of fluorescent particles applied to micro-fluidic measurements. *J. Micromech. Microeng*. 16:1689-1699.

Ma, H.L., J. Pedel, P. Fife, and W.P. Johnson. 2009. Hemispheres-in-cell geometry to predict colloid deposition in porous media. *Environ. Sci. Technol*. 43:8573-8579.

MacDonald, J.D. and J.M. Duniway. 1978. Influence of soil texture and temperature on the motility of *Phytophthora cryptogea* and *Phytophthora megasperma* zoospores. *Phytophathol*. 68:1627-1630.

Manz, B., F. Volke, D. Goll, and H. Horn. 2003. Measuring local flow velocities and biofilm structure in biofilm systems with magnetic resonance imaging (MRI). *Biotechnol. Bioeng*. 84:424-432.

McDowell-Boyer, L.M. 1992. Chemical mobilization of micron-sized particles in saturated porous media under steady flow conditions. *Environ Sci. Technol*. 26:586-593.

Mercer, J.R., R.M. Ford, J.L. Stitz, and C. Bradbeer. 1993. Growth rate effects on fundamental transport properties of bacterial populations. *Biotechnol. Bioeng*. 42:1277–86.

Mitchell, D.J. and M.E. Kannwischer-Mitchell. 1983. Relationship of inoculum density of Phytophthora disease incidence in various hosts. Pages 259-269 in: *Phytophthora*, Its Biology, Taxonomy, Ecology and Pathology. Erwin D.C., S. Bartniki-Garcia, P.H. Tsao, eds. American Phytopathological Society, St. Paul, Minnesota.

Morales, V.L., B. Gao, and T.S. Steenhuis. 2009. Grain surface roughness effects on colloidal retention in the vadose zone. *Vadose Zone J*. 8:11-20.

Morris, B.M. and N.A.R. Gow. 1993. Mechanism of electrotaxis of zoospores of phytopathogenic fungi. *Phytopathol*. 83:77:882.

Morris, P.F. and E.W.B. Ward. 1992. Chemoattraction of zoospores of the soybean pathogen *Phytophthora sojae*, by isoflavones. *Physiol. Molec. Plant Pathol*. 40:17–22.

Moschakis, T., B.S. Murray, and E. Dickinson. 2006. Particle tracking using confocal microscopy to probe the microrheology in a phase-separating emulsion containing non-adsorbing polysaccharide. *Langmuir*. 22:4710-4719.

Nazemifard, N., J.H. Masliyah, and S. Bhattacharjee. 2006. Particle deposition onto micropatterned charge heterogeneous substrates: trajectory analysis. *J. Colloid Interface Sci*. 293:1-15.

Neher, D. and J.M. Duniway. 1992. Dispersal of *Phytophthora parasitica* in tomato fields by furrow irrigation. *Plant Dis*. 76:582-586.

Newhook, F.J., B.R. Young, S.D. Allen, and R.N. Allen. 1981. Zoospore motility of *Phytophthora cinnamomi* in particulate substrates. *Phtyopathol. Z.* 101:202-209.

Nicolau, D.V., J.P. Armitage, and P.K. Maini. 2009. Directional persistence and the optimality of run-and-tumble chemotaxis. *Comp. Biol. Chem*. 33:269-274.

Ochiai, N., E.L. Kraft, and J.S. Selker. 2006. Methods for colloid transport visualization in pore networks. *Water Res. Res*. 42:W12S06.

Ochiai, N., M.I. Dragila, and J.L. Parke. 2010. Three-Dimensional Tracking of Colloids at the Pore Scale Using Epifluorescence Microscopy. *Vadose Zone J*. 9:576-587.

Olsen, M.G. and R.J. Adrian. 2000. Out of focus effects on particle image visibility and correlation in microscopic particle image velocimetry. *Expmt Fluids*. (suppl)s166-s174.

Paraskeva, C.A., V.N. Burganos, and A.C. Payatakes. 1991. Three-dimensional trajectory analysis of particle deposition in constricted tubes. *Chem. Eng. Sci*. 108:23-48.

Pedley, T.J. and J.O. Kessler. 1992. Hydrodynamic phenomena in suspensions of swimming microorganisms. *Ann. Rev. Fluid Mech.* 24:313-358.

Pedley, T.J., N.A. Hill, and J.O. Kessler. 1988. The growth of bioconvection patterns in a uniform suspension of gyrotactic micro-organisms. *J. Fluid Mech.* 195:223-237.

Petri, 1925.Osservazioni biologiche sulla '*Blepharospora cambivora*.' Reprinted from Ann R Ist Sup Agario e Forestale Ser. 2A in the *Review of Applied Mycology* 10:122-123 (1931).

Platt, J.R. 1961. "Bioconvection patterns" in cultures of free-swimming organisms. *Science.* 133:1766-1767.

Plesset , M.S. and C.G. Whipple. 1974. Viscous effects in Rayleigh-Taylor instability. *Phys. Fluids.* 17:1-7.

Plesset, M.S., and H. Winet. 1974. Bioconvection patterns in swimming microorganism cultures as an example of Rayleigh-Taylor instability. *Nature.* 248:441-443.

Rajagopalan, R. and C. Tien. 1976. Trajectory analysis of deep-bed filtration with sphere-in-cell porous media model. *AIChE*. 22:523-533.

Rafai, S., L. Jibuti, and P. Peyla. 2010. Effective viscosity of microswimmer suspensions. *Phys. Rev. Letters.* 104:098102.

Redman, J.A., S.L. Walker, and M. Elimelech. 2004. Bacterial adhesion and transport in porous media: role of the secondary energy minimum. *Environ. Sci. Technol*. 38:1777-1785.

Reid, B., B.M. Morris, and N.A.R. Gow. 1995. Calcium-dependent, genus-specific, autoaggregation of zoospores of phytopathogenic fungi. *Experimental Mycol.* 19:202-213.

Roberts, A.M. 2006. Mechanisms of gravitaxis in *Chlamydomonas*. *Biological Bulletin* 210:78-80.

Roberts, P.D., R.R. Urs, R.D. French-Monar, M.S. Hoffine, T.E. Sijo, and R.J. McGovern. 2005. Survival and recovery of *Phytophthora capsici* and oomycetes in tailwater and soil from vegetables fields in Florida. *Annals of Appl. Biol.* 146:351-359.

Saintillan, D. and M.J. Shelley. 2008. Instabilities and pattern formation in active particle suspensions: Kinetic theory and continuum simulations. *Phys. Rev. Letters*. 100:178103.

Schneider, G. 2003. X-ray microscopy: methods and perspectives. *Anal. Bioanal. Chem.* 376:558-561.

Schroth, M.H., S.J. Ahearn, J.S. Selker, and J.D. Istok. 1995. Characterization of miller-similar silica sands for laboratory studies. *Soil Sci. Soc. Amer. J*. 60:1331-1339.

Semenov, A.V., L. van Overbeek, and A.H.C. van Bruggen. 2009. Percolation and survival of *Escherichia coli* O157:H7 and *Salmonella enterica Serovar Typhimurium* in soil amended with contaminated dairy manure or slurry. *Appl. Environ. Microbiol*. 75:3206-3215.

Singleton, L.L., J.D. Mihail, and C.M. Rush. 1992. Methods for research on soil borne phytopathogenic fungi. APS Press, St. Paul, Minn. 265 pp.

Smith, J., B. Gao, H. Funabashi, T.N. Tran, D. Luo, B.A. Ahner, T.S. Steenhuis, A.G. Hay, and M.T. Walter. 2008. Pore-scale quantification of colloid transport in saturated porous media. *Environ Sci. Technol*. 42:517-523.

Sirivithayapakorn, S. and A. Keller. 2003. Transport of colloids in saturated porous media: A pore-scale observation of the size exclusion effect and colloid acceleration. *Water Res. Res*. 39:1109.

Small, H. Hydrodynamic chromatography - technique for size analysis of colloidal particles. *J. Colloid Interface. Sci*. 48:147-161.

Snyder, L.J. and W.E. Stewart. 1966. Velocity and pressure profiles for Newtonian creeping flow in regular packed beds of shapes. *AIChE J*. 12:161-173.

Sokolov, A. and I.S. Aranson. 2009. Reduction of viscosity in suspension of swimming bacteria. *Phys. Rev. Letters*. 103:148101.

Song, L., P.R. Johnson, and M. Elimelech. 1994. Transient deposition of colloidal particles in heterogeneous porous media. *J. Colloid Interface Sci*. 167:301-313.

Speidel, M., A. Jonas, and E.L. Florin. 2003. Three-dimensional tracking of fluorescent nano-particles with subnanometer precision by use of off-focus imaging. *Optics Letters*. 28:69-71.

Spielman, L.A. and P.M. Cukor. 1973. Deposition of non-brownian particles under colloidal forces. *J. Colloid Interface Sci*. 43:51-65.

Svendsen, J.C., J. Skov, M. Bildsoe, and J.F. Steffensen. Intra-school positional preference and reduced tail beat frequency in trailing positions in schooling roach under experimental conditions. *J. Fish Biol.* 62:834-846.

Thomas, D.D. and A.P. Peterson. 1990. Chemotactic auto-aggregation in the water mould *Achlya*. *J. Gen. Microbiol.* 136:847-853.

Tong, M. and W.P. Johnson. 2006. Excess colloid retention in porous media as a function of colloid size, fluid velocity and grain angularity. *Environ. Sci. Technol*. 40:7725-7731.

Tong, M., H. Ma, and W.P. Johnson. 2008. Funneling of flow into grain-to-grain contacts drives colloid-colloid aggregation in the presence of an energy barrier. *Environ. Sci. Technol*. 42:2826-2832.

Torkzaban, S., S.A. Bradford, and S.L. Walker. 2007. Resolving the coupled effects of hydrodynamics and DLVO forces on colloid attachment in porous media. *Langmuir*. 23:9652-9660.

Torkzaban, S., S.S. Tazehkand, S.L. Walker, and S.A. Bradford. 2008. Transport and fate of bacteria in porous media: coupled effects of chemical conditions and pore space geometry. *Water Res. Res*. 44:W0403.

Tufenkji, N. 2007. Modeling microbial transport in porous media: Traditional approaches and recent developments. *Adv. Water Res*. 30:1455-1469.

Tufenkji, N. and M. Elimelech. 2004. Deviation from the classical colloid filtration theory in the presence of repulsive DLVO interactions. *Langmuir*. 20:10818-10828.

Tufenkji, N. and M. Elimelech. 2005. Breakdown of colloid filtration theory: role of the secondary energy minimum and surface charge heterogeneities. *Langmuir*. 21:841-852.

Tufenkji, N., J.A. Redman, and M. Elimelech. 2003. Interpreting deposition patterns of microbial particles in laboratory-scale column experiments. *Environ. Sci. Technol*. 37:616-623.

Tuller, M. and D. Or. 2002. Unsaturated hydraulic conductivity of structure porous media: a review of liquid configuration –based models. *Vadose Zone J*. 1:14–37.

van West, P., A.A. Appiah, N.A.R. Gow. 2003. Advances in research on oomycete root pathogens. *Physiol. Molec. Plant Pathol.* **62:**99-113.

Verwey, E.J.W. and J.T.G. Overbeek. 1948. Theory of the stability of lyophobic colloids. Elsevier, Amsterdam.

Walkera, C.A. and P. van West. 2007. Zoospore development in the oomycetes. *Fungal Biol. Rev.* 21:10-18.

Weimerskirch, H., J. Martin, Y. Clerquin, P. Alexandre, and S. Jiraskova. 2001. Energy saving in flight formation. *Nature*. 413:697-698.

Winet, H. and T.L. Jahn. 1972. On the origin of bioconvective fluid instabilities in *Tetrahymena* culture systems. *Biorheol*. 9:87-104.

Wolgemuth, C.W. 2008. Collective swimming and dynamics of bacterial turbulence. *Biophys. J*. 95:1564-1574.

Wu, X.L. and A. Libchaber. 2000. Particle diffusion in a quasi-two-dimensional bacterial bath. *Phys. Rev. Letters*. 84:3017-3020.

Wu, M., J.W. Roberts, S.Kim, D.L. Koch, and M.P. DeLisa. 2006. Collective bacterial dynamics revealed using a three-dimensional population-scale defocused particle tracking technique. *Appl. Environ. Microbiol*. 72:4987-4994.

Yao, K.M., M.T. Habibian, and C.R. O'Melia. 1971. Water and waste water filtration: concepts and applications. *Environ. Sci. Technol*. 5:1105-1112.

Yoon, J.S., J.T. Germaine, and P.J. Culligan. 2006. Visualization of particle behavior within a porous medium: mechanisms for particle filtration and retardation during downward transport. *Water Res. Res*. 42:W06417.

Zhang, P.F., W.P. Johnson, M.J. Piana, C.C. Fuller, and D.L. Naftz. 2001. Potential artifacts in interpretation of differential breakthrough of colloids and dissolved tracers in the context of transport in zero-valent iron permeable reactive barrier. *Ground Water*. 39:831-840.

Young, B.R., F.J. Newhook, and R.N. Allen. 1979. Motility and chemotactic response of *Phytophthora cinnnamomi* zoospores in 'ideal soils.' *Trans. Br. Mycol. Soc.* 72:395-401.

Zentmeyer, G.A. 1961. Chemotaxis of zoospores for root exudates. *Science.* 133:1595-1596.

Zhang, P.F., W.P. Johnson, M.J. Piana, C.C. Fuller, D.L. Naftz. 2001. Potential artifacts in interpretation of differential breakthrough of colloids and dissolved tracers in the context of transport in zero-valent iron permeable reactive barrier. *Ground Water*. 39:831-840.